12-1-1995

Transient performance of parallel-flow and cross-flow direct transfer type heat exchangers with a step temperature change on the minimum capacity rate fluid stream

Brian D. Cole

Transient Performance of Parallel-Flow and Cross-Flow Direct Transfer Type Heat Exchangers with a Step Temperature Change on the Minimum Capacity Rate Fluid Stream

by

Brian D. Cole

A thesis submitted in partial fulfillment
of the requirements for the degree of
Master of Science in Mechanical Engineering

Approved By:

Professor Satish G. Kandlikar ____________________
(Thesis Advisor)

Professor Balwant V. Karlekar ____________________

Professor Alan H. Nye ____________________

Professor Charles W. Haines ____________________
(Department Head)

DEPARTMENT OF MECHANICAL ENGINEERING
COLLEGE OF ENGINEERING
ROCHESTER INSTITUTE OF TECHNOLOGY

DECEMBER 1995

Abstract

Parallel and cross-flow with both fluids unmixed, direct transfer type heat exchangers are modeled utilizing a thermal network consisting of nodes and resistors. A commercially available software package, Thermonet, calculates the transient outlet temperatures for a steady-state model introduced to a sudden change (step input) in inlet temperature of the C_{min} fluid stream. Both models are validated against analytical solutions provided in literature. Solutions are verified to within a maximum percent mean difference of 4 % of analytical solutions for parallel-flow, and 8 % of analytical solutions for cross-flow heat exchangers. Tables are generated which provide new dimensionless transient outlet temperature effectiveness values for parallel and cross-flow with both fluids unmixed, heat exchangers. The parallel-flow temperature responses are presented in graphical form for the specific parameters: NTU equal to 0.5, 1.0, and 3.0; C^* equal to 0.2, 0.6, and 1.0; R^* equal to 0.5, 1.0, and 2.0; C_w^* equal to 1.0, 10.0, and 1000.0; and t_d^* equal to 0.25, 1.0, and 4.0. The cross-flow temperature responses are presented in graphical form for the same parameters listed above except NTU is equal to 1.0. Discussion regarding the dimensionless parameters' effects on the transient response of the heat exchanger is provided. The transient performance tables provide a quick reference for transient outlet temperature solutions required for practical industrial heat exchanger analysis.

Acknowledgments

I wish to express my sincerest thanks and appreciation to Dr. Satish Kandlikar. His careful guidance, support, and knowledge made completion of this work possible. Also, I am deeply grateful to my wife, Joan, for her continuous support, patience, and encouragement throughout this process.

Permission Granted

I, Brian D. Cole, hereby grant permission to the Wallace Memorial Library of the Rochester Institute of Technology to reproduce my thesis entitled "Transient Performance of Parallel-Flow and Cross-Flow Direct Transfer Type Heat Exchangers with a Step Temperature Change on the Minimum Capacity Rate Fluid Stream" in whole or in part. Any reproduction will not be for commercial use or profit.

December 14, 1995

Brian D. Cole

Table of Contents

I
List of Tables

II
List of Figures

III
Nomenclature

A	heat transfer area, m^2
c_p	specific heat at constant pressure, J/(kg K)
C	fluid heat capacity rate, Wc_p or $\dot{m}c_p$, J/(s K)
$\overline{C}$	fluid stream heat capacitance, Mc_p, J/K
C*	dimensionless heat capacity rate, C_{min}/C_{max}
$\overline{C}_w$	wall heat capacitance, $(Mc_p)_w$, J/K
$\overline{C}_w^*$	dimensionless wall heat capacitance, $(Mc_p)_w/(Mc_p)_{min}$
$\dot{E}$	energy per unit time, J/s or Watts
h	convection heat transfer coefficient, $W/(m^2\ K)$
hgt	height, m
k	thermal conductivity, W/(m K)
L	heat exchanger length, m
$\dot{m}$	mass flow rate of the fluid stream, kg/s
M	mass of fluid or wall material in the heat exchanger, kg
NTU	dimensionless number of heat transfer units, UA/C_{min}
q	heat transfer rate, J/s or Watts
R^*	dimensionless thermal resistance ratio, $(hA)_{max}/(hA)_{min}$
T	temperature, K or °C
T(0)	Steady state outlet temperature before transient input has been applied, K or °C
T(t)	Outlet temperature at time t, K or °C
T(∞)	New steady state outlet temp. after transient input has been applied, K or °C
thk	thickness, m
t	time, starting with zero at beginning of the step change, s
t*	dimensionless time, $t/t_{d,min}$
t_d	dwell time, the time required for a fluid particle to pass through the heat exchanger, s
t_d^*	dimensionless dwell time, $t_{d,min}/t_{d,max}$
$t_{d,min}$	dwell time of C_{min} fluid, s
$t_{d,max}$	dwell time of C_{max} fluid, s
U	overall heat transfer coefficient, $W/(m^2\ K)$
V	fluid velocity, m/s
$\dot{V}$	volumetric flowrate, m^3/min
wdth	heat exchanger width, m
W	mass flow rate of the fluid stream, kg/s
X*	dimensionless distance, x/L
x	position in the heat exchanger along the flow direction, m

Greek Letters

η_0	fin efficiency
ε	dimensionless steady-state effectiveness
ε_f^*	dimensionless temperature effectiveness, $=[T(t)-T(0)]/[T(\infty)-T(0)]$
ρ	density, kg/m^3

Subscripts

0	at the beginning of the transient change
1,a	fluid with stepped change in its inlet temperature, stepped fluid
2,b	fluid with no change (unstepped) in its inlet temperature, unstepped fluid
∞	Infinite time after the step change is imposed, new steady state condition
f	fluid
in	inlet
out	outlet
min	minimum heat capacity rate fluid
max	maximum heat capacity rate fluid
w	heat exchanger wall

Superscripts

*	dimensionless quantity

1
Introduction

The intent of this thesis is to develop and validate simplified thermal network models for both parallel and cross-flow direct transfer type heat exchangers. Then provide easy to use transient performance effectiveness tables which cover a wide range of dimensionless heat exchanger design parameters.

Knowledge regarding the transient performance of heat exchangers is important for process engineers and heat exchanger design engineers. Process engineers are interested in transient response to reduce cycle time between product changes, reduce start-up time, and for process control. This knowledge assists the heat exchanger design engineer when analyzing internal stresses, in optimizing the heat exchanger geometry, and in reducing the cost to manufacture new heat exchangers.

Three common types of transient temperature inputs exist. They are the step input, frequency input, and the impulse input. Figure 1.1 shows a step input which is a sudden change in inlet temperature or flow rate to a new, constant value.

Figure 1.1: Step Input

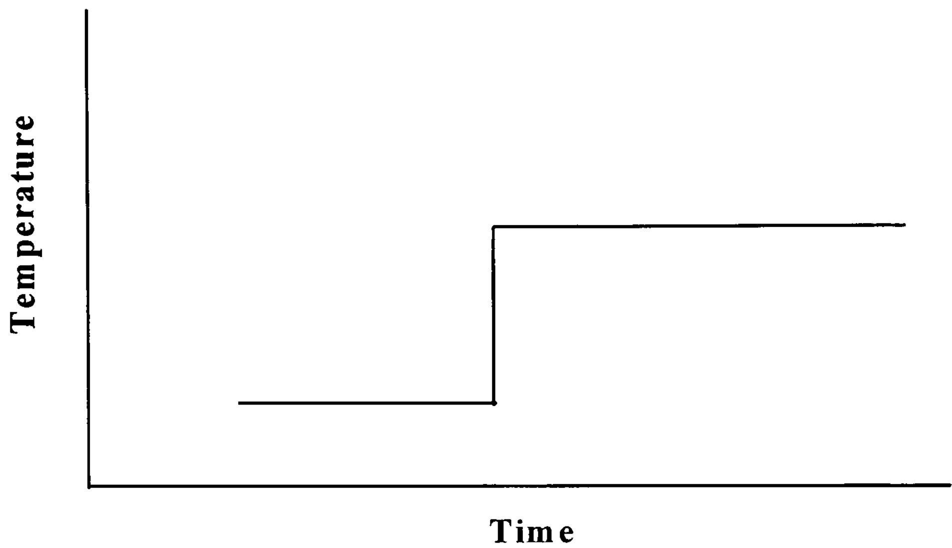

The frequency input, shown in figure 1.2, is a periodically varying change in inlet temperature or flow rate.

Figure 1.2: Frequency Input

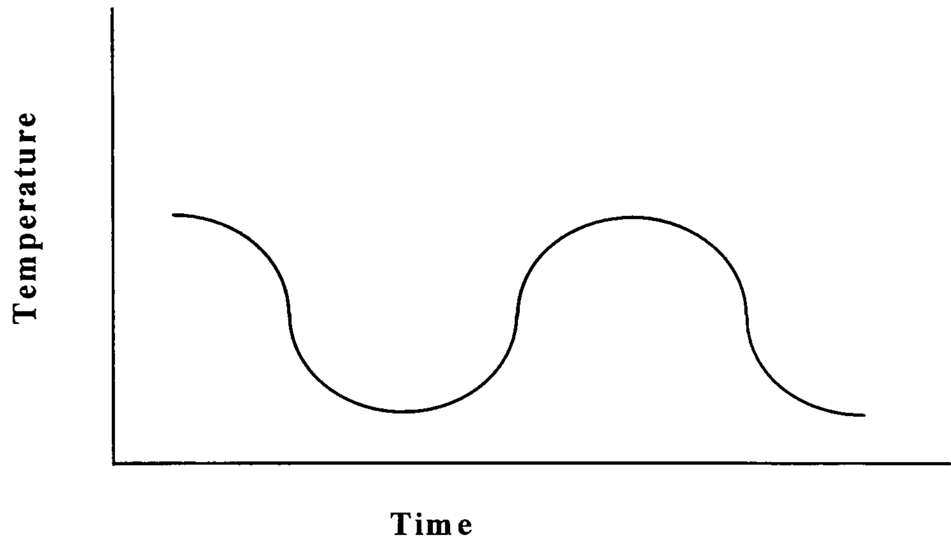

Figure 1.3 shows an impulse input which is a change in inlet temperature or flow rate of infinite amplitude, but infinitesimal duration.

Figure 1.3: Impulse Input

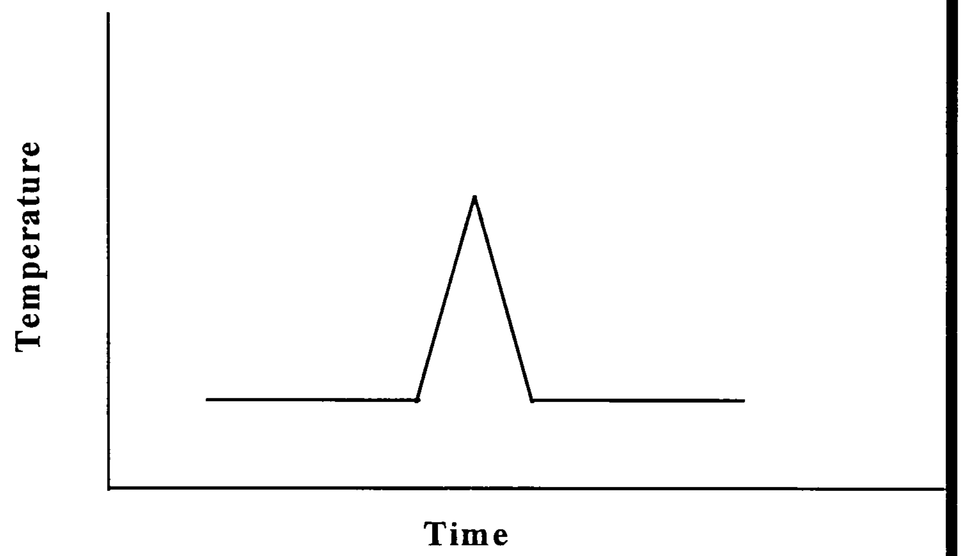

A common transient disturbance associated with heat exchangers is the step input at the heat exchanger inlet. Therefore the present work will focus on providing transient outlet temperature solutions which occur due to a step input at the inlet of both parallel and cross-flow direct transfer type heat exchangers.

A heat exchanger is a device which transfers internal thermal energy between two or more fluids at different temperatures. The type of exchangers selected for this thesis are commonly utilized in manufacturing industries. The selected exchangers are parallel and cross-flow single-pass, direct transfer type heat exchangers. Parallel-flow refers to both fluids flowing in the same direction through the heat exchanger. Cross-flow means the two fluids are flowing perpendicular to each other. Single-pass indicates the fluids cross paths only once within the heat exchanger. Finally, direct transfer type means the two fluids are separated by a thin wall through which heat transfer occurs. There are no moving parts in the heat exchanger. Both fluids flow simultaneously with no mixing between the two fluids. Figure 1.4 shows a typical parallel-flow single-pass, direct transfer type heat exchanger.

Figure 1.4: Direct Transfer Parallel-flow Heat Exchanger Cross Section

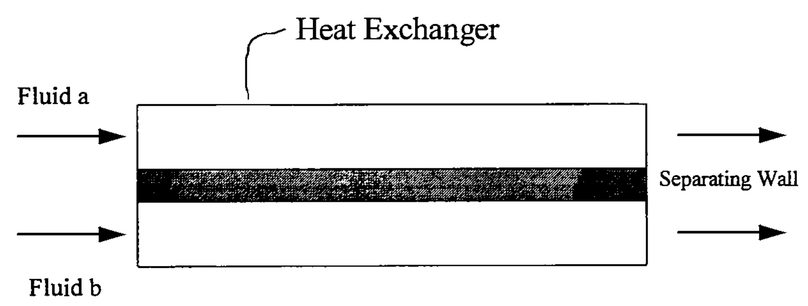

A typical cross-flow single-pass, direct transfer type heat exchanger is shown in figure 1.5.

Figure 1.5: Direct Transfer Cross-Flow Heat Exchanger Single-Pass, Both Fluids Unmixed

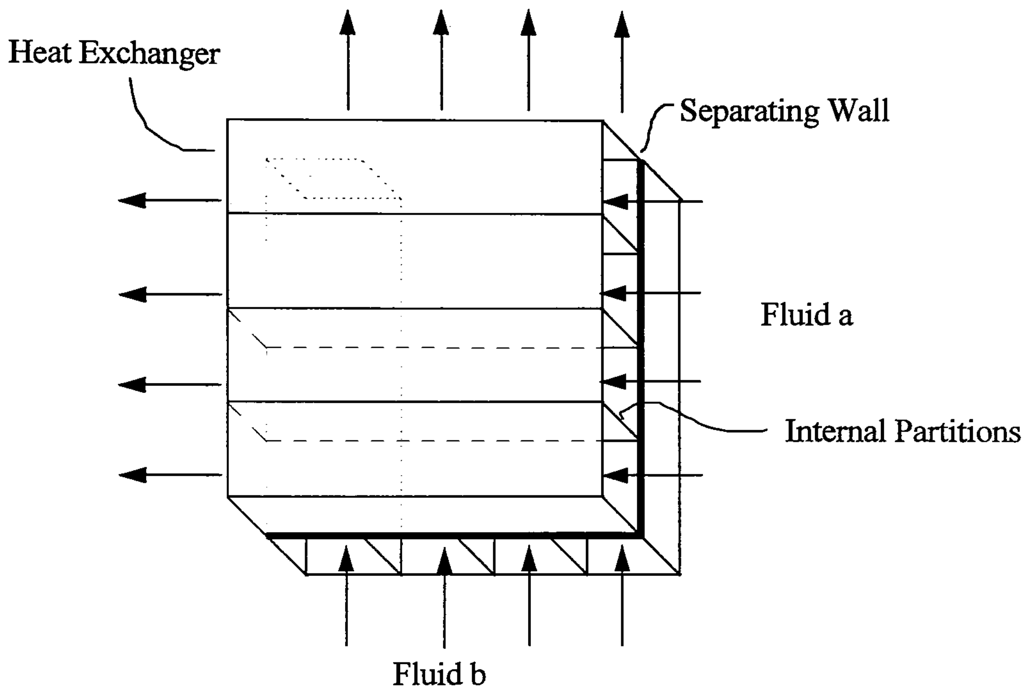

For cross-flow heat exchangers, individual fluid streams are considered either mixed or unmixed. The cross-flow heat exchanger model in this thesis is for both fluids unmixed. That means the internal partitions prevent fluid motion in a direction transverse to the main flow direction for each individual fluid stream.

Typical steady state operating conditions before and after a step change in the hot fluid inlet temperature are shown in figure 1.6 for a parallel-flow heat exchanger.

Figure 1.6: Steady-state Operating Conditions before and after a step change in hot fluid inlet temperature - Parallel-Flow

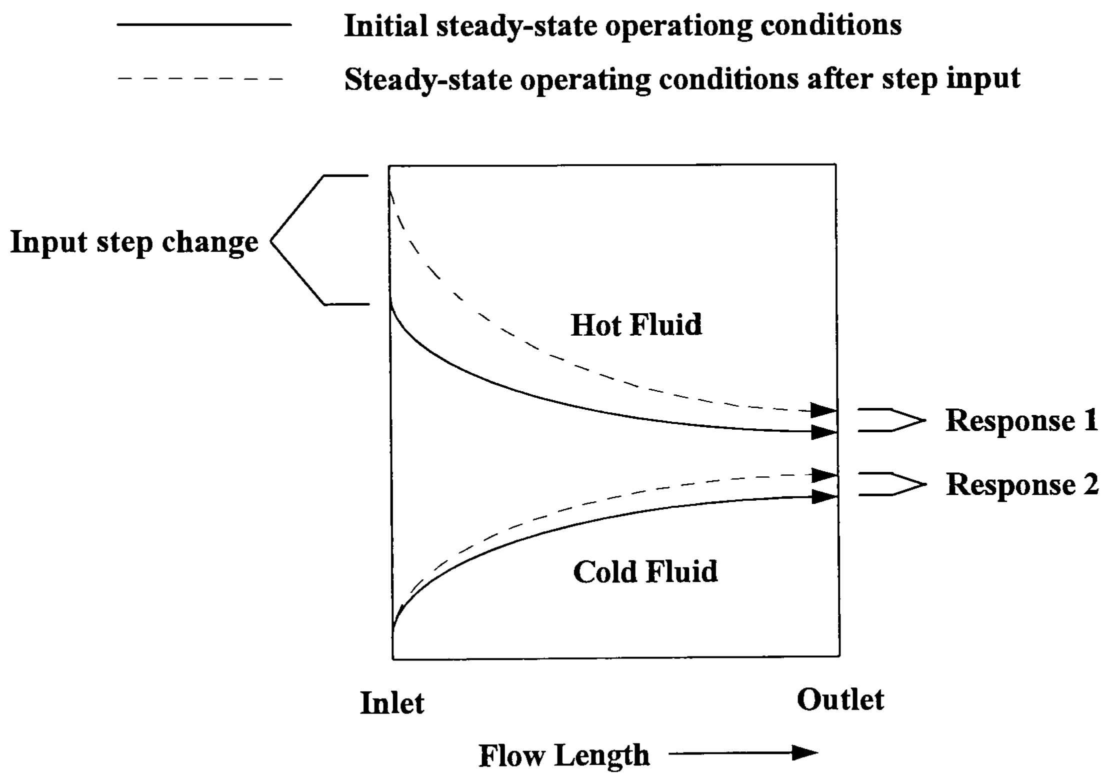

The typical inlet and outlet temperature distribution for a cross-flow heat exchanger is shown in figure 1.7.

Figure 1.7: Typical Outlet Temperature Distributions for a Cross-Flow Heat Exchanger

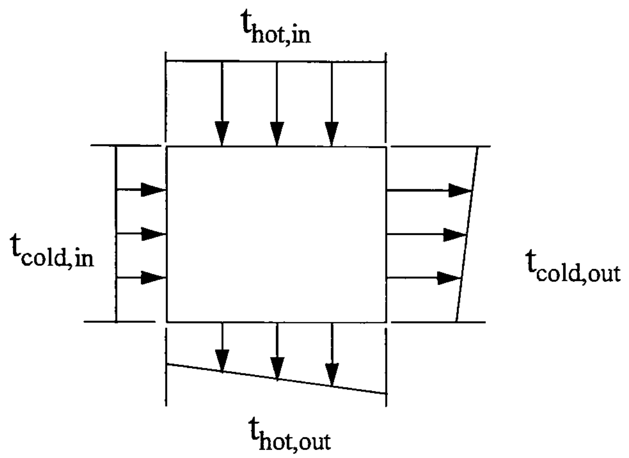

Typical steady state operating conditions before and after a step change in the hot fluid inlet temperature are shown in figure 1.8 for a cross-flow heat exchanger.

Figure 1.8: Steady-state Operating Conditions before and after a step change in hot fluid inlet temperature - Cross-Flow

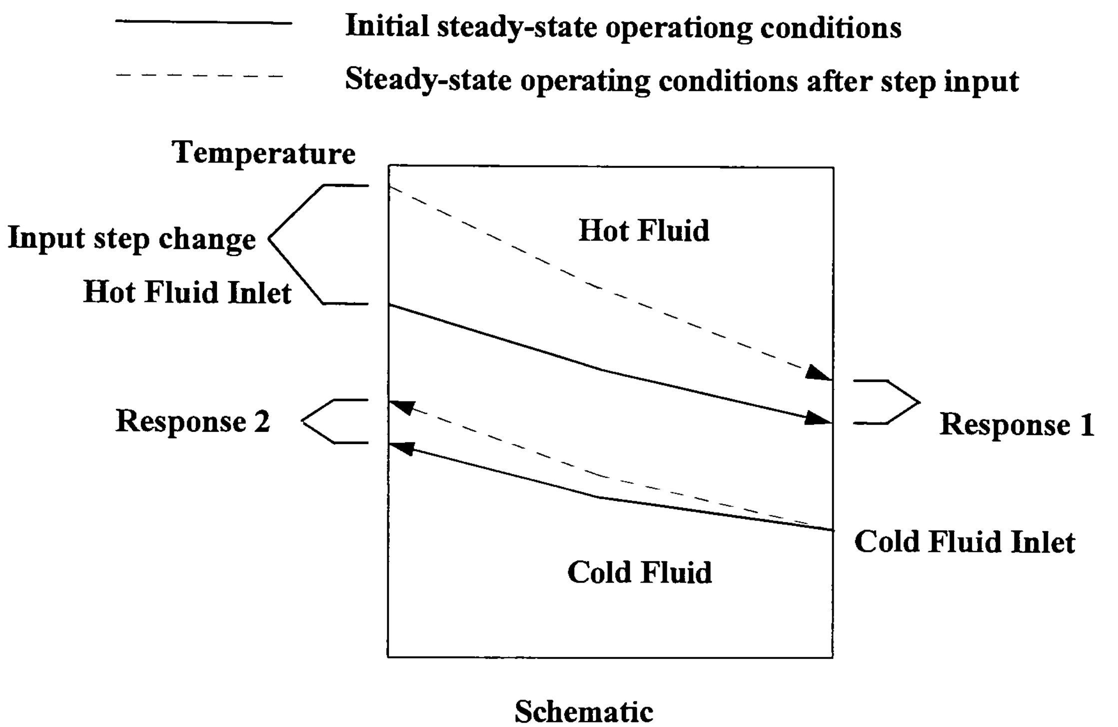

It is apparent from figure 1.6 that there will be two distinct fluid outlet temperatures for the parallel-flow heat exchanger. The cross-flow heat exchanger will have varying outlet temperatures for each fluid depending upon the location chosen across the flow direction. The typical technique for handling this variance is to average each fluids outlet temperatures to provide two distinct mean outlet temperatures.

The transient condition analyzed is described as follows. A heat exchanger system initially at steady state conditions is suddenly introduced to a transient in the form of a step input. A step input is a sudden change in either the inlet temperature or flowrate of one of the fluids to a new, constant value. The transient analysis begins with the step input and ends once the system reaches the new steady state conditons.

The parallel and cross-flow heat exchangers described above were modeled using a thermal network scheme. A thermal network is comprised of nodes and resistors connected in combinations to represent the heat exchangers fluids and thermal resistances. Specifically, nodes represent the fluids and separating wall, and resistors represent the fluid flow capacitance and convective resistances. The network was analyzed using a finite difference solution technique on a commercially available thermal network solver, Thermonet - TransHX.

The basic governing equations for parallel and cross-flow heat exchangers described by Shah (1981), were reduced to dimensionless parameters typical for heat exchanger design. The dimensionless parameters utilized include NTU, C^*, R^*, $\overline{C}_w^*$, t_d^*, and t^*. Tables were generated which provide dimensionless transient outlet temperature effectiveness values (ε_1^*, and ε_2^*) for parallel and cross-flow heat exchangers covering a wide range of dimensionless input parameters. The individual fluid temperature effectiveness, ε_1^*, and ε_2^* are solutions that indicate heat exchanger performance. The temperature effectiveness values range from 0 to 1. Zero is the initial steady-state dimensionless temperature, and 1 is the steady-state dimensionless temperature after the step input has been applied. The tables generated provide a quick reference for transient outlet temperature solutions.

2
Theoretical Background

The purpose of this section is to state the assumptions, show the governing differential equations describing the transient behaviour of heat exchangers, state the initial and boundary conditions, list the dimensionless parameters utilized to describe parallel and cross-flow heat exchangers, and give a feel for the complexities associated with analytical solutions for transient heat exchanger performance. The following idealizations presented by Shah (1981) are utilized in deriving the governing differential equations.

1. The temperatures of both fluids and the wall are functions of time and position (one dimension for parallel-flow heat exchangers, two dimensions for cross-flow heat exchangers).
2. Heat transfer between the exchanger and the surroundings is negligible. There are no thermal energy sources within the exchanger.
3. The mass flow rates of both fluids, although may be different, do not vary with time. The fluids are uniformly distributed along the flow passages.
4. The velocity and temperature of each fluid at the inlet are uniform over the flow cross section and are constant with time except for the imposed step change.
5. The convective heat transfer coefficient on each side, and the thermal properties of both fluids and the wall are constant, independent of temperature, time and position.
6. Longitudinal heat conduction within the fluids and wall as well as the transverse conduction within the fluid is neglected.

7. The heat transfer surface area on each fluid side is uniformly distributed.

8. Either the wall thermal resistance and fouling resistances are negligible or they are lumped with convective thermal resistances on hot and cold sides.

9. The thermal capacitance of the heat exchanger shell is considered negligible relative to that of the heat transfer surface.

An energy balance, utilizing equation 2.1, applied to incremental control volumes for the

$$\dot{E}_{in} - \dot{E}_{out} = \dot{E}_{stored} \qquad (2.1)$$

hot fluid, cold fluid, and separating wall shown in figure 2.1 results in the following simplified

Figure 2.1: Parallel-flow Heat Exchanger and Incremental Control Volume

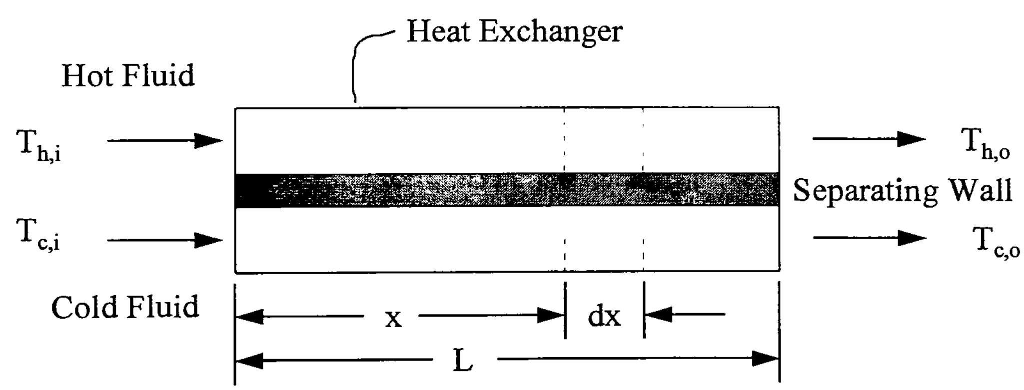

differential equations similar to counter-flow differential equations simplified by Shah (1981):

Hot fluid differential equation:

$$\overline{C}_h \frac{\partial T_h}{\partial t} + C_h L \frac{\partial T_h}{\partial x} + (\eta_0 hA)_h (T_h - T_w) = 0 \tag{2.2}$$

Cold fluid differential equation:

$$\overline{C}_c \frac{\partial T_c}{\partial t} + C_c L \frac{\partial T_c}{\partial x} + (\eta_0 hA)_c (T_c - T_w) = 0 \tag{2.3}$$

Wall differential equation:

$$\overline{C}_w \frac{\partial T_w}{\partial t} - (\eta_0 hA)_h (T_h - T_w) + (\eta_0 hA)_c (T_w - T_c) = 0 \tag{2.4}$$

where

$$\overline{C}_w = M_w c_{p,w} \equiv \text{Wall heat capacitance} \tag{2.5}$$

$$\overline{C}_h = M_h c_{p,h} \equiv \text{Hot fluid heat capacitance} \tag{2.6}$$

$$\overline{C}_c = M_c c_{p,c} \equiv \text{Cold fluid heat capacitance} \tag{2.7}$$

$$C_h = \dot{m}_h c_{p,h} \equiv \text{Hot fluid heat capacity rate} \tag{2.8}$$

$$C_c = \dot{m}_c c_{p,c} \equiv \text{Cold fluid heat capacity rate} \tag{2.9}$$

and other terms are defined in the nomenclature.

The initial conditions for the fluids and wall are obtained from the steady-state temperatures before the step input. The boundary conditions are the inlet temperature change of the stepped fluid to it's new value and the constant inlet temperature of the unstepped fluid.

It is apparent from the differential equations that the dependent fluid and wall temperatures are functions of eleven independent variables and parameters:

$$T_h = f\left[x, T_{h,i}, T_{c,i}, C_h, C_c, (\eta_0 hA)_h, (\eta_0 hA)_c, \text{Flow Arrangement}, t, \overline{C}_w, \overline{C}_h, \overline{C}_c\right] \tag{2.10a}$$

$$T_c = g\left[x, T_{h,i}, T_{c,i}, C_h, C_c, (\eta_0 hA)_h, (\eta_0 hA)_c, \text{Flow Arrangement}, t, \overline{C}_w, \overline{C}_h, \overline{C}_c\right] \quad (2.10b)$$

$$T_w = h\left[x, T_{h,i}, T_{c,i}, C_h, C_c, (\eta_0 hA)_h, (\eta_0 hA)_c, \text{Flow Arrangement}, t, \overline{C}_w, \overline{C}_h, \overline{C}_c\right] \quad (2.10c)$$

Dimensionless parameters have been formulated from the differential equations to provide steady-state and transient dimensionless groups for ease in separating the parameters for either analysis. Selection was also based on typical variables associated with heat exchanger design. The dimensionless parameters are defined as follows:

T^*: $$T^* = \frac{T(t) - T(0)}{T(\infty) - T(0)} \equiv \text{dimensionless temperature response} \quad (2.11)$$

X^*: $$X^* = \frac{x}{L} \equiv \text{dimensionless flow length variable} \quad (2.12)$$

NTU: $$NTU = \frac{UA}{C_{min}} \equiv \text{number of transfer units} \quad (2.13)$$

C^*: $$C^* = \frac{C_{min}}{C_{max}} \equiv \text{capacity rate ratio} \quad (2.14)$$

R^*: $$R^* = \frac{(\eta_0 hA)_{max}}{(\eta_0 hA)_{min}} \equiv \text{thermal resistance ratio} \quad (2.15)$$

$\overline{C}_w^*$: $$\overline{C}_w^* = \frac{\overline{C}_w}{\overline{C}_{min}} \equiv \text{wall capacitance ratio} \quad (2.16)$$

t_d^*: $$t_d^* = \frac{t_{d,min}}{t_{d,max}} \equiv \text{dwell time ratio} \quad (2.17)$$

t^*: $$t^* = \frac{t}{t_{d,min}} \equiv \text{dimensionless time variable} \quad (2.18)$$

The dimensionless parameters reduce the independent variables from eleven to seven.

$$T_h^* = f\left[X^*, NTU, C^*, t^*, R^*, \overline{C}_w^*, t_d^*\right] \tag{2.19a}$$

$$T_c^* = g\left[X^*, NTU, C^*, t^*, R^*, \overline{C}_w^*, t_d^*\right] \tag{2.19b}$$

Interest only in the transient outlet temperature response of each fluid further simplifies the analysis by eliminating X^* which equals 0 or 1 at either end of the heat exchanger.

Cima and London (1958) proposed another designation for the dependent dimensionless variables which is utilized in this work to reduce confusion between T^* and T. Instead of using T^*, they proposed to use dimensionless temperature effectiveness variables defined by equations 2.20 and 2.21.

$\varepsilon_{f,1}^*$: $$\varepsilon_{f,1}^* = \frac{T_1(t) - T_1(0)}{T_1(\infty) - T_1(0)} \tag{2.20}$$

$\varepsilon_{f,2}^*$: $$\varepsilon_{f,2}^* = \frac{T_2(t) - T_2(0)}{T_2(\infty) - T_2(0)} \tag{2.21}$$

Subscripts f, 1 and f, 2 refer to the stepped and unstepped fluids, respectively. All temperatures in equations 2.20 and 2.21 are outlet temperatures. T_1 (t) is the outlet temperature for the stepped fluid at any specified time t during the transient response to a step input. T_1 (0) is the steady state outlet temperature for the stepped fluid before the transient input has been applied to the heat exchanger. T_1 (∞) is the new steady state outlet temperature for the stepped fluid after the transient input has been applied. Subscripts 1 and 2 as described above refer to the stepped and unstepped fluids, respectively.

Finally, the independent dimensionless parameters are reduced to the six parameters shown in equations 2.22a and 2.22b.

$$\varepsilon_{f,1}^{*} = f\left[NTU,\ C^{*}, t^{*}, R^{*}, \overline{C}_{w}^{*}, t_{d}^{*}\right] \tag{2.22a}$$

$$\varepsilon_{f,2}^{*} = g\left[NTU,\ C^{*}, t^{*}, R^{*}, \overline{C}_{w}^{*}, t_{d}^{*}\right] \tag{2.22b}$$

Transient analysis of cross-flow heat exchangers is more difficult compared to parallel-flow heat exchangers because the temperature is a function of time and two position variables (x and z). Fortunately, all of the dimensionless parameters derived for parallel-flow heat exchangers are applicable for cross-flow heat exchangers.

Further reduction of the dimensionless parameters is typically performed for reducing the complexity of the analytical solution for specific cases of interest. These further reductions limit the ability to provide transient solutions for a wide range of dimensionless parameters. The numerical solution technique employed in this thesis provides for transient performance solutions which cover a wide range of dimensionless parameters.

3
Literature Review

Two comprehensive literature reviews regarding the transient performance of heat exchangers exist. Literature was reviewed up to 1981 by Shah (1981). Bunce and Kandlikar (1995) reviewed literature up to 1995. It was noted by Bunce and Kandlikar (1995) that several complex analytical solutions are presented in a difficult to utilize format.

3.1 PARALLEL-FLOW

Solutions for parallel-flow configurations are summarized in Table 3.1.

Table 3.1: Available Solutions for parallel-flow configurations

Restrictions	Solution Method	Reference
Dwell time of fluids are equal or both fluids are gases	Analytical	Romie (1985)
Thermal capacitance of the core is assumed to be negligible compared to the thermal capacitance of the stepped fluid.	Analytical	Li (1986)
Both fluids must be gases.	Analytical	Gvozdenac (1987)

Romie (1985) presents analytical solutions utilizing four dimensionless parameters θ, E, R, and NTU. Several graphical solutions are presented for specific dimensionless groups. Both fluids are restricted to equal velocities or both fluids are gases. This analytical technique requires the integration of Bessel functions. The thermal capacitance of the core is assumed negligible compared to the thermal capacitance of the stepped fluid.

Li (1986) presents an analytical solution technique which is valid for liquid to liquid and liquid to gas heat exchangers where the stepped fluid is the liquid. The fluid velocities can be different. The technique utilizes the Laplace transform and requires the integration of Bessel functions.

Gvozdenac (1987) presents solutions where both fluids are gases, the thermal capacities of the two fluids are negligible relative to the thermal capacity of the heat exchanger core, and it is valid for any type of input temperature change (sinusoidal, exponential, step function, etc.).

3.2 CROSS-FLOW

Table 3.2 summarizes the available literature and solution techniques for cross-flow heat exchangers.

Table 3.2: Available Solutions for Cross-Flow Configurations

Restrictions	Solution Method	Reference
	Finite Difference	Dusinberre (1959)
One fluid mixed, other unmixed mixed fluid stepped C_w* large	Analytical	Myers et al. (1967)
Both fluids unmixed	Finite Difference	Yamashita et al. (1978)
Both fluids gases Both fluids unmixed	Analytical	Romie (1983)
Both fluids gases Both fluids unmixed	Analytical	Gvozdenac (1986)
Both fluids gases Both fluids unmixed	Analytical	Spiga, Spiga (1987)
Delta input only Both fluids unmixed	Analytical	Spiga, Spiga (1988)
Delta input only Both fluids unmixed	Analytical	Chen, Chen (1991)
Both fluids gases Both fluids unmixed	Analytical	Chen, Chen (1992)
Both fluids unmixed	Analytical	Spiga, Spiga (1992)

Dusinberre (1959) presented the first paper to obtain the transient performance of gas-to-gas cross-flow heat exchangers with both fluids unmixed. He utilized a finite difference technique. Solutions were not verified with any other source.

Myers et al. (1967) determined the transient behavior of gas-to-gas cross-flow heat exchangers with the stepped, hot fluid mixed. Response to this step change was found utilizing a complex analytical approach which involves the integration of Bessel functions. All solutions were found for the case where the wall capacitance $\overline{C}_w^*$ was considered large. Graphical solutions are presented showing a 90 % response time for the mean outlet temperatures.

Yamashita et al. (1978) calculated the transient outlet temperature response with neither fluid mixed and no limit regarding the wall capacitance size for a step change in inlet temperature utilizing finite difference techniques. Effects of the governing parameters t_d^*, $1/\overline{C}_w^*$, R^*, NTU, and C^* were illustrated graphically by varying each parameter with the other values fixed to be unity.

Romie (1983) applied a Laplace transform technique to gas-to-gas cross-flow heat exchangers. Graphical solutions were presented for single-pass exchangers with neither gas mixed. A unit step increase was applied to the entrance temperature of either gas. Exit mean temperature solutions are given in graphical form for the following range of dimensionless parameters: NTU (1-8), E (0.6-1.67), and R (0.5-2.0).

Gvozdenac (1986) provided analytical solutions for gas-to-gas, large wall capacitance, single-pass cross-flow heat exchangers with both fluids unmixed. Solutions are presented graphically for arbitrary time varying initial and inlet temperatures.

capabilities for the fluids to be gases or liquids, and a finite wall heat capacity to be utilized. Results are valid for arbitrary time varying initial and inlet temperatures.

Chen and Chen (1991, 1992) simplified the implementation of the Spiga and Spiga (1987, 1988) work by proposing straight forward fortran computer code techniques that decrease computer time. Chen and Chen (1991) analyzed gas-to-gas cross-flow heat exchangers with neither gas mixed and provide graphical output.

Spiga and Spiga (1992) propose an exact analytical solution for a step change in the inlet temperature of the hot fluid. Both fluids are unmixed gases or liquids. Finite wall capacitance is utilized.

The literature review shows solutions exist for the transient outlet temperature response of a heat exchanger to a step input on the inlet side of the heat exchanger given specific restrictions. All of the parallel-flow solutions are analytical. Two of the cross-flow solutions utilize finite difference techniques while the remaining eight utilize analytical solution techniques. The finite difference techniques are not as accurate as the analytical solutions, however finite difference solutions can cover a wider range of independent parameters. All of the available solutions are restricted to a narrow range of dimensionless parameters. These restrictions make it difficult to provide reference tables which cover a wide range of heat exchanger design or process conditions.

4
Application of Thermal Network Solver

This analysis deals with parallel-flow and cross-flow direct-transfer type heat exchangers. These heat exchangers consist of two independent flowing fluids separated by a fixed, very thin material or wall. The entering fluids are at different temperatures resulting in heat transfer from the higher temperature fluid to the lower temperature fluid. Fluid flow rates are constant. The parallel-flow heat exchanger fluids enter the exchanger on the same side, flow in the same direction, and exit the exchanger on the opposite side from where they entered. The fluids flow perpendicular to each other in the cross-flow heat exchanger. This application consists of both fluids and the heat exchanger initially at steady-state conditions. Steady-state conditions indicate the exchanger and fluid temperatures do not change with time. The minimum capacity rate fluid stream temperature is instantaneously increased to a new, constant value. This inlet step temperature change causes the entire system to change temperature over time until it reaches new steady-state conditions. The response of interest to the process engineer is the transient outlet temperature response of each fluid to this step input change. Thermal network models were developed to represent parallel and cross-flow heat exchangers. Nodes represent the fluids or wall regions in the heat exchanger, and resistors are utilized to represent heat transfer resistance. These models were set-up in Thermonet - a commercially available thermal network software package which was utilized to calculate the transient outlet temperature responses for this application. Solutions were obtained for the following dimensionless parameters: NTU, C^*, R^*, C_W^*, t_d^*, and t^*.

4.1 PARALLEL-FLOW HEAT EXCHANGERS

Simplified 10 and 20 segment direct-transfer parallel-flow heat exchanger cross-sections are shown in Figures 4.1 and 4.3, respectively. This simplified model utilizes nodes (dots) to symbolize the fluids and separating wall in the heat exchanger. Each node represents a specific volume of fluid or wall region represented by the "boxed" region surrounding each node. Both fluids enter the exchanger on the same side, flow parallel to each other, and exit the same but opposite side from the inlet. Equivalent thermal network node-resistor models are generated from the simplified cross-sections as shown directly below each cross-section in figures 4.2 and 4.4, respectively.

Figure 4.1: Direct Transfer Parallel-flow Heat Exchanger Cross Section (10 Segment Model Schematic Diagram)

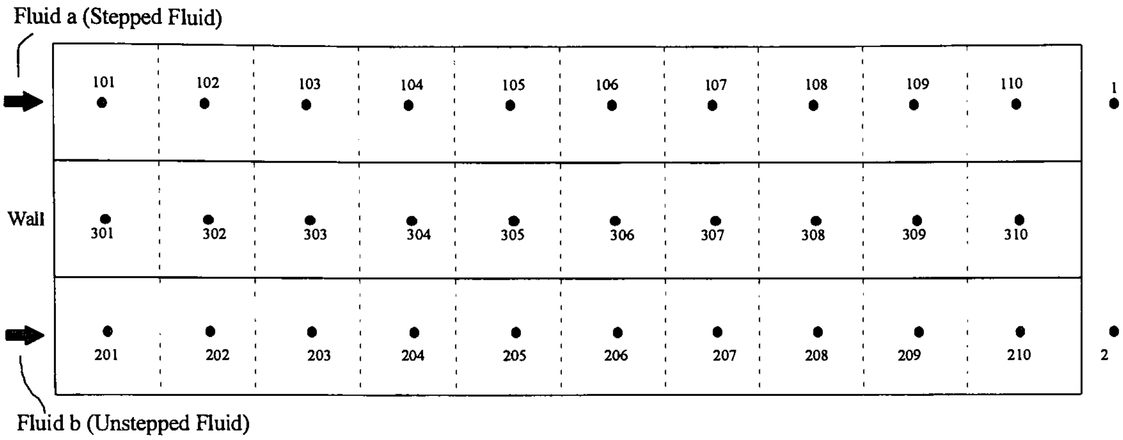

Nodes:

100 - Fluid a nodes
200 - Fluid b nodes
300 - Wall nodes

Figure 4.2: Direct Transfer Parallel-Flow Heat Exchanger Thermal Network Model No Wall Thermal Resistance (10 Segment Model)

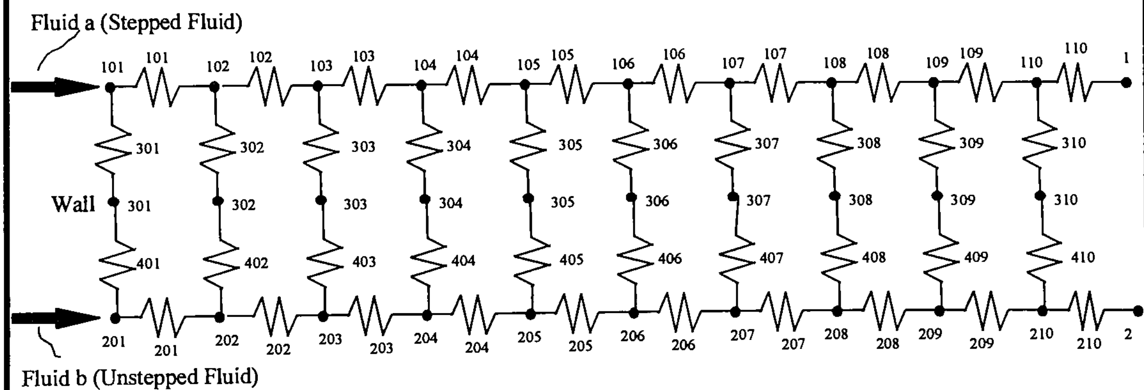

Resistors:

100 - Fluid a Flow Capacitance 1/mCp
200 - Fluid b Flow Capacitance 1/mCp
300 - Fluid a Convective Resistance 1/hA
400 - Fluid b Convective Resistance 1/hA

Figure 4.3: Direct Transfer Parallel-Flow Heat Exchanger Cross Section (20 Segment Model Schematic Diagram)

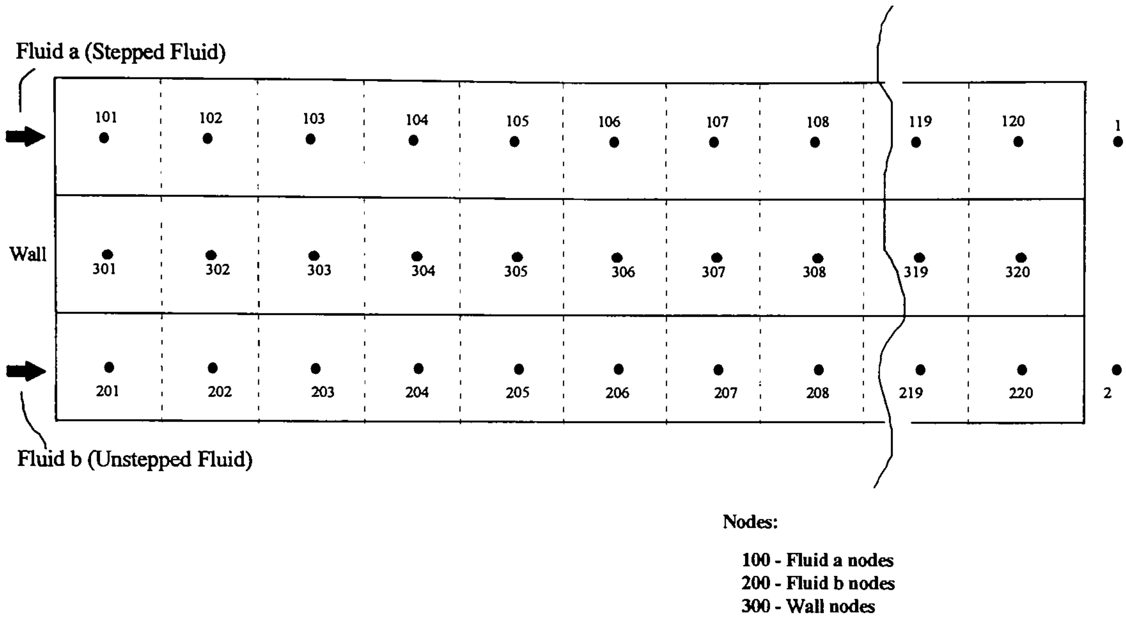

Figure 4.4: Direct Transfer Parallel-Flow Heat Exchanger Cross Section Thermal Network Model No Wall Thermal Resistance (20 Segment Thermal Network Model)

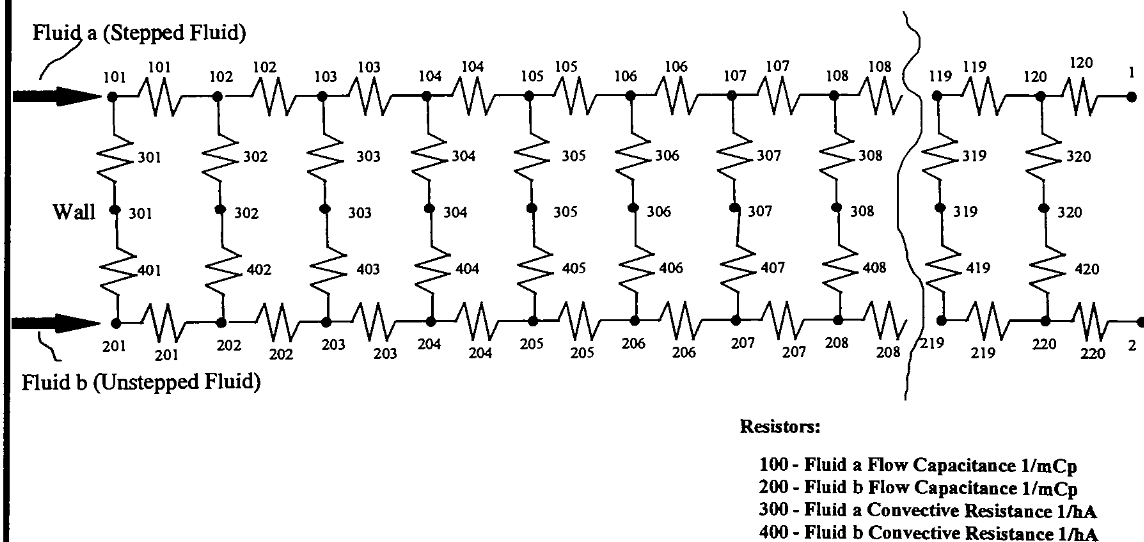

Heat transfer resistances are added to the simplified models. Fluid nodes are separated by fluid flow resistors (1/[mass flow rate times specific heat]), and convective resistance between the fluid node and wall node. Fluid flow resistors emerge from an energy balance as shown in figure 4.5 and the derivation below:

Figure 4.5: Control Volume for Fluid Flow Resistance Derivation

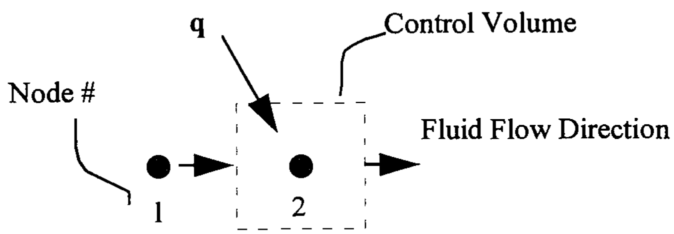

$$\dot{E}_{in} - \dot{E}_{out} + \dot{E}_{generated} = \dot{E}_{stored} \tag{4.1}$$

where $\dot{E}_{generated} = 0$

$$=> \quad q^{n+1} + \dot{m}c_p(T_1^{n+1} - T_2^{n+1}) = m_{cv}c_p \frac{(T_2^{n+1} - T_2^{n})}{\Delta\tau} \tag{4.2}$$

where $\dot{m}c_p(T_1^{n+1} - T_2^{n+1})$ is represented as

$$\frac{(T_1^{n+1} - T_2^{n+1})}{R} \tag{4.3}$$

$$\text{where } R = \frac{1}{\dot{m}c_p} \equiv \text{Fluid Flow capacitance (Kelvin/Watt)} \tag{4.4}$$

$$=> \quad q^{n+1} + \frac{(T_1^{n+1} - T_2^{n+1})}{R} = m_{cv}c_p \frac{(T_2^{n+1} - T_2^{n})}{\Delta\tau} \tag{4.5}$$

The stepped fluid is represented by nodes numbered in the one hundreds, the unstepped fluid by nodes numbered in the two hundreds, and the wall by nodes numbered in the three hundreds. The outlet temperature node for the stepped fluid is numbered one, and the unstepped fluid is numbered 2. This allows for quick recognition during modeling, and also for ease of expansion to larger segment models. A 10 segment model indicates the heat exchanger has been divided into 10 specific regions in the direction of fluid flow. The 20 segment model indicates a division into 20 regions. Increased segment models typically lead to more accurate outlet temperature calculations coupled with increased computer run time. Thermal wall resistance perpendicular to the fluid flow direction was excluded from this model because of the style heat exchangers being analyzed. The separating wall between the two fluids is extremely thin. Therefore wall thermal resistance perpendicular to the flow direction is considered negligible. Thermal resistance in the separating wall in the flow direction is considered infinite because the separating wall is extremely thin. The relative heat conduction in the flow direction is negligible relative to the heat transfer perpendicular to the flow direction. The optimal time step and number of segments required for maintaining accuracy and minimize computer run time was determined by Bunce (1995). These values limited the error to less than 1 percent. For $NTU \leq 2$, a 10 segment model was required. For $2 < NTU \leq 10$, a 20 segment model was sufficient. A timestep input required for Thermonet of half the dwell time of the fastest flowing fluid was determined sufficient for all cases by Bunce (1995).

This technique models the parallel-flow heat exchanger utilizing nodes and resistors which are solved by Thermonet a thermal network solver. Thermonet can solve steady-state and transient heat transfer problems. The heat transfer system is represented as a thermal network using the following electrical analogy:

Heat flow rate, Q	=>	Current, I
Temperature difference, ΔT	=>	Voltage, V and
Thermal resistance, R	=>	Electrical resistance, R.

A backward-difference scheme is employed to provide an unconditionally stable solver for steady-state and transient problems. The term unconditionally stable means the solution remains stable for all space and time intervals. Thermonet can handle variable thermal conductivity, variable convection heat transfer coefficients, radiation and fluid streams. It has an easy-to-use interactive windows front end. The basic equations employed are described in Incropera and De Witt (pages 221 - 222).

Individual fluid temperature effectiveness values ε_1^*, and ε_2^* were generated utilizing dimensionless parameters set-up in a spreadsheet to generate resistor and node values to be used by Thermonet. Thermonet utilizes the resistor data and initial fluid inlet temperatures to calculate the initial steady-state temperature distribution of the heat exchanger. This steady-state data is then transferred to the spreadsheet for use in the node data table. The node data table contains node volume and initial steady state temperature information for each node in the model. The node table is transferred to Thermonet. Thermonet utilizes both the resistor and node table data to calculate the transient outlet temperature response of both fluids to a step input change for the C_{min} fluid. The transient outlet temperature response was transferred to the spreadsheet and ε_1^*, and ε_2^* were calculated for appropriate t^* values. Values of t^* were selected to include the full ε^* range from 0 to 1 for the wide range of input dimensionless parameters.

4.2 CROSS-FLOW HEAT EXCHANGERS

A simplified 4 x 4 segment single pass direct-transfer cross-flow heat exchanger is shown in Figure 4.6.

Figure 4.6: Direct Transfer Cross-Flow Heat Exchanger Both Fluids Unmixed (4 x 4 Segment Model)

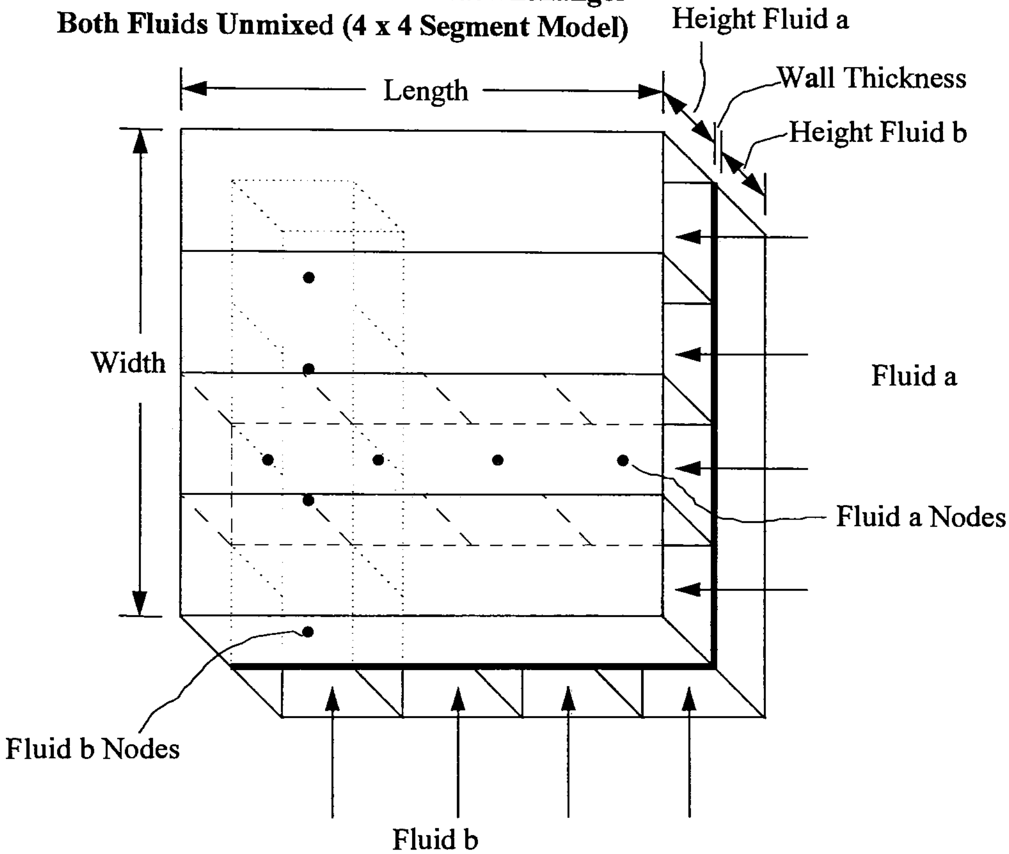

The two fluids are unmixed, separated by a wall, and flow perpendicular to each other. Each node represents a specific volume of fluid or wall region. Equivalent thermal network node-resistor models are shown for a 3 x 3, 6 x 6, and 10 x 10 segment models in figures 4.7, 4.8 and 4.9, respectively.

Figure 4.7: Direct Transfer Cross-Flow Heat Exchanger Thermal Network Model Single Pass/Both Fluids Unmixed (3 x 3 Segment Model)

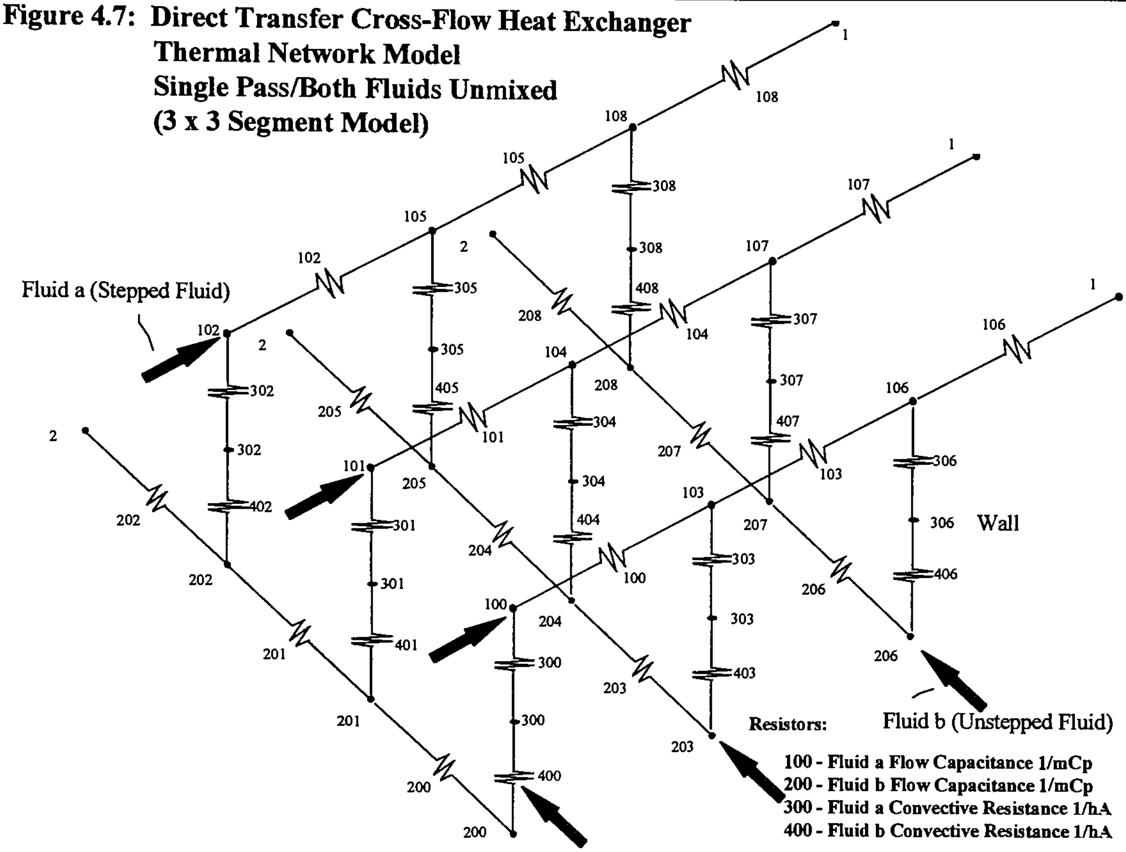

Figure 4.8: Direct Transfer Cross-Flow Heat Exchanger Thermal Network Model Single Pass/Both Fluids Unmixed (6 x 6 Segment Model)

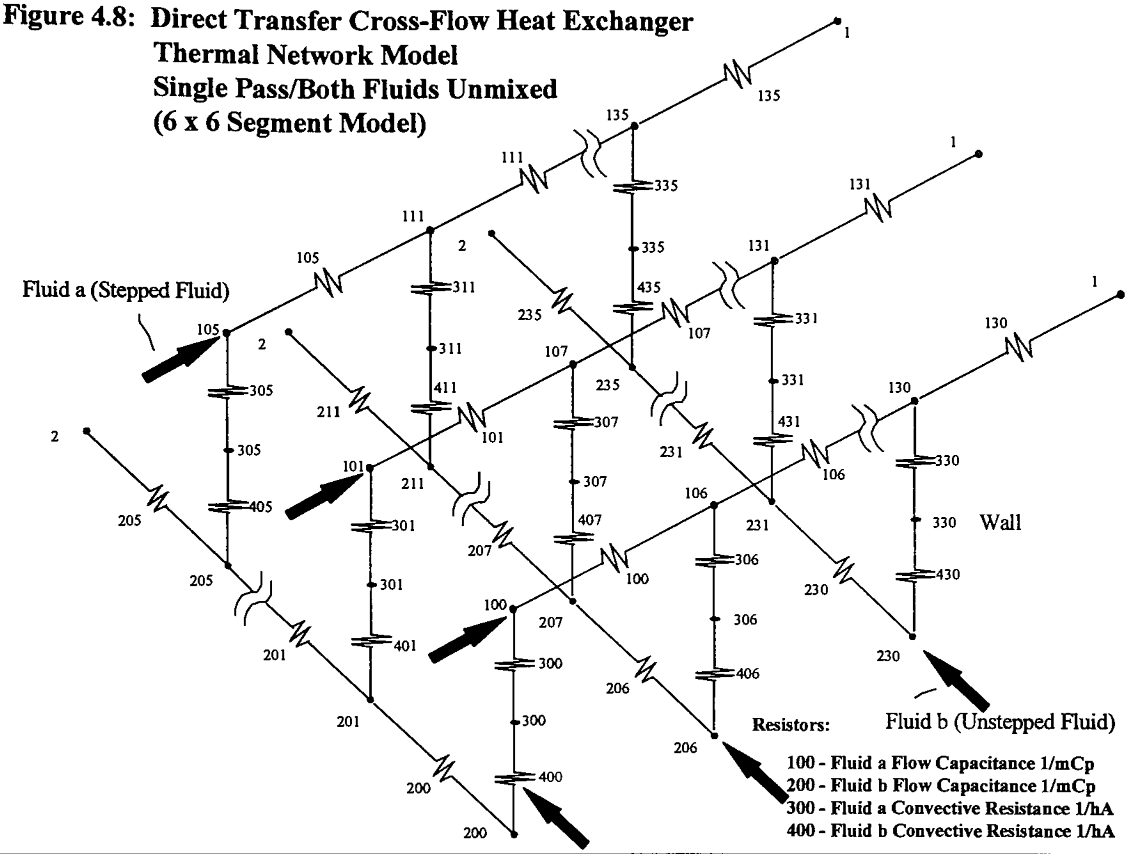

Figure 4.9: Direct Transfer Cross-Flow Heat Exchanger Thermal Network Model Single Pass/Both Fluids Unmixed (10 x 10 Segment Model)

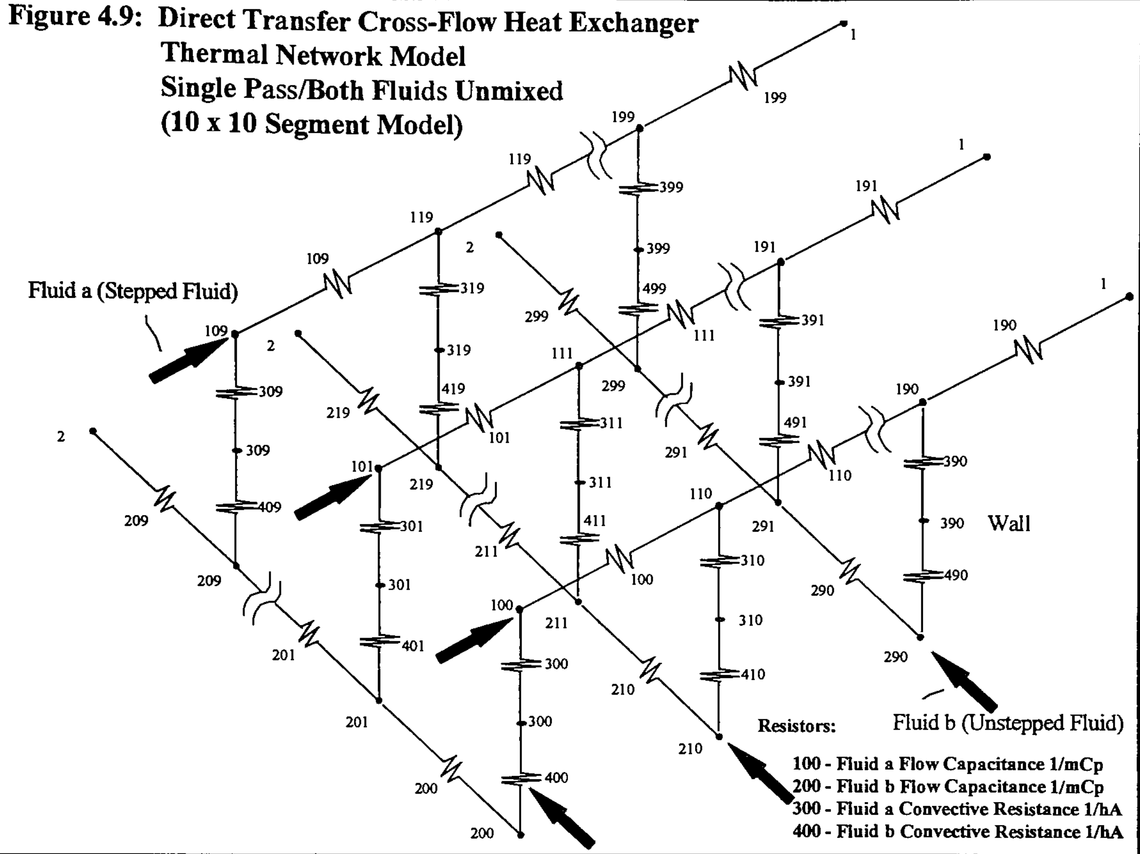

These equivalent thermal-network models are generated from equivalent simplified three dimensional models similar to the one shown in figure 4.6. Fluid nodes are separated by fluid flow resistors (1/[mass flow rate times specific heat]), and convective resistance between the fluid node and wall node. Each individual fluid stream node is connected only in it's flow direction. This makes each fluid unmixed. For a 3 x 3 segment model, it requires 9 nodes for fluid a, 9 nodes for fluid b, 9 nodes for the wall (neglecting wall resistance), and 6 nodes for the outlet temperatures of fluids a and b. This gives a total of 33 nodes required for a 3 x 3 segment model. A 3 segment parallel-flow model requires only 11 nodes. A 6 x 6 segment model requires 120 nodes versus 20 for a 6 segment parallel-flow model. A 10 x 10 segment model requires 320 nodes versus 32 for a 10 segment parallel-flow model. The current Thermonet software package utilized for this analysis is limited to 1000 node models which restricts the total number of segments to 17 x 17 requiring 901 nodes. Thermal wall resistance was excluded from this model.

The optimal number of segments required for maintaining accuracy and minimizing computer run time was determined by comparing steady state Thermonet runs to actual theoretical outlet temperature values calculated by the effectiveness-NTU method. Comparison was performed for the dimensionless parameter range listed in table 4.1:

Table 4.1: Dimensionless Values Utilized for Optimal Comparison for Cross-Flow Heat Exchangers

C_w^*	NTU	C^*	R^*	td^*
10	0.5 - 2.0	0.2 - 1.0	0.5 - 2.0	1.0

Table 4.2 shows the percent deviation from actual for the range of parameters listed above and also the total run time for each case.

Table 4.2: Optimal Number of Segment Analysis for Cross-Flow Heat Exchangers Both Fluids Unmixed/Single Pass

Cw*	NTU	C*	R*	td*	Eff.	Inlet	Outlet Temperatures (Degrees C)				Deviation from Theoretical (%)			Run Time		
						Temperature		Thermonet						Thermonet (Seconds)		
						(Degrees C)	3x3-Segment	6x6 Segment	10x10 Segment	E-NTU	3x3-Segment	6x6 Segment	10x10 Segment	3x3-Segment	6x6 Segment	10x10 Segment
10	0.50	0.2	0.5	1.00	0.376	100	69.9713	69.7756	69.7315	69.9013	0.1002	0.1795	0.2429	5	40	140
						20	26.0057	26.0446	26.0537	26.0197	0.0536	0.0965	0.1305			
			1	1.00			69.6773	69.7517	69.7233		0.0343	0.2140	0.2546	7	40	150
							26.0245	26.0497	26.0553		0.0164	0.1149	0.1367			
			2	1.00			69.6773	69.7369	69.7161		0.0343	0.2323	0.2621	6	36	155
							26.0245	26.0522	26.0564		0.0164	0.1246	0.1406			
		0.6	0.5	1.00	0.344	100	72.1969	71.9662	71.9379	72.4593	0.3621	0.6501	0.7196	5	27	110
						20	36.6616	36.6071	36.6372	36.5244	0.4309	0.7739	0.8564			
			1	1.00			72.1297	71.9706	71.9319		0.4549	0.6744	0.7276	6	39	125
							36.7222	36.6176	36.6406		0.5414	0.8026	0.8663			
			2	1.00			72.1165	71.9673	71.9303		0.4703	0.6790	0.7301	4	25	100
							36.7269	36.6196	36.6416		0.5599	0.8062	0.9690			
		1.00	0.5	1	0.315	100	74.2440	74.0031	73.9416	74.7641	0.6956	1.0176	1.0996	6	31	110
						20	45.7560	45.9969	46.0562	45.2359	1.1496	1.6623	1.8177			
			1.00	1.00			74.2062	73.9932	73.9392		0.7434	1.0311	1.1032	5	15	90
							45.7916	46.0066	46.0606		1.2267	1.7041	1.8234			
			2.00	1.00			74.2440	74.0031	73.9416		0.6956	1.0179	1.0996	6	24	105
							45.7560	45.9969	46.0562		1.1496	1.6623	1.8177			
10	1.00	0.2	0.5	1.00	0.596	100	53.4916	52.6377	52.4220	52.3196	2.2396	0.6075	0.1952	11	60	370
						20	29.3017	29.4725	29.5156	29.5360	0.7935	0.2152	0.0692			
			1	1.00			53.1166	52.5261	52.3604		1.5267	0.3942	0.1156	12	60	260
							29.3763	29.4946	29.5239		0.5409	0.1397	0.0410			
			2	1.00			52.9269	52.4726	52.3602		1.1604	0.2920	0.0773	6	60	205
							29.4146	29.5055	29.5279		0.4111	0.1035	0.0274			
		0.6	0.5	1.00	0.529	100	56.6775	57.9276	57.6556	57.7146	2.0150	0.3694	0.1021	7	45	200
						20	44.6735	45.2433	45.4066	45.3713	1.5379	0.2620	0.0779			
			1	1.00			56.6463	57.6506	57.6246		1.6144	0.2356	0.1554	5	45	170
							44.6122	45.2696	45.4251		1.2322	0.1799	0.1196			
			2	1.00			56.6197	57.6462	57.6245		1.5663	0.2261	0.1560	6	45	160
							44.6262	45.2923	45.4253		1.1970	0.1741	0.1190			
		1.00	0.5	1	0.469	100	63.6919	62.5933	62.2415	62.5171	1.6793	0.1219	0.4406	7	45	195
						20	56.3061	57.4067	57.7565	57.4629	2.0436	0.1326	0.4793			
			1.00	1.00			63.5905	62.5521	62.2227		1.7169	0.0561	0.4709	5	25	90
							56.4095	57.4476	57.7773		1.6673	0.0610	0.5121			
			2.00	1.00			63.6913	62.6933	62.2415		1.6763	0.1219	0.4406	6	50	170
							96.3067	57.4067	57.7565		2.0426	0.1326	0.4793			
10	2.00	0.2	0.5	1.00	0.816	100	36.6616	36.4764	35.7563	34.7213	11.4067	5.0547	2.9610	14	170	600
						20	32.2636	32.7947	32.8467	33.0557	2.3963	1.0619	0.6263			
			1	1.00			36.0047	36.1994	35.6373		9.4566	4.2570	2.6363	9	130	525
							32.3990	32.7601	32.8725		1.9666	0.6943	0.5543			
			2	1.00			37.6356	36.0767	35.5907		6.3933	3.9006	2.5039	12	120	450
							32.4729	32.7649	32.8619		1.7633	0.6195	0.5260			
		0.6	0.5	1.00	0.713	100	49.3021	45.5645	Locked after	42.9574	14.7696	6.1157	-	15	120	Locked up
						20	50.4167	52.6493	32 minutes	54.2256	7.0203	2.9069	-			
			1	1.00			49.0737	45.6431	44.4152		14.2379	6.2519	3.3936	11	105	690
							50.5556	52.6142	53.3509		6.7676	2.9717	1.6131			
			2	1.00			49.0066	45.3604	44.4200		14.0623	5.5936	3.4046	14	125	2700
							50.5959	52.7636	53.3460		6.6936	2.6566	1.6163			
		1.00	0.5	1	0.816	100	56.2620	53.2926	Locked after	50.7674	10.6625	4.9745	-	32	90	Locked up
						20	63.7160	66.7072	40 minutes	69.2326	7.9653	3.6477	-			
			1.00	1.00			96.3646	53.2927	52.1696		11.0644	4.9741	2.6016	45	60	960
							63.6156	96.7073	67.6103		6.1134	3.6475	2.0544			
			2.00	1.00			96.2624	Locked after	Locked after		10.6631	-	-	36	Locked up	Locked up
							63.7176	10 minutes	40 minutes		7.9666	-	-			

Computer run time increased anywhere from 2 to 14 times the total time for the 3 x 3 versus the 6 x 6 segment model. The 10 x 10 segment model took from 3 to 22 times longer compared to the 6 x 6 model. Total computer run time was longer as NTU increased for each segment model.

For NTU = 0.5, percent deviation from theoretical is less than 2 % for the 3 x 3, 6 x 6, and 10 x 10 segment models shown in Figure 4.10.

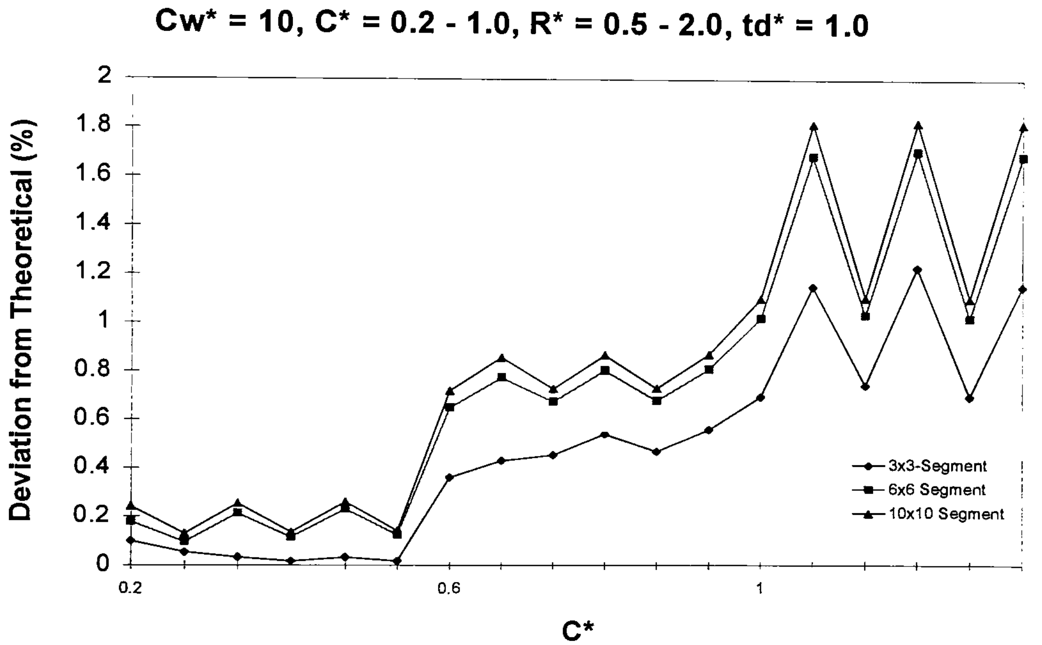

Figure 4.10: Optimal Number of Segments for NTU = 0.5

For NTU = 1.0, percent deviation from theoretical is less than 1 % for the 6 x 6, and 10 x 10 segment models, and less than 2.2% for the 3 x 3 segment model shown in figure 4.11.

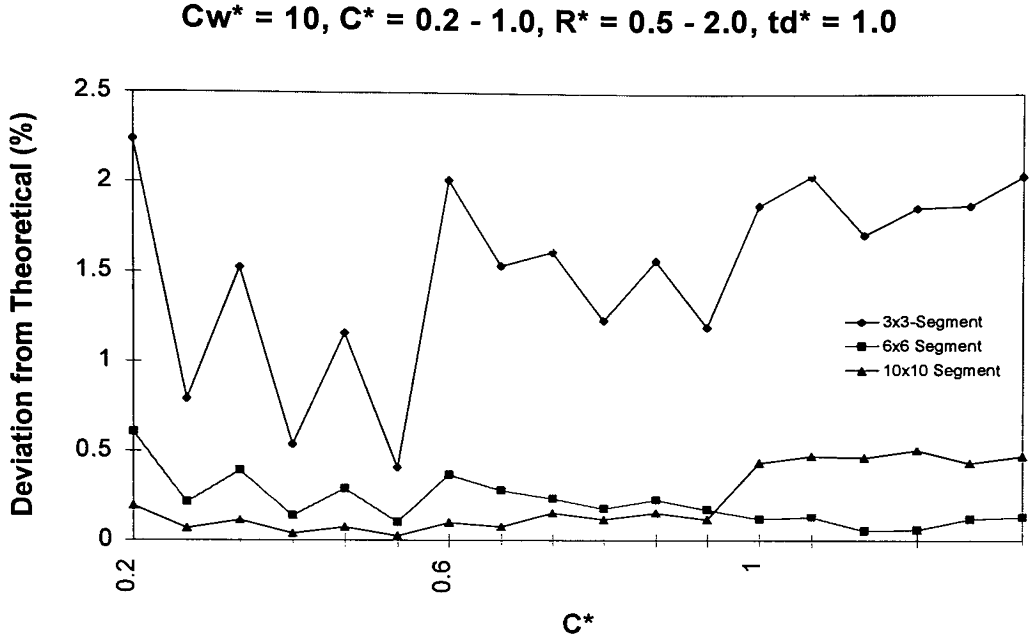

Figure 4.11: Optimal Number of Segments for NTU = 1.0

For NTU = 2.0, percent deviation from theoretical is less than 3.4 % for the 10 x 10 segment model, less than 6.3 % for the 6 x 6 segment model, and less than 14.8% for the 3 x 3 segment model as shown in figure 4.12.

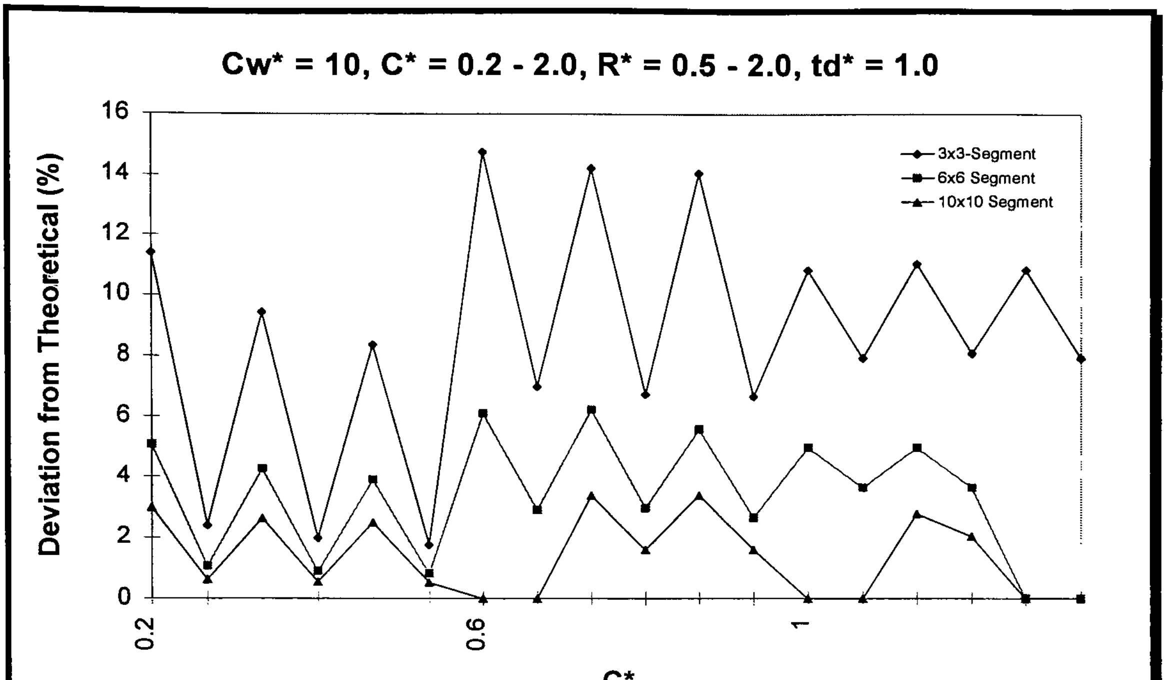

Figure 4.12: Optimal Number of Segments for NTU = 2.0

Therefore, the 6 x 6 segment model is recommended for NTU $\leq$ 1.0 to achieve accuracy within 1% and minimize computer run time. For NTU $\leq$ 2.0 the 10 x 10 segment model is recommended to achieve accuracy within 3.4%. Following previous recommendations from Bunce (1995) regarding the timestep, a timestep of half the dwell time of the fastest flowing fluid was determined sufficient for all cases.

This technique models the cross-flow heat exchanger utilizing nodes and resistors which are solved by Thermonet. The same method described for parallel-flow heat exchangers is applied to cross-flow heat exchangers. Individual fluid temperature effectiveness values ε_1^*, and ε_2^* were generated utilizing dimensionless parameters for NTU = 1.0 utilizing the 6 x 6 segment model.

5
Validation of Thermal Network Solver Accuracy

Thermonet results for transient performance of parallel-flow and cross-flow heat exchangers were each validated against three separate papers found in the literature review. Each paper solved for the transient solutions utilizing analytical techniques. Thermonet transient results were compared to literature results by calculating the percent mean difference given by equation 5.1.

$$\% \text{ Mean Difference} = \frac{\text{Average difference between solutions over the time domain}}{\text{Total change in fluid outlet temperature from time } t=0 \text{ to } t=\infty} \times 100 \qquad (5.1)$$

5.1 PARALLEL-FLOW

Thermonet results for transient performance of parallel-flow heat exchangers were validated for three separate cases as shown in Table 5.1.

Table 5.1: Transient Performance Validation for Parallel-Flow Heat Exchangers

Author	Application	Solution Method	Comparison Figure #	Stepped Fluid % Mean Difference	Unstepped Fluid % Mean Difference
Romie (1985)	Parallel-Flow $C^* = 1.0$	Analytical	5.1	0.23	0.65
Romie (1985)	Parallel-Flow $C^* = 0.8$	Analytical	5.2	0.48	0.50
Myers et al. (1967)	$C^* = 0$ Step change in C_{min} Fluid	Analytical	5.3 - 5.4	3.80 1.84	
Rizika (1956)	$C^* = 0$ $0 \leq t^* \leq 1$ Step change in C_{max} Fluid	Analytical	5.5 - 5.6	1.74 0.81	

C^* = 0 cases by Myers (1967), and Rizika (1956) were validated by Bunce (1995). Myers (1967) and Rizika (1956) modeled the Cmax = ∞ fluid as having a dwell time of zero. Bunce (1995) modeled the Cmax = ∞ fluid in Thermonet as having a constant temperature, no flow. Therefore, the Thermonet validations for C^* = 0 are flow direction independent for the Cmin fluid relative to the C_{max} fluid. This makes those validations applicable to both parallel-flow and counter-flow heat exchangers.

Percent mean difference between Thermonet solutions versus each case ranged from 0.23 0.65% (Romie, 1985), 1.84 - 3.18 % (Myers et al., 1967), and 0.81 1.74 % (Rizika, 1956). Comparison to Romie (1985) and Myers et al. (1967) may vary more than actual from Thermonet due to readability error of the graphical representation given in each paper. Bunce (1995) calculated directly from Rizika's (1956) analytical expression in the Rizika (1956) comparison. Figures 9-12 compare the transient performance given by Thermonet versus each analytical solution. Each case modeled was for different, specific C^*, NTU, R^*, and $\overline{C}_w^*$ values.

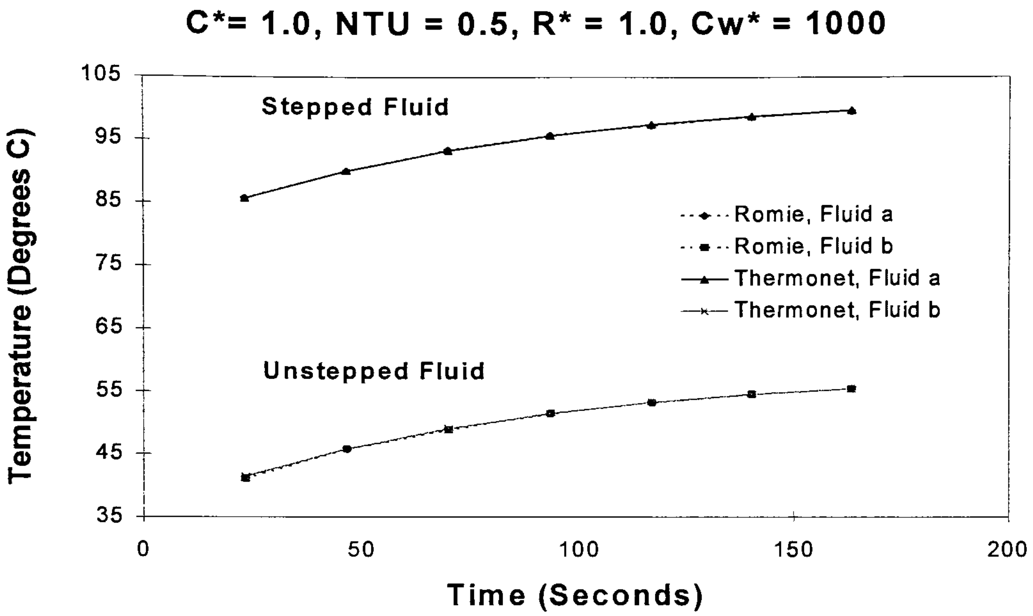

Figure 5.1: Thermonet Versus Romie (1985) Validation

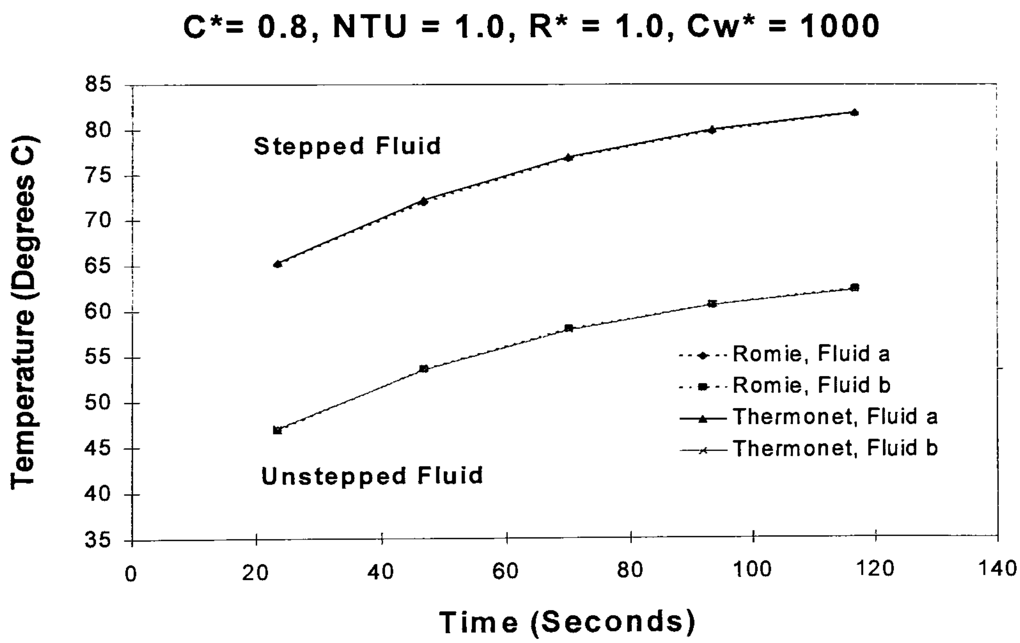

Figure 5.2: Thermonet Versus Romie (1985) Validation

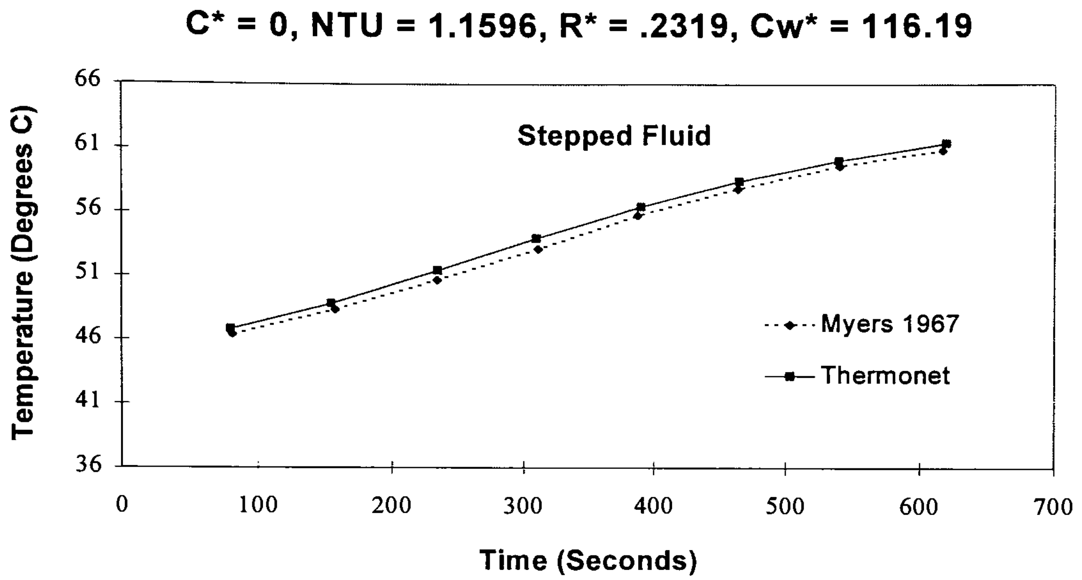

Figure 5.3: Bunce (1995) Comparison of Thermonet solution to solution by Myers et al. (1967)

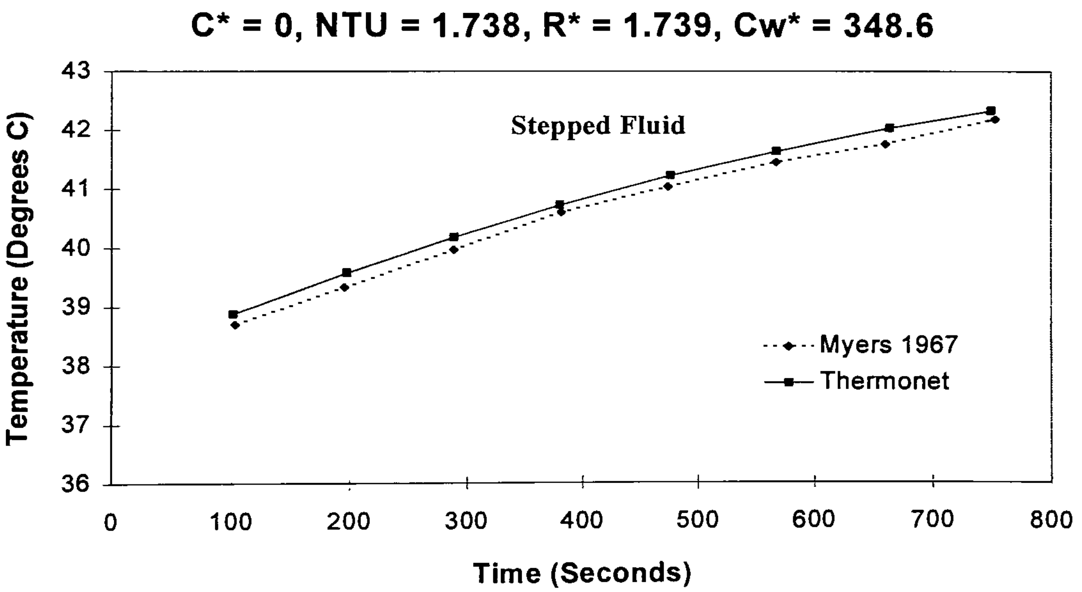

Figure 5.4: Bunce (1995) Comparison of Thermonet solution to solution by Myers et al. (1967)

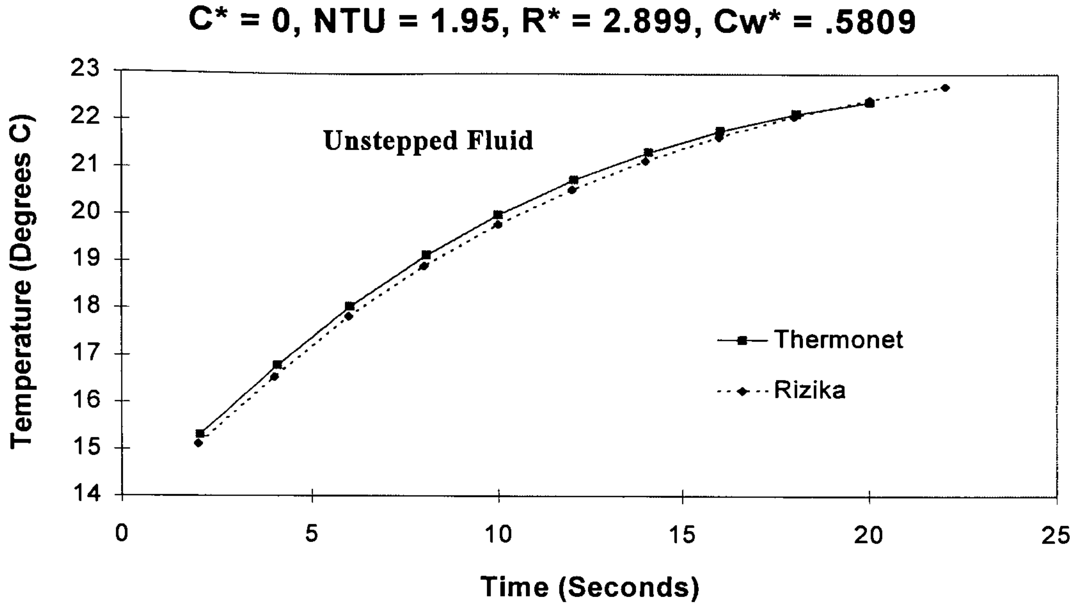

Figure 5.5: Bunce (1995) Comparison of Thermonet solution to solution by Rizika (1956)

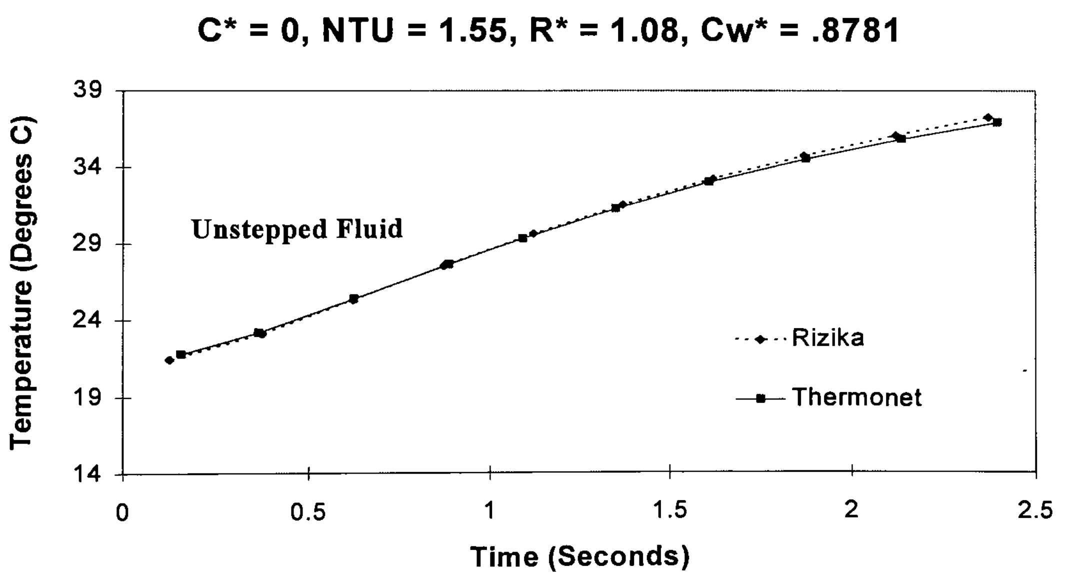

Figure 5.6: Bunce (1995) Comparison of Thermonet solution to solution by Rizika (1956)

5.2 CROSS-FLOW

Thermonet results for transient performance of cross-flow heat exchangers were validated against three analytical solutions as shown in Table 5.2.

Table 5.2: Transient Performance Validation for Cross-Flow Heat Exchangers

Author	**Application**	**Solution Method**	**Comparison Figure #**	**Stepped Fluid % Mean Difference**	**Unstepped Fluid % Mean Difference**
Chen, Chen (1992)	Cross-Flow Both fluids gases Both fluids unmixed	Analytical	5.7 5.8	4.06	2.31
Spiga, Spiga (1987)	Cross-Flow Both fluids gases Both fluids unmixed	Analytical	5.9 5.10	3.37	1.73
			5.11 5.12	1.64	3.57
			5.13 5.14	15.97	16.88
Romie (1983)	Cross-Flow Both fluids gases Both fluids unmixed NTU: 1 - 8 E: .6 - 1.67 R: .5 - 2.0	Analytical	5.15 5.16	1.69	2.37
			5.17 5.18	4.58	4.91
			5.19 5.20	2.95	0.38
			5.21	0.73	--
			5.22	7.40	--
			5.23	5.40	--
			5.24	0.96	--
			5.25	7.95	--
			5.26	4.42	--

The 6 x 6 segment thermal network model was utilized for all comparisons shown in Table 5.2. This was chosen based on the accuracy and computer run time considerations for NTU = 1.0 cases. Cross-flow heat exchanger validations ranged from 2.31 - 4.06 % (Chen, Chen/1992), 1.64 - 3.57 % (Spiga, Spiga/1987), and 0.73 7.95 % (Romie/1983) for NTU $\leq$ 1.0. For NTU = 2.0, Spiga, Spiga (1987) versus Thermonet showed a % mean difference range from 15.97 to 16.88 %.

Figures 5.7 - 5.26 compare the transient performance given by Thermonet versus each analytical solution.

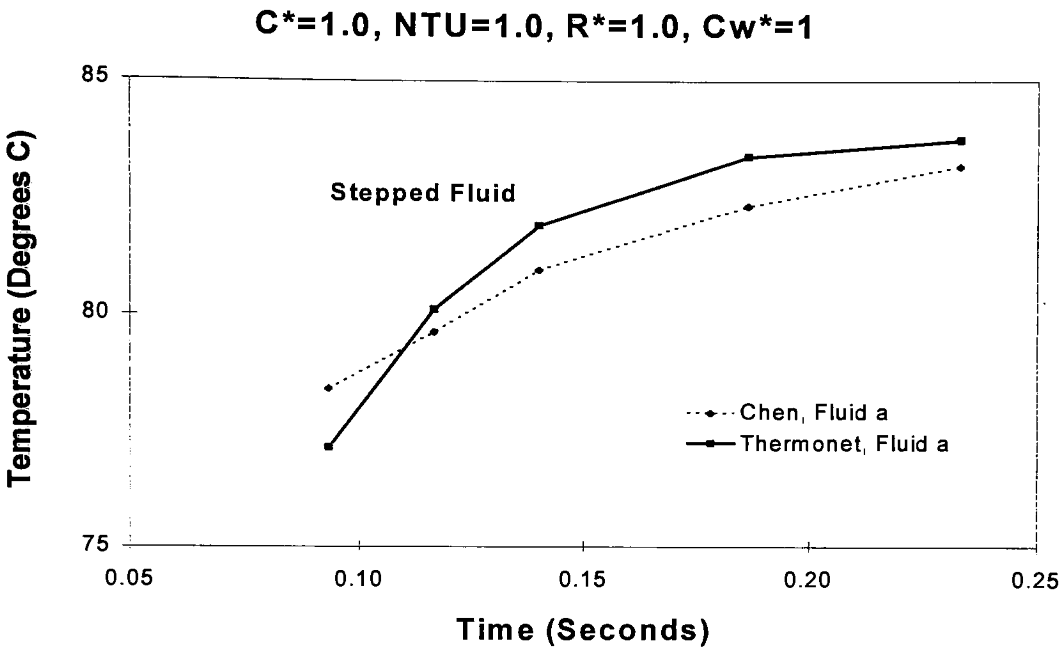

Figure 5.7: Thermonet Versus Chen (1992) Validation

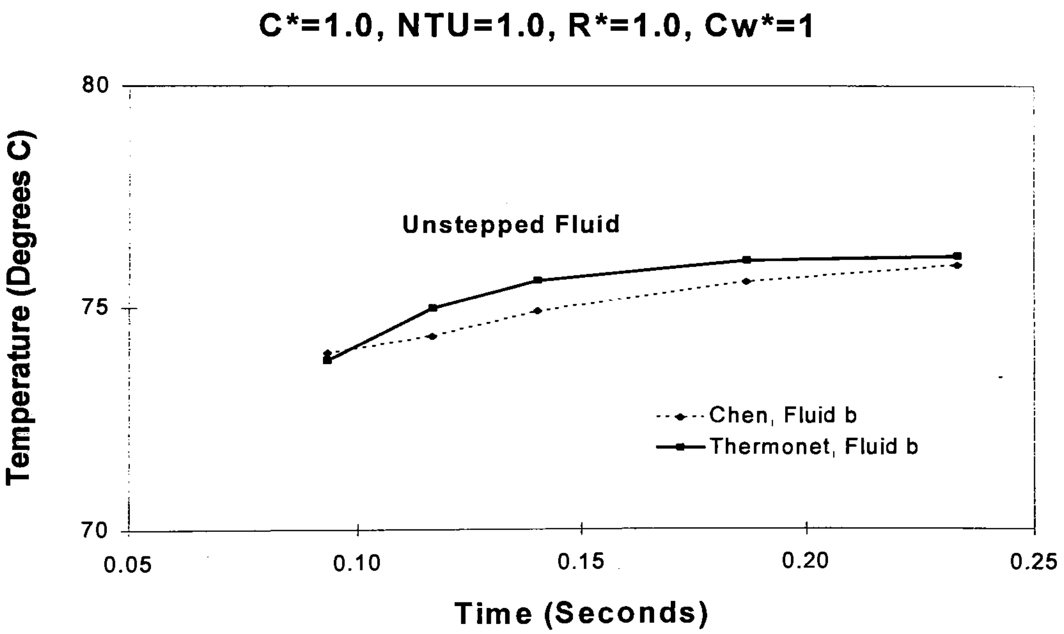

Figure 5.8: Thermonet Versus Chen (1992) Validation

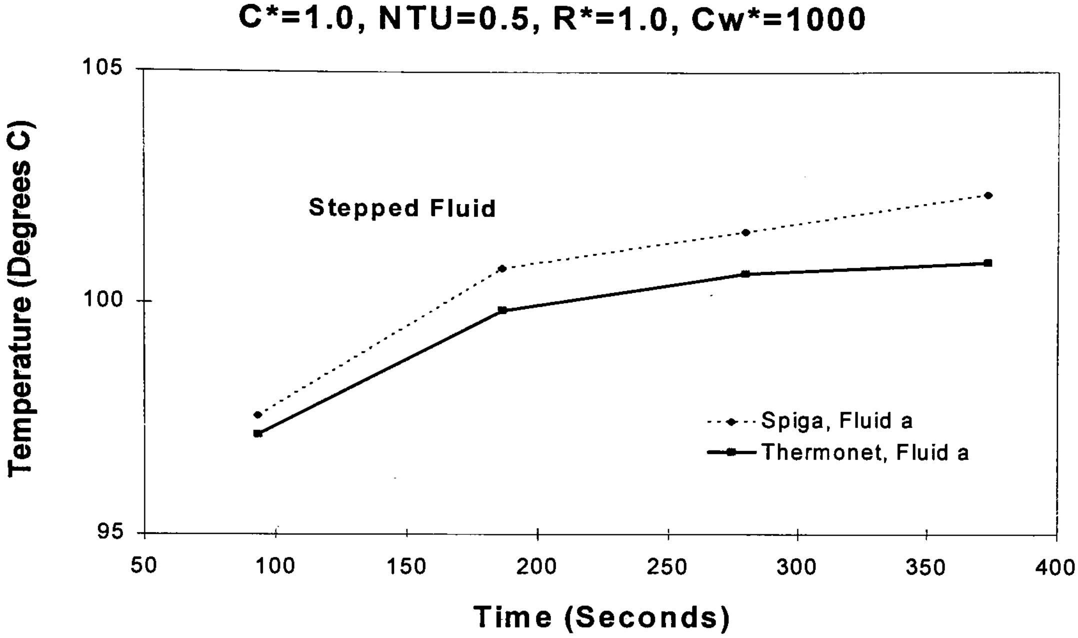

Figure 5.9: Thermonet Versus Spiga (1987) Validation

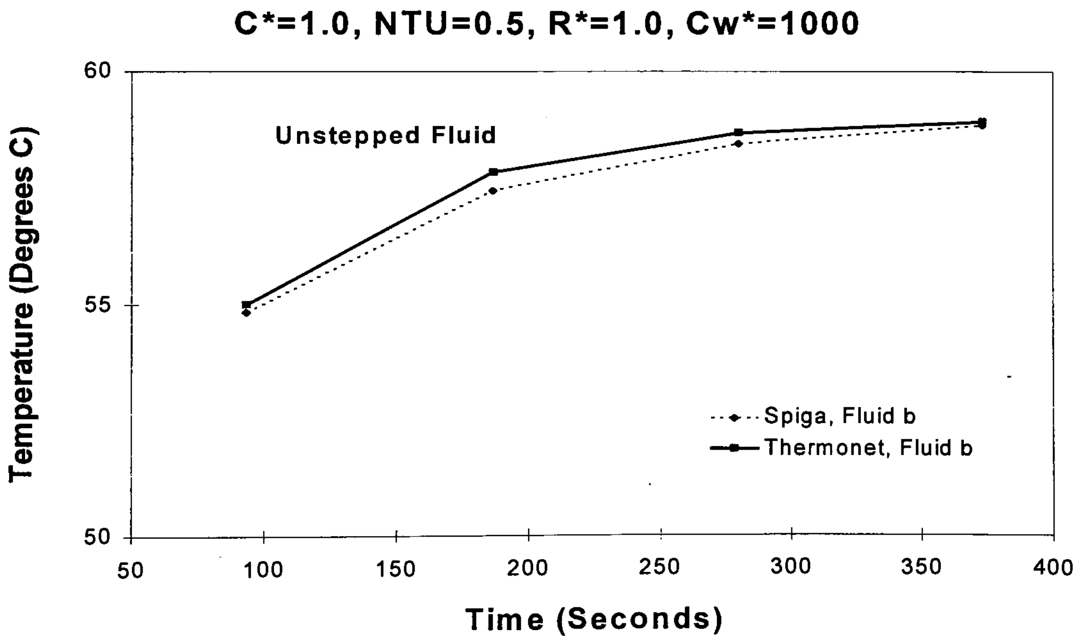

Figure 5.10: Thermonet Versus Spiga (1987) Validation

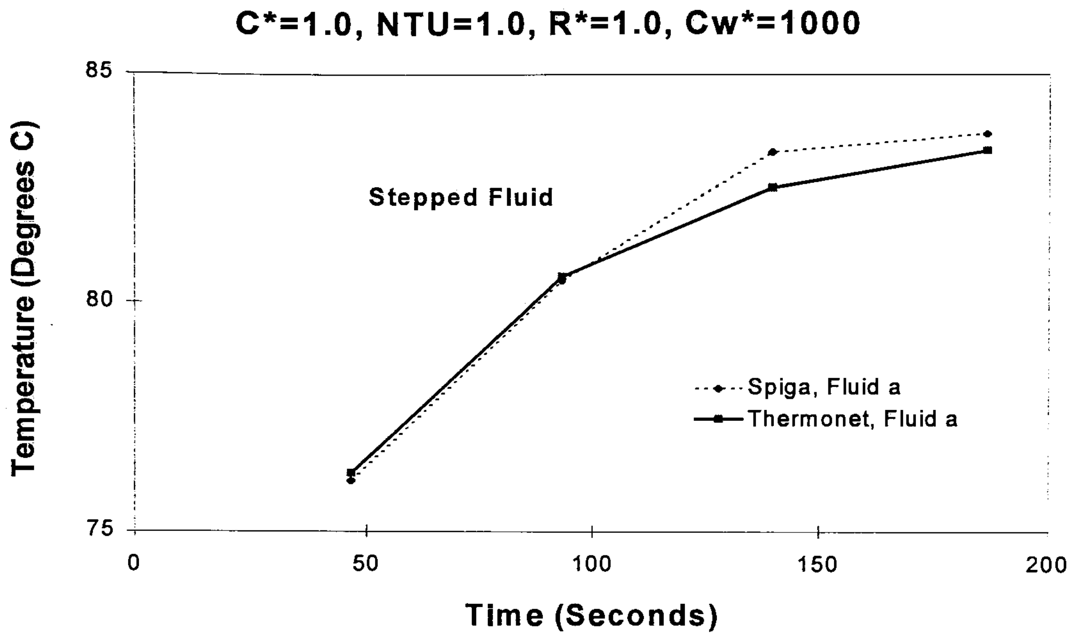

Figure 5.11: Thermonet Versus Spiga (1987) Validation

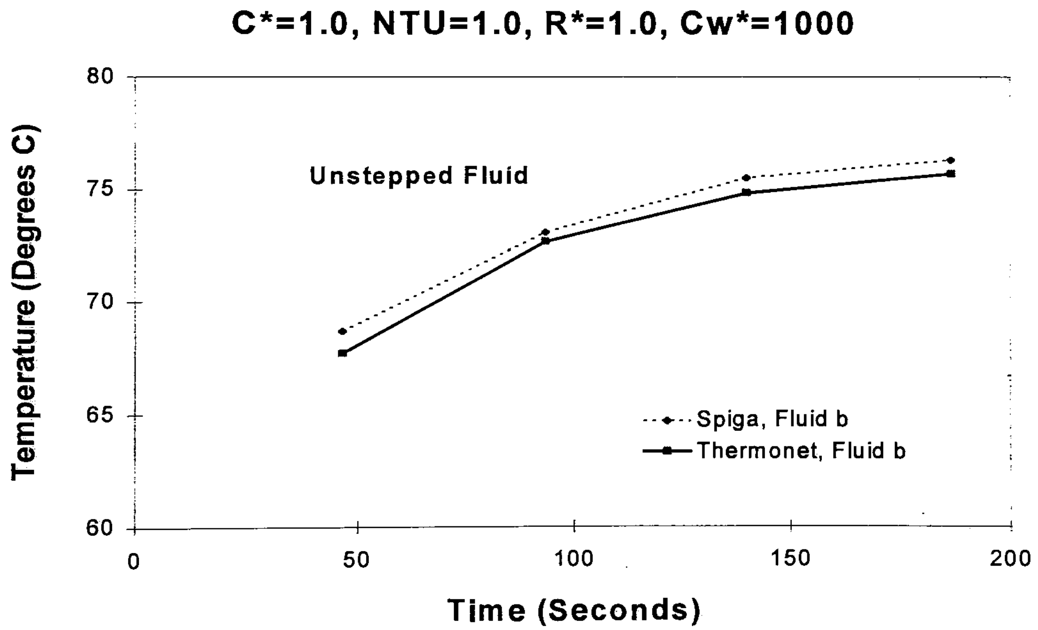

Figure 5.12: Thermonet Versus Spiga (1987) Validation

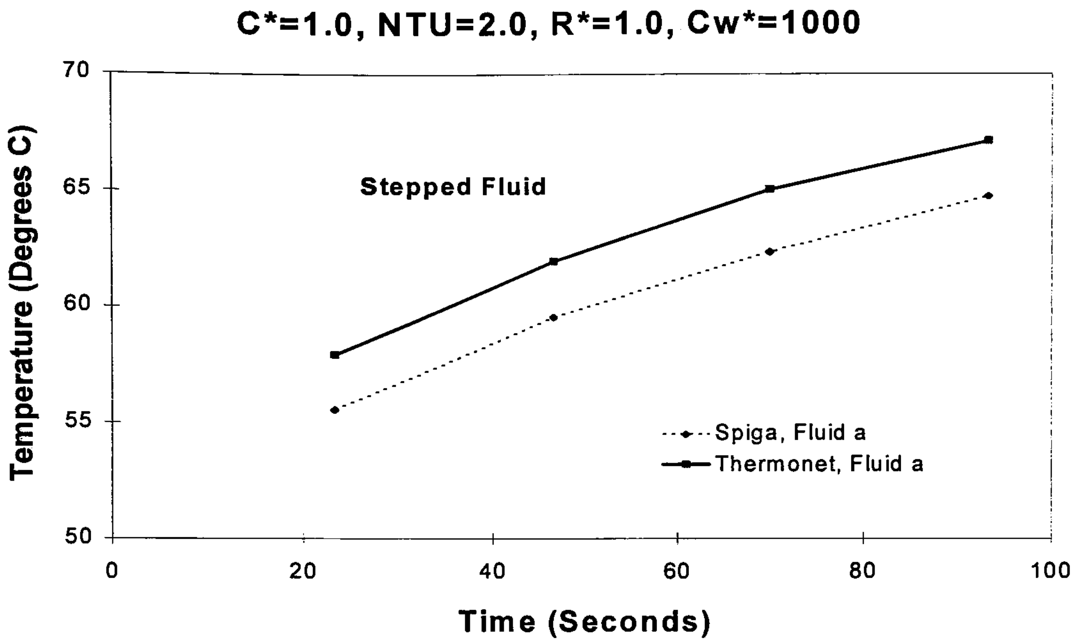

Figure 5.13: Thermonet Versus Spiga (1987) Validation

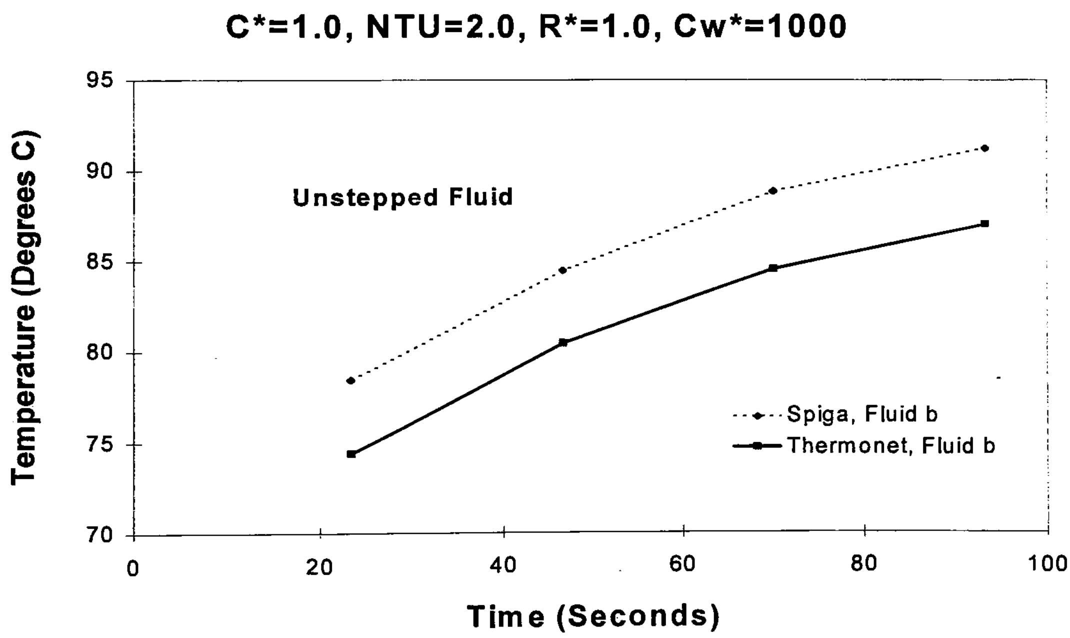

Figure 5.14: Thermonet Versus Spiga (1987) Validation

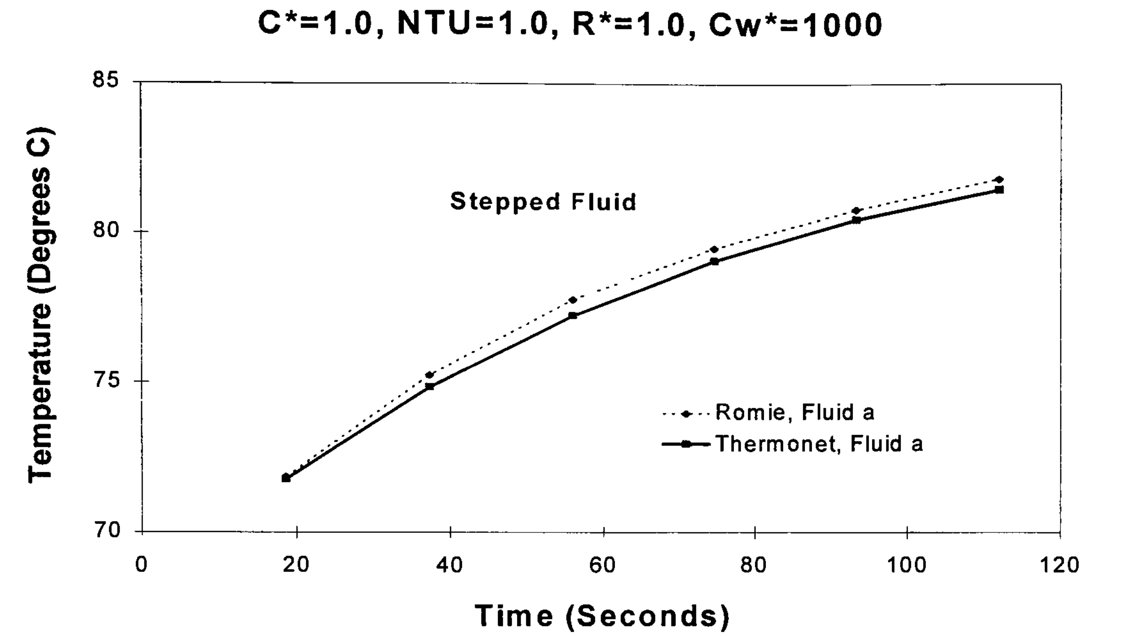

Figure 5.15: Thermonet Versus Romie (1983) Validation

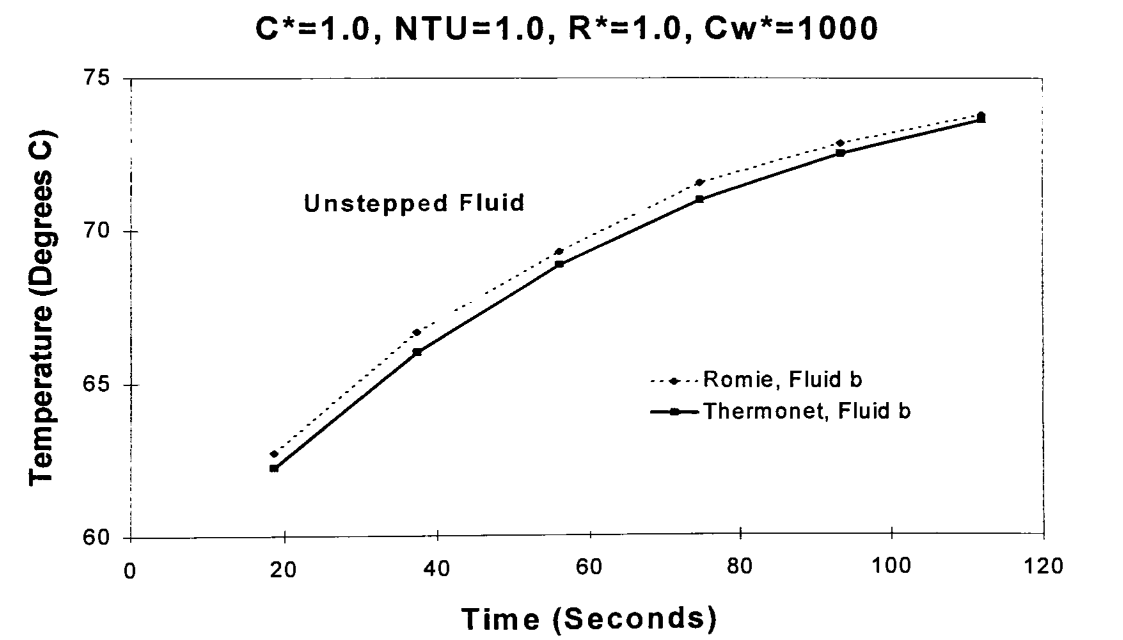

Figure 5.16: Thermonet Versus Romie (1983) Validation

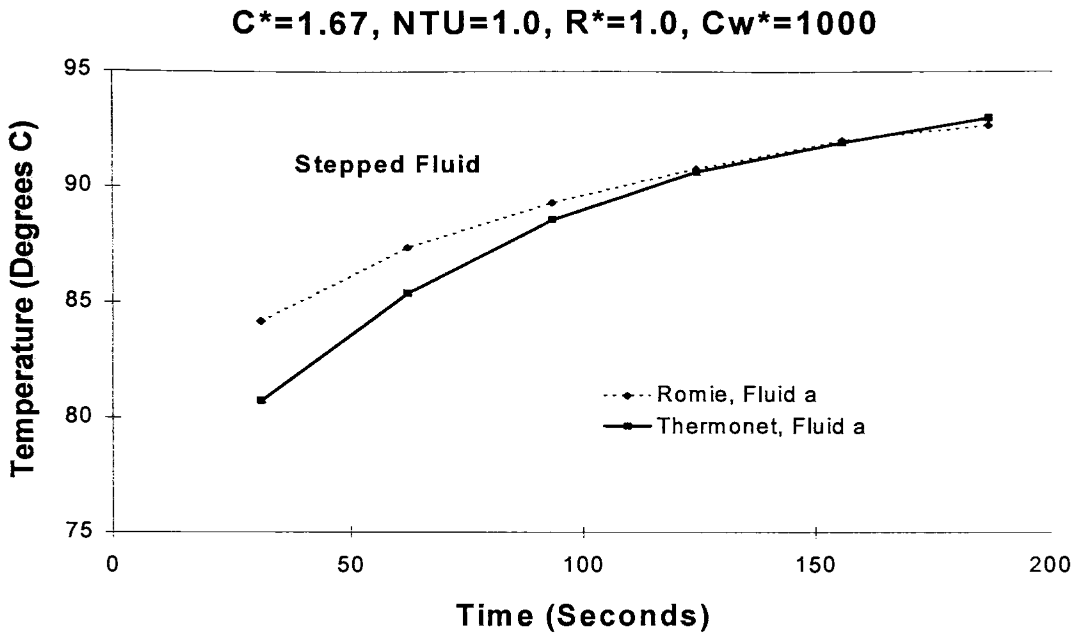

Figure 5.17: Thermonet Versus Romie (1983) Validation

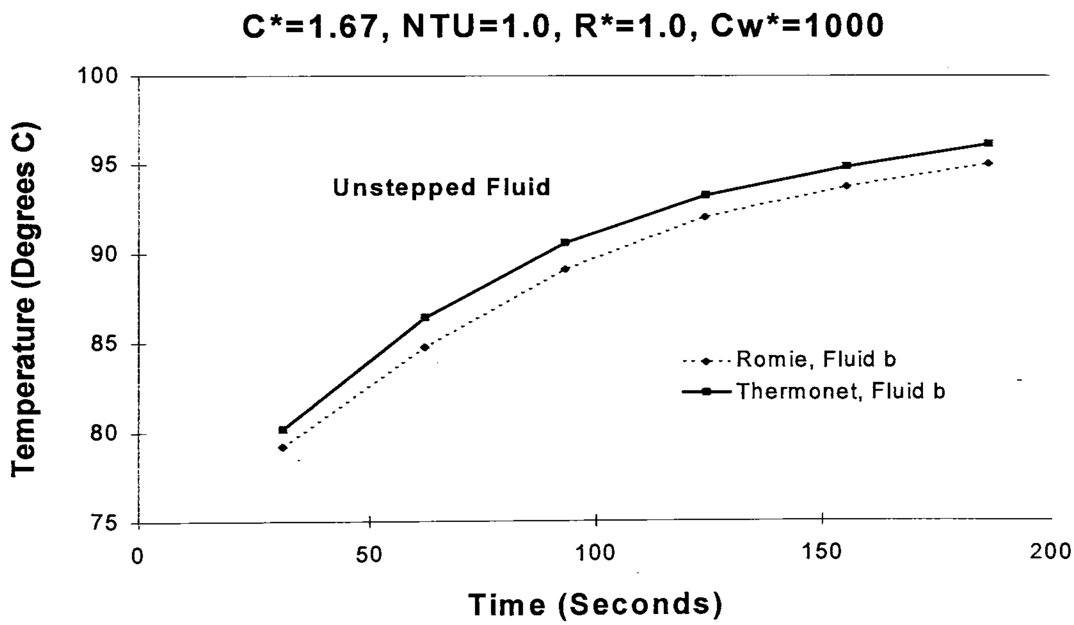

Figure 5.18: Thermonet Versus Romie (1983) Validation

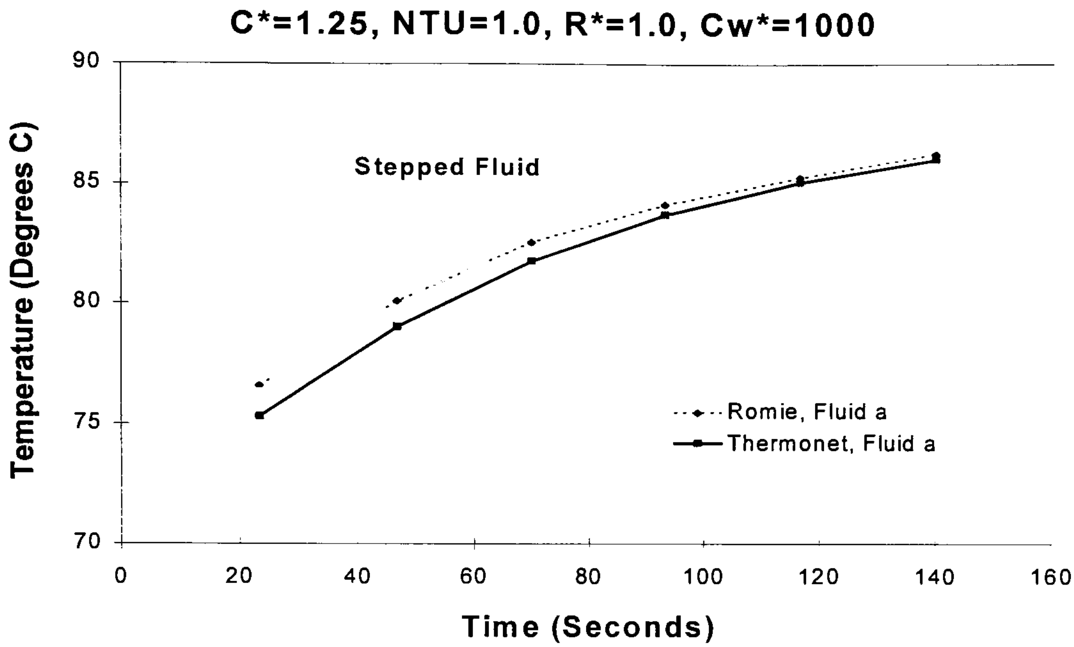

Figure 5.19: Thermonet Versus Romie (1983) Validation

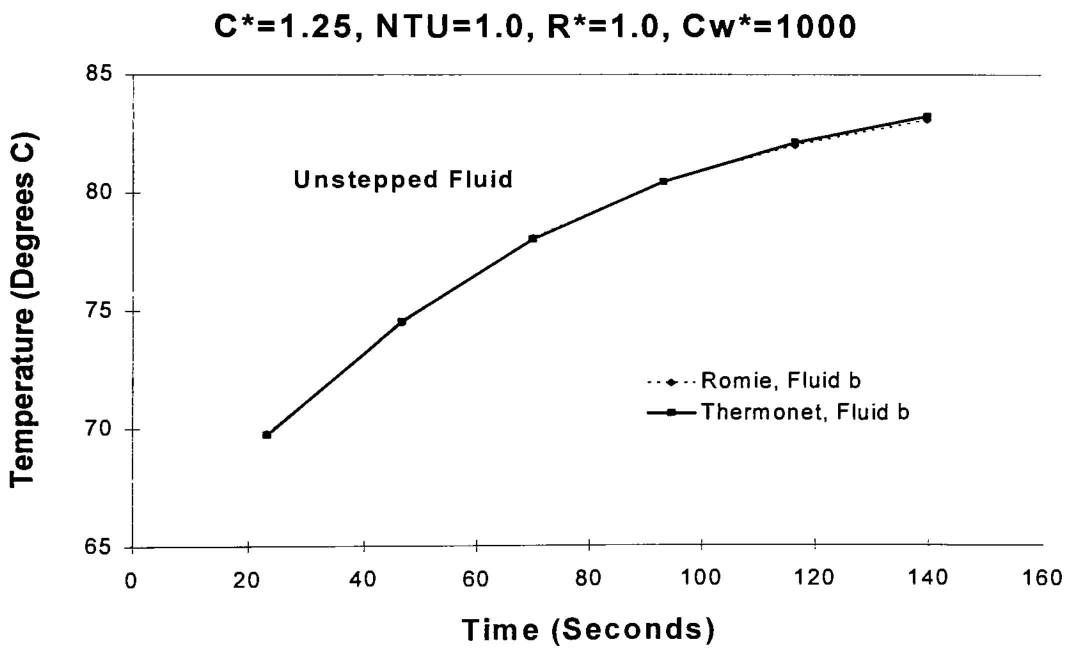

Figure 5.20: Thermonet Versus Romie (1983) Validation

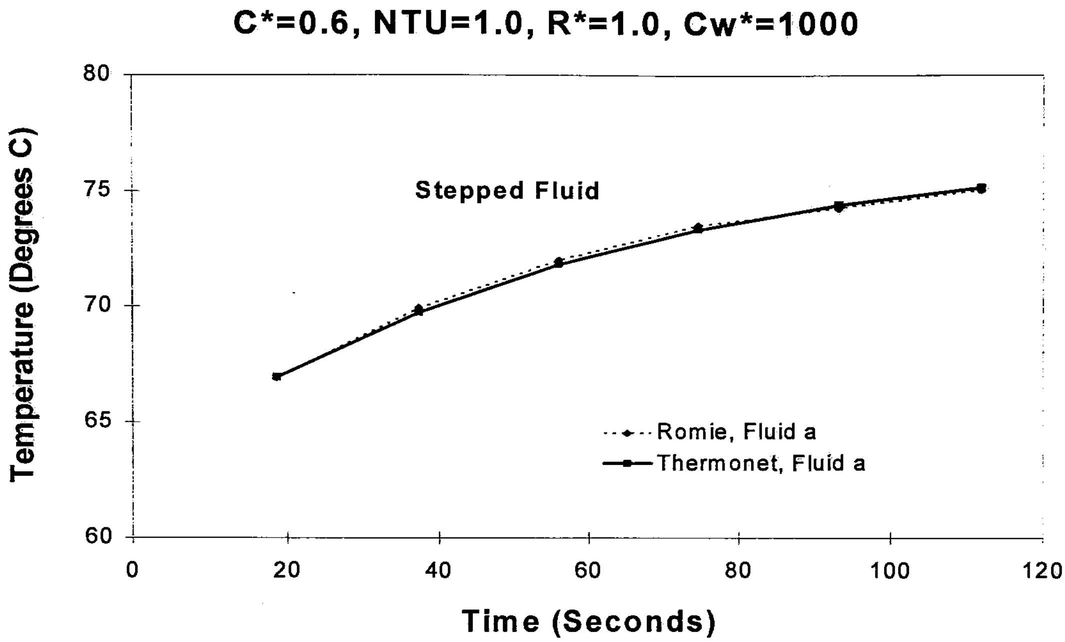

Figure 5.21: Thermonet Versus Romie (1983) Validation

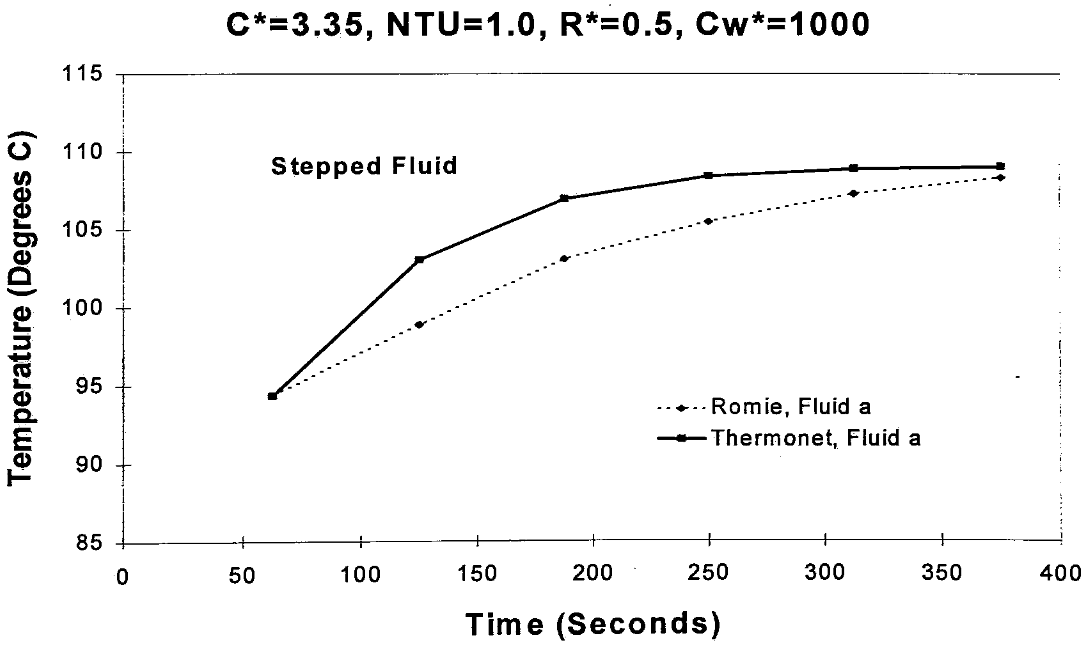

Figure 5.22: Thermonet Versus Romie (1983) Validation

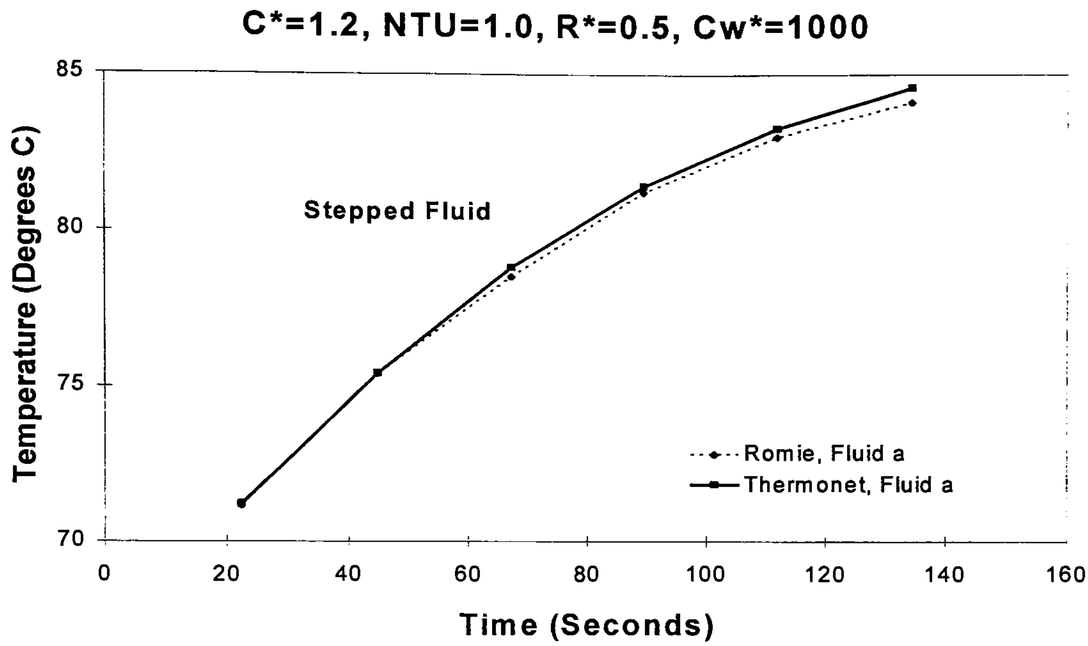

Figure 5.23: Thermonet Versus Romie (1983) Validation

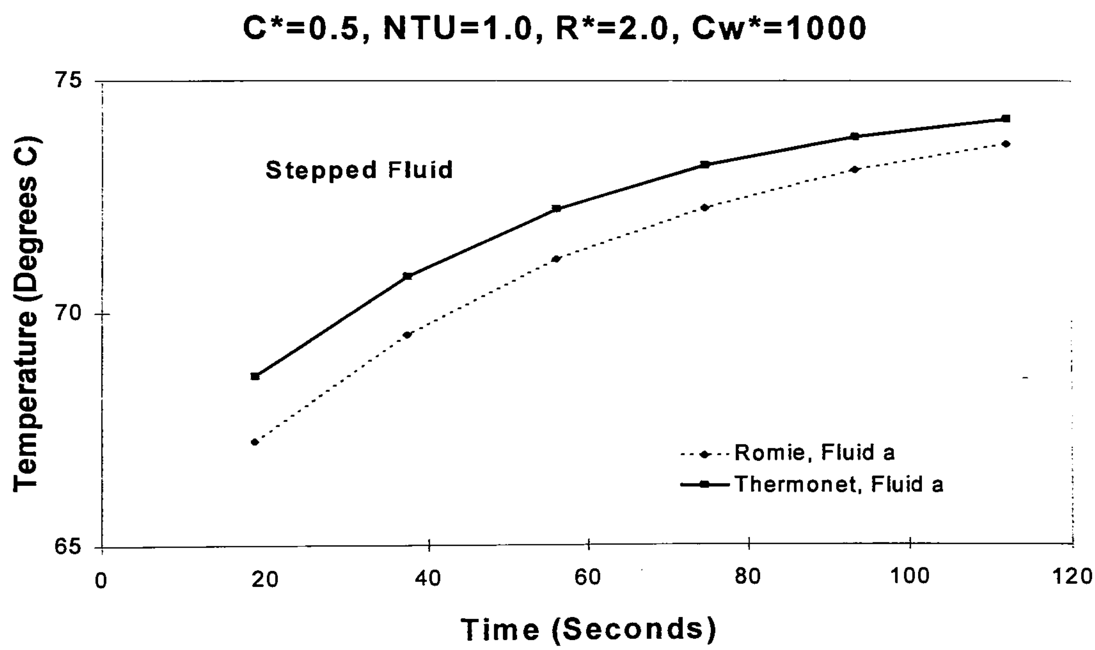

Figure 5.24: Thermonet Versus Romie (1983) Validation

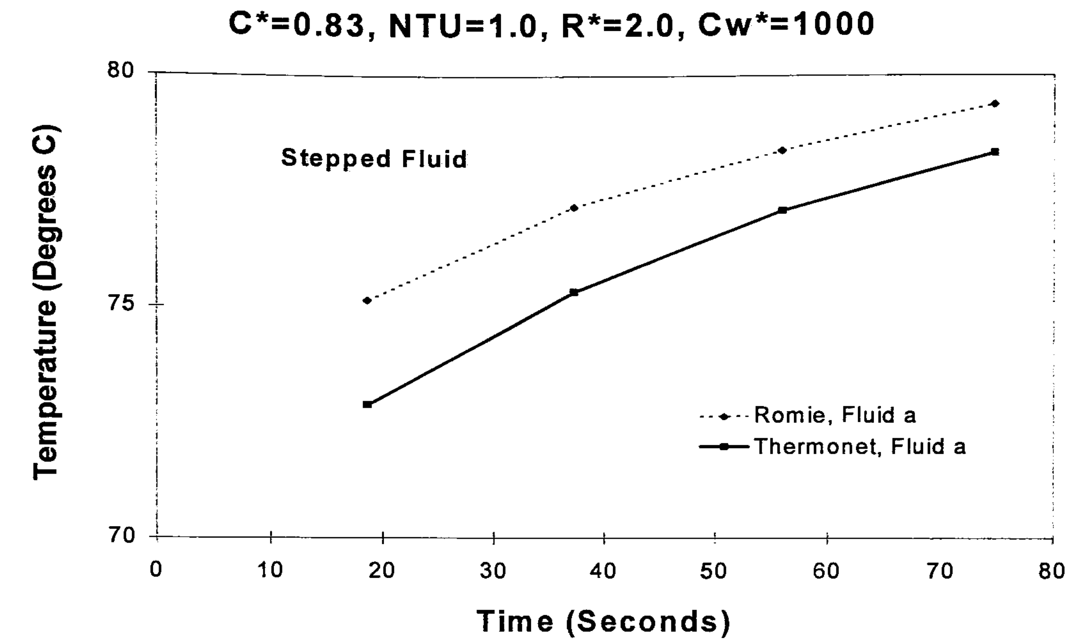

Figure 5.25: Thermonet Versus Romie (1983) Validation

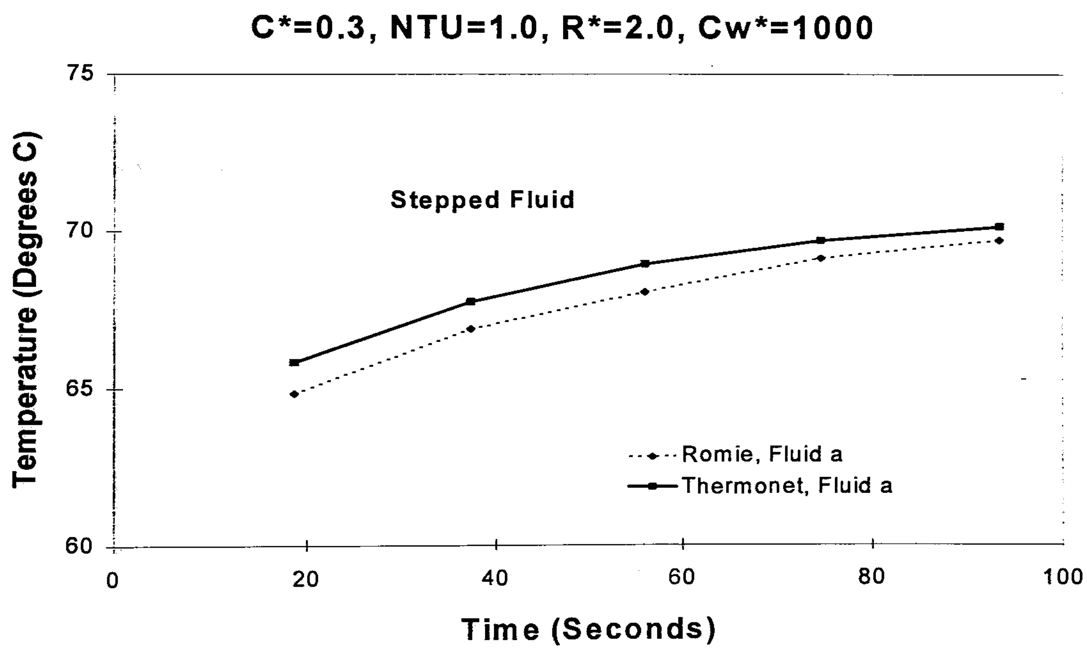

Figure 5.26: Thermonet Versus Romie (1983) Validation

6
Results

6.1 PARALLEL-FLOW HEAT EXCHANGERS

Transient performance effectiveness tables were generated for a step input change to the C_{min} fluid for the range of dimensionless parameters listed in table 6.1.

Table 6.1: Dimensionless Parameters Used in this Analysis for Direct Transfer Parallel-Flow Heat Exchangers

Dimensionless Parameter	Parameter Values		
NTU	0.5	1.0	3.0
C^*	0.2	0.6	1.0
R^*	0.5	1.0	2.0
C_w^*	1.0	10.0	1000.0
t_d^*	0.25	1.0	4.0

Transient temperature effectiveness values (ε_1^* and ε_2^*) generated for parallel-flow heat exchangers are shown in Tables 6.2 - 6.8.

Table 6.2: Transient Temperature Effectiveness Values for NTU = 0.5, Wall Capacitance Ratio = 1.0, Parallel-Flow Heat Exchangers

NTU = 0.5 $C_w^* = 1.0$																		
$t_d^*=0.25$	$C^* = 0.2$						$C^* = 0.6$						$C^* = 1.0$					
	$R^* = 0.5$		$R^* = 1$		$R^* = 2$		$R^* = 0.5$		$R^* = 1$		$R^* = 2$		$R^* = 0.5$		$R^* = 1$		$R^* = 2$	
t^*	$\varepsilon_{f,1}^*$	$\varepsilon_{f,2}^*$	$\varepsilon_{f,1}^*$	$\varepsilon_{f,2}^*$	$\varepsilon_{f,1}^*$	$\varepsilon_{f,2}^*$	$\varepsilon_{f,1}^*$	$\varepsilon_{f,2}^*$	$\varepsilon_{f,1}^*$	$\varepsilon_{f,2}^*$	$\varepsilon_{f,1}^*$	$\varepsilon_{f,2}^*$	$\varepsilon_{f,1}^*$	$\varepsilon_{f,2}^*$	$\varepsilon_{f,1}^*$	$\varepsilon_{f,2}^*$	$\varepsilon_{f,1}^*$	$\varepsilon_{f,2}^*$
0.7	0.154	0.006	0.194	0.008	0.224	0.009	0.146	0.007	0.185	0.008	0.213	0.010	0.140	0.007	0.178	0.008	0.204	0.010
1.4	0.530	0.062	0.623	0.068	0.690	0.079	0.506	0.064	0.595	0.070	0.659	0.080	0.487	0.068	0.572	0.073	0.634	0.082
2.1	0.784	0.189	0.855	0.200	0.906	0.222	0.754	0.194	0.822	0.203	0.872	0.222	0.730	0.201	0.795	0.209	0.845	0.225
2.8	0.904	0.363	0.940	0.374	0.967	0.401	0.878	0.368	0.912	0.375	0.939	0.396	0.857	0.378	0.890	0.382	0.917	0.397
3.5	0.958	0.543	0.974	0.550	0.986	0.576	0.938	0.546	0.953	0.548	0.966	0.566	0.923	0.556	0.936	0.553	0.951	0.563
4.2	0.983	0.699	0.988	0.702	0.994	0.722	0.969	0.700	0.974	0.696	0.981	0.709	0.959	0.707	0.963	0.698	0.971	0.703
4.9	0.994	0.817	0.995	0.817	0.998	0.832	0.985	0.815	0.987	0.809	0.990	0.817	0.979	0.821	0.980	0.809	0.984	0.809
5.6	1.00	0.898	1.00	0.896	1.00	0.905	0.994	0.894	0.994	0.888	0.996	0.891	0.990	0.897	0.990	0.886	0.992	0.884
6.3	1.00	0.948	1.00	0.945	1.00	0.951	0.999	0.943	0.998	0.937	0.999	0.939	0.997	0.944	0.996	0.935	0.997	0.933
7.0	1.00	0.977	1.00	0.974	1.00	0.977	1.00	0.971	1.00	0.967	1.00	0.968	1.00	0.972	0.999	0.965	1.00	0.963
7.7	1.00	0.992	1.00	0.991	1.00	0.991	1.00	0.986	1.00	0.984	1.00	0.984	1.00	0.987	1.00	0.982	1.00	0.981
8.4	1.00	1.00	1.00	0.999	1.00	0.999	1.00	0.994	1.00	0.993	1.00	0.993	1.00	0.994	1.00	0.992	1.00	0.990
$t_d^*=1.0$	$C^* = 0.2$						$C^* = 0.6$						$C^* = 1.0$					
	$R^* = 0.5$		$R^* = 1$		$R^* = 2$		$R^* = 0.5$		$R^* = 1$		$R^* = 2$		$R^* = 0.5$		$R^* = 1$		$R^* = 2$	
t^*	$\varepsilon_{f,1}^*$	$\varepsilon_{f,2}^*$	$\varepsilon_{f,1}^*$	$\varepsilon_{f,2}^*$	$\varepsilon_{f,1}^*$	$\varepsilon_{f,2}^*$	$\varepsilon_{f,1}^*$	$\varepsilon_{f,2}^*$	$\varepsilon_{f,1}^*$	$\varepsilon_{f,2}^*$	$\varepsilon_{f,1}^*$	$\varepsilon_{f,2}^*$	$\varepsilon_{f,1}^*$	$\varepsilon_{f,2}^*$	$\varepsilon_{f,1}^*$	$\varepsilon_{f,2}^*$	$\varepsilon_{f,1}^*$	$\varepsilon_{f,2}^*$
0.5	0.071	0.027	0.091	0.028	0.106	0.032	0.068	0.026	0.087	0.026	0.101	0.028	0.065	0.026	0.084	0.025	0.097	0.026
1.0	0.315	0.179	0.388	0.183	0.440	0.203	0.303	0.171	0.371	0.172	0.421	0.183	0.293	0.170	0.359	0.166	0.407	0.170
1.5	0.581	0.425	0.674	0.433	0.742	0.471	0.562	0.411	0.650	0.410	0.717	0.432	0.547	0.404	0.632	0.397	0.696	0.405
2.0	0.765	0.649	0.841	0.659	0.897	0.702	0.747	0.634	0.819	0.633	0.875	0.658	0.732	0.624	0.800	0.615	0.856	0.625
2.5	0.873	0.802	0.923	0.811	0.960	0.847	0.859	0.790	0.906	0.788	0.944	0.811	0.847	0.780	0.891	0.770	0.930	0.781
3.0	0.934	0.892	0.962	0.898	0.984	0.923	0.924	0.884	0.951	0.882	0.974	0.899	0.915	0.876	0.941	0.868	0.964	0.877
3.5	0.967	0.940	0.982	0.944	0.994	0.960	0.961	0.937	0.975	0.935	0.988	0.947	0.955	0.931	0.968	0.925	0.982	0.932
4.0	0.984	0.966	0.992	0.968	0.999	0.978	0.981	0.965	0.988	0.964	0.995	0.971	0.977	0.962	0.983	0.957	0.991	0.962
4.5	0.993	0.978	0.997	0.980	1.00	0.985	0.991	0.980	0.995	0.979	0.999	0.984	0.989	0.979	0.991	0.975	0.996	0.978
5.0	0.998	0.985	1.00	0.986	1.00	0.989	0.997	0.988	1.00	0.987	1.00	0.990	0.995	0.987	0.996	0.985	0.999	0.987
5.5	1.00	0.988	1.00	0.989	1.00	0.991	1.00	0.992	1.00	0.992	1.00	0.993	0.998	0.992	0.998	0.991	1.00	0.991
6.0	1.00	0.990	1.00	0.991	1.00	0.992	1.00	0.994	1.00	0.994	1.00	0.994	1.00	0.994	1.00	0.994	1.00	0.994
$t_d^*=4.0$	$C^* = 0.2$						$C^* = 0.6$						$C^* = 1.0$					
	$R^* = 0.5$		$R^* = 1$		$R^* = 2$		$R^* = 0.5$		$R^* = 1$		$R^* = 2$		$R^* = 0.5$		$R^* = 1$		$R^* = 2$	
t^*	$\varepsilon_{f,1}^*$	$\varepsilon_{f,2}^*$	$\varepsilon_{f,1}^*$	$\varepsilon_{f,2}^*$	$\varepsilon_{f,1}^*$	$\varepsilon_{f,2}^*$	$\varepsilon_{f,1}^*$	$\varepsilon_{f,2}^*$	$\varepsilon_{f,1}^*$	$\varepsilon_{f,2}^*$	$\varepsilon_{f,1}^*$	$\varepsilon_{f,2}^*$	$\varepsilon_{f,1}^*$	$\varepsilon_{f,2}^*$	$\varepsilon_{f,1}^*$	$\varepsilon_{f,2}^*$	$\varepsilon_{f,1}^*$	$\varepsilon_{f,2}^*$
0.4	0.045	0.081	0.057	0.079	0.067	0.086	0.043	0.081	0.055	0.077	0.064	0.078	0.042	0.066	0.053	0.060	0.062	0.057
0.8	0.206	0.283	0.258	0.283	0.295	0.307	0.200	0.275	0.249	0.267	0.285	0.276	0.194	0.241	0.241	0.228	0.275	0.224
1.2	0.430	0.500	0.516	0.505	0.580	0.544	0.419	0.485	0.501	0.480	0.562	0.500	0.408	0.448	0.486	0.434	0.545	0.436
1.6	0.627	0.669	0.718	0.679	0.786	0.722	0.613	0.655	0.700	0.654	0.766	0.682	0.601	0.623	0.683	0.612	0.747	0.623
2.0	0.767	0.788	0.843	0.799	0.900	0.838	0.754	0.777	0.826	0.778	0.882	0.807	0.742	0.753	0.810	0.746	0.866	0.760
2.4	0.859	0.866	0.913	0.875	0.954	0.906	0.847	0.858	0.899	0.860	0.940	0.885	0.837	0.841	0.886	0.836	0.927	0.852
2.8	0.915	0.914	0.951	0.921	0.979	0.943	0.906	0.909	0.940	0.911	0.968	0.931	0.898	0.899	0.930	0.895	0.959	0.909
3.2	0.951	0.944	0.973	0.949	0.990	0.964	0.943	0.942	0.964	0.943	0.982	0.957	0.937	0.936	0.957	0.933	0.976	0.944
3.6	0.972	0.962	0.985	0.965	0.996	0.975	0.965	0.961	0.978	0.962	0.990	0.972	0.961	0.959	0.973	0.956	0.986	0.965
4.0	0.985	0.973	0.993	0.975	0.999	0.980	0.979	0.973	0.987	0.973	0.994	0.981	0.976	0.973	0.983	0.971	0.991	0.977
4.4	0.992	0.979	0.997	0.980	1.00	0.983	0.988	0.980	0.992	0.980	0.996	0.986	0.985	0.981	0.989	0.980	0.995	0.985
4.8	0.997	0.983	0.999	0.984	1.00	0.985	0.993	0.984	0.995	0.985	0.997	0.988	0.991	0.986	0.993	0.985	0.996	0.989

Table 6.3: Transient Temperature Effectiveness Values for NTU = 1.0, Wall Capacitance Ratio = 1.0, Parallel-Flow Heat Exchangers

NTU = 1.0 $C_w^* = 1.0$

$t_d^*=0.25$	$C^*=0.2$						$C^*=0.6$						$C^*=1.0$					
	$R^*=0.5$		$R^*=1$		$R^*=2$		$R^*=0.5$		$R^*=1$		$R^*=2$		$R^*=0.5$		$R^*=1$		$R^*=2$	
t^*	$\varepsilon_{f,1}^*$	$\varepsilon_{f,2}^*$	$\varepsilon_{f,1}^*$	$\varepsilon_{f,2}^*$	$\varepsilon_{f,1}^*$	$\varepsilon_{f,2}^*$	$\varepsilon_{f,1}^*$	$\varepsilon_{f,2}^*$	$\varepsilon_{f,1}^*$	$\varepsilon_{f,2}^*$	$\varepsilon_{f,1}^*$	$\varepsilon_{f,2}^*$	$\varepsilon_{f,1}^*$	$\varepsilon_{f,2}^*$	$\varepsilon_{f,1}^*$	$\varepsilon_{f,2}^*$	$\varepsilon_{f,1}^*$	$\varepsilon_{f,2}^*$
0.55	0.053	0.000	0.076	0.001	0.096	0.002	0.044	0.001	0.064	0.001	0.080	0.002	0.038	0.001	0.056	0.002	0.072	0.002
1.10	0.323	0.023	0.421	0.029	0.500	0.036	0.273	0.025	0.356	0.031	0.423	0.038	0.244	0.028	0.318	0.034	0.379	0.041
1.65	0.626	0.098	0.721	0.112	0.793	0.130	0.539	0.104	0.621	0.119	0.686	0.135	0.491	0.113	0.565	0.127	0.625	0.142
2.20	0.812	0.227	0.864	0.245	0.901	0.268	0.720	0.236	0.768	0.253	0.805	0.272	0.671	0.252	0.715	0.266	0.752	0.282
2.75	0.907	0.388	0.928	0.404	0.944	0.426	0.829	0.394	0.850	0.407	0.869	0.423	0.790	0.414	0.810	0.422	0.830	0.432
3.30	0.954	0.553	0.961	0.563	0.968	0.582	0.895	0.553	0.903	0.558	0.914	0.569	0.868	0.573	0.875	0.572	0.886	0.575
3.85	0.980	0.702	0.980	0.705	0.984	0.720	0.938	0.691	0.940	0.690	0.946	0.696	0.921	0.708	0.922	0.702	0.928	0.699
4.40	0.996	0.822	0.993	0.819	0.995	0.831	0.966	0.799	0.965	0.796	0.968	0.797	0.955	0.813	0.954	0.803	0.957	0.798
4.95	1.00	0.911	1.00	0.904	1.00	0.912	0.983	0.877	0.982	0.873	0.983	0.872	0.977	0.887	0.975	0.877	0.976	0.871
5.50	1.00	0.974	1.00	0.964	1.00	0.967	0.994	0.929	0.992	0.925	0.993	0.924	0.990	0.935	0.988	0.927	0.988	0.921
6.05	1.00	1.00	1.00	1.00	1.00	1.00	1.00	0.962	0.999	0.959	0.999	0.958	0.998	0.965	0.996	0.960	0.996	0.954
6.60	1.00	1.00	1.00	1.00	1.00	1.00	1.00	0.982	1.00	0.979	1.00	0.979	1.00	0.983	1.00	0.979	1.00	0.975

$t_d^*=1.0$	$C^*=0.2$						$C^*=0.6$						$C^*=1.0$					
	$R^*=0.5$		$R^*=1$		$R^*=2$		$R^*=0.5$		$R^*=1$		$R^*=2$		$R^*=0.5$		$R^*=1$		$R^*=2$	
t^*	$\varepsilon_{f,1}^*$	$\varepsilon_{f,2}^*$	$\varepsilon_{f,1}^*$	$\varepsilon_{f,2}^*$	$\varepsilon_{f,1}^*$	$\varepsilon_{f,2}^*$	$\varepsilon_{f,1}^*$	$\varepsilon_{f,2}^*$	$\varepsilon_{f,1}^*$	$\varepsilon_{f,2}^*$	$\varepsilon_{f,1}^*$	$\varepsilon_{f,2}^*$	$\varepsilon_{f,1}^*$	$\varepsilon_{f,2}^*$	$\varepsilon_{f,1}^*$	$\varepsilon_{f,2}^*$	$\varepsilon_{f,1}^*$	$\varepsilon_{f,2}^*$
0.40	0.020	0.007	0.029	0.008	0.036	0.010	0.017	0.007	0.024	0.007	0.030	0.008	0.015	0.007	0.022	0.007	0.027	0.007
0.80	0.157	0.104	0.218	0.112	0.269	0.127	0.136	0.095	0.188	0.099	0.232	0.105	0.125	0.091	0.170	0.092	0.209	0.092
1.20	0.401	0.338	0.507	0.359	0.593	0.395	0.361	0.314	0.451	0.323	0.528	0.337	0.338	0.298	0.417	0.299	0.486	0.300
1.60	0.637	0.597	0.738	0.623	0.817	0.667	0.594	0.566	0.680	0.577	0.754	0.596	0.566	0.542	0.643	0.541	0.710	0.544
2.00	0.806	0.784	0.875	0.805	0.927	0.842	0.770	0.759	0.831	0.768	0.883	0.787	0.746	0.736	0.800	0.734	0.848	0.738
2.40	0.906	0.890	0.945	0.903	0.974	0.927	0.882	0.878	0.917	0.883	0.948	0.896	0.845	0.860	0.896	0.858	0.925	0.861
2.80	0.959	0.941	0.978	0.949	0.991	0.962	0.945	0.940	0.963	0.944	0.979	0.951	0.933	0.930	0.949	0.927	0.965	0.930
3.20	0.985	0.965	0.992	0.968	0.998	0.975	0.977	0.971	0.985	0.972	0.992	0.977	0.970	0.966	0.977	0.964	0.985	0.965
3.60	0.997	0.975	0.999	0.976	1.00	0.980	0.992	0.985	0.995	0.986	0.998	0.987	0.988	0.983	0.990	0.981	0.994	0.981
4.00	1.00	0.980	1.00	0.979	1.00	0.982	0.999	0.991	0.999	0.991	1.00	0.992	0.996	0.991	0.997	0.990	0.998	0.989
4.40	1.00	0.981	1.00	0.981	1.00	0.982	1.00	0.993	1.00	0.993	1.00	0.993	1.00	0.994	1.00	0.994	1.00	0.992
4.80	1.00	0.982	1.00	0.981	1.00	0.983	1.00	0.994	1.00	0.994	1.00	0.994	1.00	0.996	1.00	0.995	1.00	0.994

$t_d^*=4.0$	$C^*=0.2$						$C^*=0.6$						$C^*=1.0$					
	$R^*=0.5$		$R^*=1$		$R^*=2$		$R^*=0.5$		$R^*=1$		$R^*=2$		$R^*=0.5$		$R^*=1$		$R^*=2$	
t^*	$\varepsilon_{f,1}^*$	$\varepsilon_{f,2}^*$	$\varepsilon_{f,1}^*$	$\varepsilon_{f,2}^*$	$\varepsilon_{f,1}^*$	$\varepsilon_{f,2}^*$	$\varepsilon_{f,1}^*$	$\varepsilon_{f,2}^*$	$\varepsilon_{f,1}^*$	$\varepsilon_{f,2}^*$	$\varepsilon_{f,1}^*$	$\varepsilon_{f,2}^*$	$\varepsilon_{f,1}^*$	$\varepsilon_{f,2}^*$	$\varepsilon_{f,1}^*$	$\varepsilon_{f,2}^*$	$\varepsilon_{f,1}^*$	$\varepsilon_{f,2}^*$
0.30	0.010	0.053	0.013	0.053	0.016	0.056	0.009	0.049	0.012	0.044	0.014	0.041	0.008	0.030	0.010	0.026	0.013	0.021
0.60	0.075	0.241	0.105	0.243	0.132	0.262	0.071	0.215	0.096	0.206	0.118	0.201	0.064	0.160	0.086	0.146	0.106	0.129
0.90	0.226	0.461	0.302	0.478	0.368	0.514	0.215	0.419	0.278	0.419	0.336	0.426	0.200	0.349	0.255	0.335	0.305	0.320
1.20	0.421	0.643	0.527	0.670	0.616	0.714	0.404	0.600	0.493	0.610	0.574	0.632	0.383	0.533	0.461	0.529	0.531	0.527
1.50	0.605	0.774	0.711	0.802	0.797	0.842	0.585	0.738	0.676	0.753	0.756	0.783	0.562	0.686	0.642	0.688	0.714	0.697
1.80	0.750	0.860	0.836	0.883	0.902	0.915	0.730	0.835	0.805	0.850	0.870	0.878	0.710	0.799	0.776	0.804	0.836	0.817
2.10	0.851	0.914	0.911	0.931	0.956	0.951	0.833	0.898	0.887	0.910	0.933	0.932	0.817	0.874	0.865	0.880	0.910	0.894
2.40	0.916	0.946	0.954	0.957	0.981	0.970	0.901	0.938	0.937	0.946	0.966	0.962	0.889	0.924	0.921	0.928	0.952	0.939
2.70	0.955	0.964	0.978	0.971	0.993	0.978	0.944	0.960	0.965	0.966	0.983	0.978	0.935	0.953	0.955	0.957	0.975	0.965
3.00	0.978	0.974	0.990	0.978	0.998	0.981	0.968	0.973	0.981	0.977	0.991	0.985	0.963	0.971	0.975	0.973	0.987	0.979
3.30	0.991	0.980	0.997	0.982	0.999	0.983	0.983	0.981	0.989	0.983	0.995	0.987	0.979	0.982	0.985	0.983	0.993	0.986
3.60	0.998	0.982	1.00	0.984	1.00	0.984	0.991	0.985	0.994	0.987	0.997	0.990	0.988	0.987	0.992	0.988	0.996	0.989

Table 6.4: Transient Temperature Effectiveness Values for NTU = 3.0, Wall Capacitance Ratio = 1.0, Parallel-Flow Heat Exchangers

NTU = 3.0 $C_w^* = 1.0$

$t_d^*=0.25$	C* = 0.2						C* = 0.6						C* = 1.0					
	R* = 0.5		R* = 1		R* = 2		R* = 0.5		R* = 1		R* = 2		R* = 0.5		R* = 1		R* = 2	
t*	$\varepsilon_{f,1}^*$	$\varepsilon_{f,2}^*$	$\varepsilon_{f,1}^*$	$\varepsilon_{f,2}^*$	$\varepsilon_{f,1}^*$	$\varepsilon_{f,2}^*$	$\varepsilon_{f,1}^*$	$\varepsilon_{f,2}^*$	$\varepsilon_{f,1}^*$	$\varepsilon_{f,2}^*$	$\varepsilon_{f,1}^*$	$\varepsilon_{f,2}^*$	$\varepsilon_{f,1}^*$	$\varepsilon_{f,2}^*$	$\varepsilon_{f,1}^*$	$\varepsilon_{f,2}^*$	$\varepsilon_{f,1}^*$	$\varepsilon_{f,2}^*$
0.6	0.016	0.001	0.024	0.001	0.033	0.002	0.008	0.001	0.013	0.012	0.018	0.002	0.007	0.001	0.011	0.002	0.015	0.003
1.2	0.119	0.016	0.157	0.021	0.191	0.026	0.078	0.020	0.102	0.026	0.126	0.031	0.071	0.024	0.093	0.030	0.115	0.036
1.8	0.300	0.078	0.343	0.090	0.378	0.101	0.233	0.096	0.266	0.108	0.297	0.120	0.229	0.112	0.260	0.124	0.288	0.135
2.4	0.488	0.207	0.518	0.222	0.543	0.236	0.431	0.244	0.458	0.257	0.484	0.269	0.438	0.277	0.463	0.288	0.485	0.296
3.0	0.657	0.388	0.675	0.402	0.693	0.414	0.626	0.439	0.642	0.446	0.658	0.453	0.642	0.482	0.655	0.485	0.666	0.484
3.6	0.795	0.582	0.805	0.591	0.817	0.601	0.782	0.633	0.789	0.634	0.798	0.635	0.799	0.675	0.803	0.670	0.805	0.662
4.2	0.893	0.748	0.898	0.754	0.906	0.761	0.888	0.789	0.890	0.786	0.894	0.783	0.901	0.821	0.900	0.812	0.898	0.801
4.8	0.953	0.865	0.956	0.870	0.961	0.875	0.950	0.893	0.950	0.890	0.951	0.886	0.958	0.913	0.956	0.905	0.952	0.895
5.4	0.986	0.937	0.988	0.940	0.991	0.945	0.982	0.953	0.981	0.951	0.981	0.948	0.985	0.964	0.984	0.959	0.980	0.950
6.0	1.00	0.974	1.00	0.978	1.00	0.983	0.996	0.983	0.996	0.982	0.996	0.980	0.997	0.988	0.997	0.986	0.993	0.979
6.6	1.00	0.992	1.00	0.996	1.00	1.00	1.00	0.996	1.00	0.996	1.00	0.995	1.00	0.998	1.00	0.998	0.999	0.993
7.2	1.00	1.00	1.00	1.00	1.00	1.00	1.00	1.00	1.00	1.00	1.00	1.00	1.00	1.00	1.00	1.00	1.00	0.999

$t_d^*=1.0$	C* = 0.2						C* = 0.6						C* = 1.0					
	R* = 0.5		R* = 1		R* = 2		R* = 0.5		R* = 1		R* = 2		R* = 0.5		R* = 1		R* = 2	
t*	$\varepsilon_{f,1}^*$	$\varepsilon_{f,2}^*$	$\varepsilon_{f,1}^*$	$\varepsilon_{f,2}^*$	$\varepsilon_{f,1}^*$	$\varepsilon_{f,2}^*$	$\varepsilon_{f,1}^*$	$\varepsilon_{f,2}^*$	$\varepsilon_{f,1}^*$	$\varepsilon_{f,2}^*$	$\varepsilon_{f,1}^*$	$\varepsilon_{f,2}^*$	$\varepsilon_{f,1}^*$	$\varepsilon_{f,2}^*$	$\varepsilon_{f,1}^*$	$\varepsilon_{f,2}^*$	$\varepsilon_{f,1}^*$	$\varepsilon_{f,2}^*$
0.4	0.007	0.007	0.008	0.008	0.051	0.051	0.027	0.033	0.000	0.000	0.001	0.000	0.000	0.000	0.000	0.000	0.000	0.000
0.8	0.077	0.115	0.102	0.123	0.199	0.202	0.119	0.141	0.030	0.035	0.043	0.035	0.015	0.021	0.023	0.021	0.032	0.022
1.2	0.310	0.401	0.373	0.423	0.423	0.430	0.286	0.324	0.259	0.287	0.312	0.294	0.170	0.202	0.208	0.206	0.247	0.552
1.6	0.611	0.703	0.680	0.728	0.646	0.655	0.492	0.536	0.630	0.660	0.688	0.676	0.504	0.545	0.551	0.550	0.596	0.824
2.0	0.831	0.884	0.876	0.902	0.814	0.821	0.679	0.717	0.872	0.886	0.904	0.899	0.793	0.819	0.822	0.821	0.848	0.948
2.4	0.940	0.958	0.962	0.968	0.919	0.923	0.821	0.847	0.963	0.966	0.975	0.972	0.935	0.944	0.946	0.946	0.957	0.987
2.8	0.982	0.982	0.990	0.988	0.969	0.970	0.906	0.922	0.986	0.986	0.990	0.989	0.981	0.984	0.985	0.985	0.989	0.996
3.2	0.995	0.988	0.998	0.992	0.993	0.992	0.955	0.962	0.991	0.989	0.993	0.991	0.993	0.993	0.995	0.995	0.997	0.997
3.6	0.998	0.990	0.999	0.994	1.00	1.00	0.981	0.984	0.991	0.990	0.993	0.992	0.995	0.995	0.997	0.997	0.998	0.998
4.0	0.999	0.990	1.00	0.994	1.00	1.00	0.991	0.992	0.991	0.990	0.993	0.992	0.995	0.995	0.997	0.997	0.998	0.998
4.4	0.999	0.990	1.00	0.994	1.00	1.00	0.996	0.996	0.991	0.990	0.993	0.992	0.995	0.995	0.997	0.997	0.998	0.998
4.8	0.999	0.990	1.00	0.994	1.00	1.00	0.998	0.997	0.991	0.990	0.993	0.992	0.995	0.995	0.997	0.997	0.998	0.998

$t_d^*=4.0$	C* = 0.2						C* = 0.6						C* = 1.0					
	R* = 0.5		R* = 1		R* = 2		R* = 0.5		R* = 1		R* = 2		R* = 0.5		R* = 1		R* = 2	
t*	$\varepsilon_{f,1}^*$	$\varepsilon_{f,2}^*$	$\varepsilon_{f,1}^*$	$\varepsilon_{f,2}^*$	$\varepsilon_{f,1}^*$	$\varepsilon_{f,2}^*$	$\varepsilon_{f,1}^*$	$\varepsilon_{f,2}^*$	$\varepsilon_{f,1}^*$	$\varepsilon_{f,2}^*$	$\varepsilon_{f,1}^*$	$\varepsilon_{f,2}^*$	$\varepsilon_{f,1}^*$	$\varepsilon_{f,2}^*$	$\varepsilon_{f,1}^*$	$\varepsilon_{f,2}^*$	$\varepsilon_{f,1}^*$	$\varepsilon_{f,2}^*$
0.4	0.046	0.181	0.048	0.180	0.055	0.182	0.070	0.132	0.029	0.082	0.029	0.068	0.016	0.044	0.015	0.035	0.014	0.026
0.8	0.247	0.538	0.284	0.560	0.333	0.587	0.235	0.359	0.212	0.364	0.235	0.356	0.142	0.239	0.151	0.224	0.160	0.206
1.2	0.529	0.783	0.602	0.815	0.678	0.848	0.451	0.592	0.527	0.668	0.580	0.685	0.400	0.524	0.433	0.524	0.468	0.523
1.6	0.765	0.908	0.832	0.931	0.888	0.951	0.651	0.766	0.782	0.865	0.832	0.886	0.670	0.764	0.712	0.775	0.754	0.787
2.0	0.903	0.959	0.941	0.971	0.967	0.979	0.802	0.878	0.920	0.953	0.947	0.965	0.854	0.903	0.883	0.913	0.911	0.925
2.4	0.963	0.977	0.979	0.982	0.987	0.986	0.900	0.943	0.974	0.984	0.985	0.988	0.945	0.965	0.959	0.970	0.973	0.976
2.8	0.984	0.981	0.990	0.985	0.992	0.987	0.951	0.973	0.991	0.993	0.994	0.994	0.981	0.987	0.986	0.989	0.991	0.992
3.2	0.990	0.982	0.992	0.985	0.992	0.987	0.978	0.987	0.996	0.995	0.996	0.995	0.992	0.993	0.994	0.994	0.995	0.995
3.6	0.992	0.983	0.992	0.985	0.992	0.987	0.990	0.993	0.997	0.996	0.996	0.995	0.995	0.995	0.996	0.996	0.996	0.996
4.0	0.992	0.983	0.993	0.986	0.992	0.987	0.995	0.996	0.997	0.996	0.996	0.995	0.996	0.996	0.996	0.996	0.997	0.996
4.4	0.993	0.983	0.993	0.986	0.992	0.987	0.997	0.997	0.997	0.996	0.996	0.995	0.996	0.996	0.997	0.996	0.997	0.996
4.8	0.993	0.983	0.993	0.986	0.992	0.987	0.998	0.997	0.998	0.996	0.996	0.995	0.996	0.996	0.997	0.996	0.997	0.996

Table 6.5: Transient Temperature Effectiveness Values for NTU = 0.5, Wall Capacitance Ratio = 10.0, Parallel-Flow Heat Exchangers

NTU = 0.5 $C_w^* = 10.0$

$0.25 < t_d^* < 1.0$	$C^* = 0.2$						$C^* = 0.6$						$C^* = 1.0$					
	$R^* = 0.5$		$R^* = 1$		$R^* = 2$		$R^* = 0.5$		$R^* = 1$		$R^* = 2$		$R^* = 0.5$		$R^* = 1$		$R^* = 2$	
t^*	$\varepsilon_{f,1}^*$	$\varepsilon_{f,2}^*$	$\varepsilon_{f,1}^*$	$\varepsilon_{f,2}^*$	$\varepsilon_{f,1}^*$	$\varepsilon_{f,2}^*$	$\varepsilon_{f,1}^*$	$\varepsilon_{f,2}^*$	$\varepsilon_{f,1}^*$	$\varepsilon_{f,2}^*$	$\varepsilon_{f,1}^*$	$\varepsilon_{f,2}^*$	$\varepsilon_{f,1}^*$	$\varepsilon_{f,2}^*$	$\varepsilon_{f,1}^*$	$\varepsilon_{f,2}^*$	$\varepsilon_{f,1}^*$	$\varepsilon_{f,2}^*$
3.5	0.53	0.225	0.708	0.237	0.837	0.275	0.506	0.213	0.676	0.218	0.799	0.239	0.487	0.202	0.650	0.202	0.769	0.21
7.0	0.702	0.526	0.823	0.541	0.911	0.602	0.678	0.501	0.794	0.504	0.880	0.536	0.659	0.479	0.769	0.469	0.853	0.481
10.5	0.814	0.714	0.893	0.727	0.951	0.784	0.795	0.69	0.87	0.689	0.928	0.722	0.778	0.668	0.849	0.654	0.907	0.666
14.0	0.886	0.83	0.936	0.839	0.974	0.883	0.872	0.811	0.919	0.807	0.958	0.836	0.859	0.792	0.903	0.777	0.942	0.789
17.5	0.932	0.899	0.962	0.905	0.986	0.938	0.921	0.885	0.950	0.882	0.976	0.905	0.912	0.871	0.939	0.858	0.965	0.869
21.0	0.959	0.941	0.978	0.944	0.993	0.967	0.952	0.931	0.969	0.928	0.986	0.946	0.946	0.921	0.962	0.911	0.979	0.919
24.5	0.976	0.966	0.987	0.968	0.996	0.983	0.972	0.959	0.981	0.957	0.993	0.969	0.967	0.952	0.976	0.945	0.988	0.951
28.0	0.986	0.98	0.993	0.981	0.998	0.991	0.983	0.976	0.989	0.974	0.996	0.983	0.98	0.971	0.986	0.966	0.993	0.97
31.5	0.992	0.988	0.996	0.989	0.999	0.996	0.99	0.986	0.993	0.985	0.998	0.991	0.988	0.983	0.992	0.979	0.996	0.982
35.0	0.996	0.993	0.998	0.994	1.00	0.998	0.995	0.992	0.996	0.991	0.999	0.996	0.993	0.990	0.995	0.988	0.998	0.989
38.5	0.998	0.996	0.999	0.997	1.00	0.999	0.997	0.995	0.998	0.995	1.00	0.999	0.996	0.994	0.998	0.993	0.999	0.994
42.0	0.999	0.998	1.00	0.998	1.00	1.00	0.999	0.997	0.999	0.997	1.00	1.00	0.998	0.997	0.999	0.996	1.00	0.996
$1.0 < t_d^* < 4.0$	$C^* = 0.2$						$C^* = 0.6$						$C^* = 1.0$					
	$R^* = 0.5$		$R^* = 1$		$R^* = 2$		$R^* = 0.5$		$R^* = 1$		$R^* = 2$		$R^* = 0.5$		$R^* = 1$		$R^* = 2$	
t^*	$\varepsilon_{f,1}^*$	$\varepsilon_{f,2}^*$	$\varepsilon_{f,1}^*$	$\varepsilon_{f,2}^*$	$\varepsilon_{f,1}^*$	$\varepsilon_{f,2}^*$	$\varepsilon_{f,1}^*$	$\varepsilon_{f,2}^*$	$\varepsilon_{f,1}^*$	$\varepsilon_{f,2}^*$	$\varepsilon_{f,1}^*$	$\varepsilon_{f,2}^*$	$\varepsilon_{f,1}^*$	$\varepsilon_{f,2}^*$	$\varepsilon_{f,1}^*$	$\varepsilon_{f,2}^*$	$\varepsilon_{f,1}^*$	$\varepsilon_{f,2}^*$
3.5	0.530	0.315	0.765	0.460	0.838	0.371	0.506	0.213	0.677	0.291	0.801	0.312	0.489	0.269	0.652	0.262	0.771	0.267
7.0	0.703	0.58	0.859	0.676	0.913	0.655	0.678	0.501	0.796	0.550	0.882	0.584	0.662	0.524	0.772	0.513	0.856	0.524
10.5	0.815	0.745	3915	0.806	0.953	0.811	0.795	0.690	0.871	0.717	0.930	0.751	0.781	0.696	0.852	0.683	0.910	0.697
14.0	0.887	0.847	0.949	0.884	0.975	0.896	0.872	0.811	0.920	0.823	0.959	0.852	0.861	0.809	0.905	0.795	0.944	0.810
17.5	0.932	0.908	0.97	0.930	0.987	0.942	0.921	0.885	0.950	0.890	0.976	0.912	0.913	0.881	0.939	0.869	0.966	0.882
21.0	0.96	0.945	0.982	0.958	0.993	0.967	0.952	0.931	0.970	0.931	0.986	0.948	0.946	0.926	0.962	0.916	0.98	0.927
24.5	0.976	0.966	0.99	0.974	0.997	0.98	0.972	0.959	0.981	0.956	0.992	0.969	0.967	0.954	0.976	0.946	0.988	0.955
28.0	0.986	0.979	0.994	0.984	0.999	0.987	0.983	0.976	0.988	0.972	0.995	0.981	0.98	0.971	0.985	0.966	0.993	0.972
31.5	0.992	0.987	0.997	0.989	1.00	0.991	0.990	0.986	0.993	0.981	0.997	0.987	0.988	0.982	0.990	0.977	0.996	0.983
35.0	0.996	0.991	0.998	0.992	1.00	0.993	0.995	0.992	0.996	0.987	0.998	0.991	0.993	0.988	0.994	0.985	0.998	0.989
38.5	0.998	0.994	0.999	0.994	1.00	0.994	0.997	0.995	0.997	0.991	0.999	0.994	0.996	0.992	0.996	0.99	0.999	0.992
42.0	0.999	0.995	1.00	0.995	1.00	0.995	0.999	0.997	0.998	0.993	1.00	0.995	0.998	0.995	0.997	0.992	1.00	0.995

Table 6.6: Transient Temperature Effectiveness Values for NTU = 1.0, Wall Capacitance Ratio = 10.0, Parallel-Flow Heat Exchangers

$NTU = 1.0 \;\; C_w^* = 10.0$

$0.25 < t_d^* < 1.0$	$C^* = 0.2$						$C^* = 0.6$						$C^* = 1.0$					
	$R^* = 0.5$		$R^* = 1$		$R^* = 2$		$R^* = 0.5$		$R^* = 1$		$R^* = 2$		$R^* = 0.5$		$R^* = 1$		$R^* = 2$	
t^*	$\varepsilon_{f,1}^*$	$\varepsilon_{f,2}^*$	$\varepsilon_{f,1}^*$	$\varepsilon_{f,2}^*$	$\varepsilon_{f,1}^*$	$\varepsilon_{f,2}^*$	$\varepsilon_{f,1}^*$	$\varepsilon_{f,2}^*$	$\varepsilon_{f,1}^*$	$\varepsilon_{f,2}^*$	$\varepsilon_{f,1}^*$	$\varepsilon_{f,2}^*$	$\varepsilon_{f,1}^*$	$\varepsilon_{f,2}^*$	$\varepsilon_{f,1}^*$	$\varepsilon_{f,2}^*$	$\varepsilon_{f,1}^*$	$\varepsilon_{f,2}^*$
2	0.235	0.102	0.420	0.120	0.587	0.147	0.199	0.090	0.354	0.102	0.495	0.114	0.178	0.080	0.315	0.088	0.440	0.093
4	0.438	0.363	0.625	0.401	0.778	0.461	0.385	0.320	0.545	0.339	0.678	0.361	0.352	0.284	0.494	0.291	0.613	0.294
6	0.603	0.583	0.754	0.622	0.869	0.689	0.549	0.526	0.680	0.543	0.785	0.568	0.513	0.478	0.629	0.479	0.725	0.480
8	0.730	0.733	0.843	0.766	0.925	0.825	0.682	0.679	0.781	0.692	0.861	0.718	0.648	0.632	0.736	0.628	0.810	0.630
10	0.822	0.831	0.902	0.857	0.958	0.903	0.783	0.787	0.854	0.796	0.912	0.819	0.754	0.747	0.816	0.740	0.871	0.744
12	0.886	0.894	0.940	0.913	0.978	0.947	0.856	0.862	0.904	0.867	0.946	0.887	0.833	0.830	0.875	0.822	0.915	0.826
14	0.929	0.934	0.964	0.948	0.989	0.972	0.907	0.911	0.939	0.914	0.968	0.930	0.889	0.888	0.917	0.880	0.945	0.884
16	0.958	0.959	0.980	0.969	0.995	0.986	0.941	0.943	0.961	0.945	0.981	0.957	0.928	0.927	0.945	0.920	0.965	0.924
18	0.976	0.974	0.989	0.982	0.999	0.993	0.964	0.964	0.976	0.965	0.990	0.974	0.954	0.952	0.965	0.947	0.979	0.950
20	0.987	0.984	0.995	0.989	1.00	0.997	0.978	0.977	0.986	0.977	0.995	0.984	0.971	0.969	0.978	0.965	0.987	0.968
22	0.994	0.989	0.998	0.994	1.00	0.999	0.988	0.985	0.992	0.985	0.998	0.990	0.983	0.980	0.986	0.977	0.993	0.979
24	0.999	0.992	1.00	0.996	1.00	1.00	0.994	0.990	0.996	0.990	0.999	0.994	0.990	0.987	0.992	0.985	0.996	0.986

$1.0 < t_d^* < 4.0$	$C^* = 0.2$						$C^* = 0.6$						$C^* = 1.0$					
	$R^* = 0.5$		$R^* = 1$		$R^* = 2$		$R^* = 0.5$		$R^* = 1$		$R^* = 2$		$R^* = 0.5$		$R^* = 1$		$R^* = 2$	
t^*	$\varepsilon_{f,1}^*$	$\varepsilon_{f,2}^*$	$\varepsilon_{f,1}^*$	$\varepsilon_{f,2}^*$	$\varepsilon_{f,1}^*$	$\varepsilon_{f,2}^*$	$\varepsilon_{f,1}^*$	$\varepsilon_{f,2}^*$	$\varepsilon_{f,1}^*$	$\varepsilon_{f,2}^*$	$\varepsilon_{f,1}^*$	$\varepsilon_{f,2}^*$	$\varepsilon_{f,1}^*$	$\varepsilon_{f,2}^*$	$\varepsilon_{f,1}^*$	$\varepsilon_{f,2}^*$	$\varepsilon_{f,1}^*$	$\varepsilon_{f,2}^*$
2	0.238	0.224	0.423	0.246	0.591	0.284	0.204	0.181	0.359	0.188	0.501	0.195	0.183	0.147	0.320	0.147	0.445	0.142
4	0.444	0.478	0.632	0.517	0.786	0.582	0.397	0.414	0.556	0.429	0.691	0.450	0.365	0.360	0.506	0.361	0.626	0.358
6	0.610	0.657	0.761	0.696	0.877	0.761	0.562	0.594	0.693	0.610	0.799	0.638	0.528	0.538	0.643	0.537	0.739	0.539
8	0.736	0.778	0.848	0.809	0.930	0.865	0.694	0.726	0.793	0.739	0.873	0.768	0.662	0.677	0.749	0.674	0.823	0.678
10	0.827	0.858	0.906	0.881	0.962	0.923	0.793	0.819	0.863	0.829	0.921	0.854	0.765	0.779	0.828	0.774	0.883	0.781
12	0.889	0.907	0.942	0.925	0.979	0.956	0.863	0.882	0.911	0.889	0.952	0.909	0.841	0.852	0.884	0.847	0.924	0.854
14	0.931	0.941	0.965	0.953	0.989	0.974	0.912	0.924	0.944	0.928	0.972	0.944	0.895	0.902	0.923	0.897	0.952	0.904
16	0.958	0.962	0.980	0.970	0.995	0.984	0.944	0.951	0.965	0.954	0.984	0.966	0.932	0.936	0.950	0.932	0.97	0.937
18	0.976	0.974	0.989	0.980	0.998	0.990	0.966	0.969	0.978	0.970	0.991	0.979	0.957	0.959	0.968	0.955	0.982	0.959
20	0.987	0.982	0.994	0.986	1.00	0.993	0.980	0.980	0.987	0.981	0.995	0.987	0.973	0.973	0.980	0.970	0.989	0.974
22	0.994	0.987	0.997	0.990	1.00	0.994	0.988	0.987	0.993	0.987	0.998	0.991	0.984	0.982	0.987	0.980	0.994	0.983
24	0.998	0.989	0.999	0.992	1.00	0.995	0.994	0.991	0.996	0.991	1.00	0.994	0.991	0.988	0.992	0.987	0.997	0.989

Table 6.7: Transient Temperature Effectiveness Values for NTU = 3.0, Wall Capacitance Ratio = 10.0, Parallel-Flow Heat Exchangers

NTU = 3.0 $C_w^* = 10.0$

$0.25 < t_d^* < 1.0$	$C^* = 0.2$						$C^* = 0.6$						$C^* = 1.0$					
	$R^* = 0.5$		$R^* = 1$		$R^* = 2$		$R^* = 0.5$		$R^* = 1$		$R^* = 2$		$R^* = 0.5$		$R^* = 1$		$R^* = 2$	
t^*	$\varepsilon_{f,1}^*$	$\varepsilon_{f,2}^*$	$\varepsilon_{f,1}^*$	$\varepsilon_{f,2}^*$	$\varepsilon_{f,1}^*$	$\varepsilon_{f,2}^*$	$\varepsilon_{f,1}^*$	$\varepsilon_{f,2}^*$	$\varepsilon_{f,1}^*$	$\varepsilon_{f,2}^*$	$\varepsilon_{f,1}^*$	$\varepsilon_{f,2}^*$	$\varepsilon_{f,1}^*$	$\varepsilon_{f,2}^*$	$\varepsilon_{f,1}^*$	$\varepsilon_{f,2}^*$	$\varepsilon_{f,1}^*$	$\varepsilon_{f,2}^*$
1.2	0.016	0.029	0.037	0.035	0.074	0.042	0.008	0.014	0.020	0.016	0.040	0.017	0.006	0.008	0.015	0.009	0.030	0.011
2.4	0.092	0.182	0.169	0.209	0.274	0.238	0.060	0.100	0.104	0.107	0.161	0.111	0.043	0.059	0.078	0.064	0.121	0.067
3.6	0.244	0.410	0.368	0.455	0.507	0.504	0.175	0.255	0.250	0.268	0.331	0.274	0.133	0.167	0.192	0.175	0.254	0.177
4.8	0.430	0.614	0.569	0.663	0.704	0.716	0.333	0.433	0.424	0.450	0.512	0.460	0.268	0.316	0.340	0.322	0.407	0.322
6.0	0.604	0.761	0.729	0.803	0.838	0.850	0.500	0.597	0.588	0.614	0.669	0.629	0.423	0.474	0.494	0.478	0.556	0.476
7.2	0.742	0.858	0.841	0.891	0.918	0.925	0.648	0.729	0.723	0.744	0.789	0.761	0.572	0.619	0.633	0.620	0.685	0.617
8.4	0.842	0.919	0.912	0.941	0.961	0.965	0.766	0.827	0.823	0.839	0.873	0.854	0.700	0.738	0.746	0.737	0.787	0.735
9.6	0.909	0.955	0.954	0.969	0.984	0.984	0.852	0.894	0.892	0.902	0.927	0.915	0.799	0.828	0.832	0.825	0.862	0.824
10.8	0.951	0.976	0.978	0.985	0.994	0.993	0.910	0.937	0.936	0.943	0.960	0.952	0.871	0.892	0.893	0.888	0.914	0.888
12.0	0.976	0.987	0.991	0.992	1.00	0.997	0.947	0.963	0.964	0.968	0.979	0.974	0.920	0.934	0.934	0.931	0.948	0.931
13.2	0.991	0.994	0.998	0.996	1.00	0.999	0.970	0.980	0.980	0.982	0.989	0.986	0.952	0.961	0.960	0.958	0.970	0.959
14.4	0.999	0.997	1.00	0.998	1.00	1.00	0.984	0.989	0.990	0.990	0.995	0.993	0.972	0.977	0.977	0.976	0.983	0.976
$1.0 < t_d^* < 4.0$	$C^* = 0.2$						$C^* = 0.6$						$C^* = 1.0$					
	$R^* = 0.5$		$R^* = 1$		$R^* = 2$		$R^* = 0.5$		$R^* = 1$		$R^* = 2$		$R^* = 0.5$		$R^* = 1$		$R^* = 2$	
t^*	$\varepsilon_{f,1}^*$	$\varepsilon_{f,2}^*$	$\varepsilon_{f,1}^*$	$\varepsilon_{f,2}^*$	$\varepsilon_{f,1}^*$	$\varepsilon_{f,2}^*$	$\varepsilon_{f,1}^*$	$\varepsilon_{f,2}^*$	$\varepsilon_{f,1}^*$	$\varepsilon_{f,2}^*$	$\varepsilon_{f,1}^*$	$\varepsilon_{f,2}^*$	$\varepsilon_{f,1}^*$	$\varepsilon_{f,2}^*$	$\varepsilon_{f,1}^*$	$\varepsilon_{f,2}^*$	$\varepsilon_{f,1}^*$	$\varepsilon_{f,2}^*$
1.2	0.038	0.150	0.063	0.160	0.107	0.169	0.023	0.073	0.035	0.066	0.055	0.056	0.011	0.026	0.020	0.023	0.035	0.020
2.4	0.160	0.391	0.248	0.426	0.370	0.467	0.110	0.224	0.157	0.224	0.218	0.215	0.067	0.113	0.102	0.110	0.145	0.103
3.6	0.335	0.590	0.467	0.640	0.618	0.698	0.253	0.398	0.332	0.410	0.419	0.415	0.178	0.248	0.237	0.248	0.298	0.241
4.8	0.514	0.737	0.654	0.786	0.790	0.842	0.419	0.563	0.512	0.583	0.605	0.601	0.325	0.405	0.397	0.408	0.464	0.403
6.0	0.668	0.837	0.790	0.877	0.892	0.920	0.578	0.700	0.666	0.722	0.749	0.745	0.482	0.558	0.552	0.562	0.615	0.561
7.2	0.787	0.903	0.879	0.932	0.948	0.961	0.711	0.804	0.784	0.823	0.850	0.846	0.625	0.689	0.685	0.692	0.738	0.694
8.4	0.870	0.943	0.934	0.963	0.976	0.981	0.811	0.877	0.866	0.892	0.914	0.912	0.742	0.792	0.788	0.794	0.830	0.797
9.6	0.925	0.967	0.966	0.980	0.990	0.990	0.882	0.926	0.920	0.936	0.953	0.951	0.831	0.866	0.863	0.867	0.894	0.871
10.8	0.959	0.980	0.983	0.988	0.996	0.994	0.929	0.956	0.954	0.963	0.975	0.973	0.893	0.917	0.915	0.917	0.936	0.921
12.0	0.980	0.988	0.993	0.993	0.999	0.996	0.959	0.975	0.974	0.979	0.987	0.986	0.935	0.950	0.948	0.949	0.963	0.953
13.2	0.991	0.992	0.997	0.995	1.00	0.997	0.977	0.985	0.986	0.988	0.993	0.992	0.961	0.970	0.969	0.970	0.979	0.973
14.4	0.998	0.994	1.00	0.996	1.00	0.997	0.987	0.991	0.992	0.993	0.997	0.996	0.978	0.983	0.982	0.982	0.988	0.984

Table 6.8: Transient Temperature Effectiveness Values for NTU =0.5,1.0,3.0, Wall Capacitance Ratio = 1000, Parallel-Flow Heat Exchangers

NTU = 0.5

C_w^*=1000	C^* = 0.2						C^* = 0.6						C^* = 1.0					
	R^* = 0.5		R^* = 1		R^* = 2		R^* = 0.5		R^* = 1		R^* = 2		R^* = 0.5		R^* = 1		R^* = 2	
t^*	$\varepsilon_{f,1}^*$	$\varepsilon_{f,2}^*$	$\varepsilon_{f,1}^*$	$\varepsilon_{f,2}^*$	$\varepsilon_{f,1}^*$	$\varepsilon_{f,2}^*$	$\varepsilon_{f,1}^*$	$\varepsilon_{f,2}^*$	$\varepsilon_{f,1}^*$	$\varepsilon_{f,2}^*$	$\varepsilon_{f,1}^*$	$\varepsilon_{f,2}^*$	$\varepsilon_{f,1}^*$	$\varepsilon_{f,2}^*$	$\varepsilon_{f,1}^*$	$\varepsilon_{f,2}^*$	$\varepsilon_{f,1}^*$	$\varepsilon_{f,2}^*$
360	0.594	0.395	0.753	0.409	0.868	0.462	0.571	0.371	0.722	0.373	0.833	0.400	0.552	0.350	0.697	0.343	0.804	0.350
720	0.749	0.639	0.853	0.653	0.929	0.713	0.728	0.613	0.827	0.612	0.902	0.646	0.710	0.588	0.805	0.576	0.878	0.588
1080	0.848	0.787	0.914	0.798	0.962	0.848	0.832	0.765	0.894	0.763	0.944	0.794	0.817	0.744	0.876	0.730	0.926	0.744
1440	0.910	0.875	0.949	0.882	0.980	0.919	0.898	0.859	0.935	0.856	0.968	0.882	0.887	0.843	0.922	0.830	0.955	0.843
1800	0.947	0.927	0.971	0.931	0.990	0.957	0.939	0.916	0.961	0.913	0.982	0.932	0.931	0.905	0.952	0.894	0.974	0.905
2160	0.969	0.958	0.983	0.960	0.995	0.977	0.964	0.951	0.977	0.948	0.990	0.962	0.959	0.943	0.970	0.934	0.985	0.943
2520	0.983	0.975	0.991	0.977	0.997	0.988	0.979	0.971	0.986	0.969	0.995	0.978	0.976	0.966	0.982	0.960	0.991	0.966
2880	0.990	0.985	0.995	0.986	0.999	0.993	0.988	0.983	0.992	0.981	0.997	0.987	0.986	0.979	0.989	0.975	0.995	0.980
3240	0.995	0.991	0.997	0.992	1.00	0.996	0.993	0.989	0.995	0.989	0.999	0.993	0.992	0.987	0.994	0.985	0.997	0.988
3600	0.997	0.994	0.999	0.995	1.00	0.998	0.996	0.993	0.997	0.993	0.999	0.996	0.995	0.992	0.996	0.990	1.00	0.992
3960	0.999	0.996	1.00	0.996	1.00	0.999	0.998	0.996	0.999	0.996	1.00	0.997	0.998	0.995	0.998	0.994	1.00	0.995
4320	1.00	0.997	1.00	0.997	1.00	1.00	0.999	0.997	0.999	0.997	1.00	0.998	0.999	0.997	0.999	0.996	1.00	0.997

NTU = 1.0

C_w^*=1000	C^* = 0.2						C^* = 0.6						C^* = 1.0					
	R^* = 0.5		R^* = 1		R^* = 2		R^* = 0.5		R^* = 1		R^* = 2		R^* = 0.5		R^* = 1		R^* = 2	
t^*	$\varepsilon_{f,1}^*$	$\varepsilon_{f,2}^*$	$\varepsilon_{f,1}^*$	$\varepsilon_{f,2}^*$	$\varepsilon_{f,1}^*$	$\varepsilon_{f,2}^*$	$\varepsilon_{f,1}^*$	$\varepsilon_{f,2}^*$	$\varepsilon_{f,1}^*$	$\varepsilon_{f,2}^*$	$\varepsilon_{f,1}^*$	$\varepsilon_{f,2}^*$	$\varepsilon_{f,1}^*$	$\varepsilon_{f,2}^*$	$\varepsilon_{f,1}^*$	$\varepsilon_{f,2}^*$	$\varepsilon_{f,1}^*$	$\varepsilon_{f,2}^*$
196	0.339	0.326	0.546	0.362	0.723	0.419	0.295	0.274	0.469	0.289	0.620	0.305	0.266	0.233	0.421	0.237	0.555	0.233
392	0.529	0.558	0.704	0.600	0.839	0.670	0.479	0.494	0.628	0.512	0.750	0.537	0.444	0.440	0.577	0.441	0.686	0.440
588	0.678	0.715	0.812	0.752	0.909	0.815	0.632	0.658	0.748	0.673	0.841	0.702	0.598	0.605	0.701	0.603	0.786	0.606
784	0.788	0.818	0.883	0.848	0.950	0.897	0.749	0.774	0.833	0.785	0.901	0.812	0.719	0.730	0.793	0.725	0.857	0.730
980	0.864	0.885	0.928	0.906	0.973	0.943	0.834	0.853	0.892	0.861	0.940	0.884	0.810	0.820	0.861	0.813	0.907	0.820
1176	0.915	0.928	0.957	0.942	0.986	0.968	0.893	0.906	0.931	0.911	0.965	0.929	0.874	0.881	0.908	0.875	0.941	0.882
1372	0.949	0.954	0.975	0.964	0.993	0.982	0.933	0.940	0.957	0.943	0.980	0.957	0.919	0.923	0.940	0.917	0.963	0.923
1568	0.970	0.970	0.986	0.977	0.997	0.989	0.959	0.962	0.974	0.964	0.989	0.974	0.948	0.950	0.962	0.946	0.978	0.951
1764	0.984	0.980	0.993	0.984	0.999	0.993	0.975	0.976	0.984	0.977	0.994	0.984	0.968	0.968	0.976	0.965	0.987	0.969
1960	0.992	0.986	0.997	0.989	1.00	0.995	0.986	0.984	0.991	0.985	0.997	0.990	0.981	0.979	0.985	0.977	0.993	0.980
2156	0.997	0.989	0.999	0.992	1.00	0.996	0.992	0.989	0.995	0.990	0.999	0.994	0.988	0.986	0.991	0.985	0.996	0.987
2352	1.00	0.991	1.00	0.993	1.00	0.997	0.996	0.992	0.998	0.993	1.00	0.996	0.993	0.990	0.995	0.990	0.999	0.991

NTU = 3.0

C_w^*=1000	C^* = 0.2						C^* = 0.6						C^* = 1.0					
	R^* = 0.5		R^* = 1		R^* = 2		R^* = 0.5		R^* = 1		R^* = 2		R^* = 0.5		R^* = 1		R^* = 2	
t^*	$\varepsilon_{f,1}^*$	$\varepsilon_{f,2}^*$	$\varepsilon_{f,1}^*$	$\varepsilon_{f,2}^*$	$\varepsilon_{f,1}^*$	$\varepsilon_{f,2}^*$	$\varepsilon_{f,1}^*$	$\varepsilon_{f,2}^*$	$\varepsilon_{f,1}^*$	$\varepsilon_{f,2}^*$	$\varepsilon_{f,1}^*$	$\varepsilon_{f,2}^*$	$\varepsilon_{f,1}^*$	$\varepsilon_{f,2}^*$	$\varepsilon_{f,1}^*$	$\varepsilon_{f,2}^*$	$\varepsilon_{f,1}^*$	$\varepsilon_{f,2}^*$
105	0.080	0.253	0.159	0.283	0.280	0.315	0.046	0.113	0.087	0.114	0.147	0.108	0.028	0.054	0.060	0.054	0.104	0.054
210	0.229	0.470	0.363	0.521	0.523	0.578	0.153	0.267	0.230	0.277	0.316	0.277	0.106	0.157	0.165	0.160	0.228	0.157
315	0.402	0.641	0.557	0.696	0.713	0.758	0.298	0.431	0.396	0.448	0.493	0.458	0.226	0.293	0.302	0.298	0.373	0.293
420	0.564	0.765	0.710	0.814	0.839	0.869	0.454	0.581	0.554	0.602	0.648	0.620	0.368	0.440	0.447	0.444	0.517	0.440
525	0.699	0.851	0.820	0.891	0.915	0.932	0.597	0.705	0.687	0.725	0.768	0.747	0.510	0.578	0.583	0.581	0.646	0.578
630	0.802	0.908	0.893	0.938	0.958	0.966	0.716	0.801	0.789	0.818	0.854	0.840	0.638	0.696	0.698	0.696	0.750	0.696
735	0.875	0.944	0.940	0.966	0.981	0.984	0.808	0.870	0.863	0.883	0.911	0.902	0.744	0.789	0.790	0.788	0.831	0.789
840	0.925	0.967	0.968	0.982	0.99	0.993	0.875	0.917	0.914	0.927	0.948	0.942	0.825	0.859	0.858	0.857	0.889	0.859
945	0.957	0.980	0.985	0.991	0.998	0.997	0.921	0.949	0.947	0.955	0.971	0.967	0.885	0.908	0.907	0.906	0.929	0.908
1050	0.978	0.988	0.994	0.996	1.00	0.999	0.952	0.969	0.968	0.973	0.984	0.981	0.926	0.942	0.940	0.939	0.956	0.942
1155	0.990	0.993	1.00	0.999	1.00	1.00	0.971	0.981	0.982	0.984	0.991	0.990	0.954	0.964	0.962	0.962	0.973	0.964
1260	0.997	0.995	1.00	1.00	1.00	1.00	0.983	0.989	0.989	0.990	0.996	0.994	0.972	0.978	0.977	0.976	0.984	0.978

6.2 CROSS-FLOW HEAT EXCHANGERS

Transient performance effectiveness tables were generated for a step input change to the C_{min} fluid for the range of dimensionless parameters listed in table 6.9.

Table 6.9: Dimensionless Parameters Used in this Analysis for Direct Transfer Cross-Flow Heat Exchangers

Dimensionless Parameter	Parameter Values		
NTU	1.0		
C^*	0.2	0.6	1.0
R^*	0.5	1.0	2.0
C_w^*	1.0	10.0	1000.0
t_d^*	0.25	1.0	4.0

Transient temperature effectiveness values (ε_1^* and ε_2^*) generated for cross-flow heat exchangers are shown in Tables 6.10 - 6.12.

Table 6.10: Transient Temperature Effectiveness Values for NTU = 1.0, Wall Capacitance Ratio = 1.0, Cross-Flow Heat Exchangers

NTU = 1.0 $C_w^* = 1.0$

$t_d^*=0.25$	C* = 0.2						C* = 0.6						C* = 1.0					
	R* = 0.5		R* = 1		R* = 2		R* = 0.5		R* = 1		R* = 2		R* = 0.5		R* = 1		R* = 2	
t*	$\varepsilon_{f,1}^*$	$\varepsilon_{f,2}^*$	$\varepsilon_{f,1}^*$	$\varepsilon_{f,2}^*$	$\varepsilon_{f,1}^*$	$\varepsilon_{f,2}^*$	$\varepsilon_{f,1}^*$	$\varepsilon_{f,2}^*$	$\varepsilon_{f,1}^*$	$\varepsilon_{f,2}^*$	$\varepsilon_{f,1}^*$	$\varepsilon_{f,2}^*$	$\varepsilon_{f,1}^*$	$\varepsilon_{f,2}^*$	$\varepsilon_{f,1}^*$	$\varepsilon_{f,2}^*$	$\varepsilon_{f,1}^*$	$\varepsilon_{f,2}^*$
2.25	0.168	0.078	0.226	0.084	0.275	0.094	0.143	0.085	0.194	0.089	0.237	0.097	0.125	0.093	0.171	0.096	0.211	0.101
4.50	0.491	0.212	0.594	0.223	0.677	0.242	0.426	0.224	0.516	0.234	0.591	0.248	0.381	0.238	0.463	0.245	0.532	0.256
6.75	0.734	0.349	0.809	0.364	0.866	0.385	0.648	0.364	0.716	0.375	0.771	0.390	0.590	0.382	0.653	0.389	0.706	0.398
9.00	0.868	0.479	0.906	0.494	0.934	0.513	0.782	0.493	0.820	0.503	0.851	0.515	0.725	0.511	0.762	0.515	0.794	0.521
11.25	0.934	0.594	0.949	0.608	0.961	0.626	0.860	0.607	0.878	0.614	0.895	0.623	0.810	0.623	0.829	0.624	0.850	0.626
13.50	0.967	0.693	0.971	0.705	0.976	0.720	0.907	0.702	0.915	0.708	0.926	0.715	0.867	0.716	0.877	0.715	0.891	0.715
15.75	0.985	0.773	0.984	0.784	0.986	0.797	0.939	0.780	0.942	0.785	0.949	0.789	0.907	0.791	0.912	0.790	0.922	0.788
18.00	0.996	0.836	0.993	0.846	0.993	0.856	0.961	0.841	0.961	0.845	0.966	0.848	0.936	0.850	0.938	0.848	0.945	0.845
20.25	1.00	0.884	0.999	0.892	0.998	0.900	0.976	0.887	0.975	0.890	0.978	0.892	0.957	0.894	0.957	0.893	0.963	0.889
22.50	1.00	0.918	1.00	0.925	1.00	0.932	0.987	0.920	0.985	0.923	0.987	0.925	0.972	0.927	0.971	0.925	0.976	0.922
24.75	1.00	0.942	1.00	0.948	1.00	0.953	0.995	0.944	0.992	0.947	0.994	0.948	0.982	0.950	0.981	0.949	0.985	0.946
27.00	1.00	0.958	1.00	0.964	1.00	0.968	1.00	0.960	0.997	0.963	0.998	0.964	0.989	0.966	0.988	0.965	0.991	0.962

$t_d^*=1.0$	C* = 0.2						C* = 0.6						C* = 1.0					
	R* = 0.5		R* = 1		R* = 2		R* = 0.5		R* = 1		R* = 2		R* = 0.5		R* = 1		R* = 2	
t*	$\varepsilon_{f,1}^*$	$\varepsilon_{f,2}^*$	$\varepsilon_{f,1}^*$	$\varepsilon_{f,2}^*$	$\varepsilon_{f,1}^*$	$\varepsilon_{f,2}^*$	$\varepsilon_{f,1}^*$	$\varepsilon_{f,2}^*$	$\varepsilon_{f,1}^*$	$\varepsilon_{f,2}^*$	$\varepsilon_{f,1}^*$	$\varepsilon_{f,2}^*$	$\varepsilon_{f,1}^*$	$\varepsilon_{f,2}^*$	$\varepsilon_{f,1}^*$	$\varepsilon_{f,2}^*$	$\varepsilon_{f,1}^*$	$\varepsilon_{f,2}^*$
0.40	0.095	0.109	0.129	0.114	0.158	0.127	0.080	0.106	0.111	0.108	0.137	0.114	0.071	0.117	0.098	0.115	0.123	0.115
0.80	0.318	0.310	0.409	0.324	0.485	0.353	0.278	0.293	0.358	0.299	0.426	0.313	0.254	0.311	0.326	0.309	0.389	0.312
1.20	0.554	0.518	0.656	0.541	0.740	0.577	0.494	0.488	0.586	0.498	0.664	0.515	0.460	0.506	0.544	0.507	0.617	0.510
1.60	0.735	0.689	0.816	0.714	0.880	0.749	0.671	0.653	0.746	0.665	0.810	0.682	0.634	0.668	0.705	0.669	0.767	0.672
2.00	0.854	0.808	0.906	0.831	0.947	0.861	0.796	0.776	0.848	0.786	0.893	0.801	0.764	0.786	0.813	0.786	0.859	0.789
2.40	0.927	0.885	0.956	0.904	0.979	0.925	0.880	0.859	0.912	0.868	0.941	0.880	0.854	0.866	0.885	0.866	0.916	0.869
2.80	0.969	0.931	0.983	0.946	0.994	0.960	0.933	0.913	0.951	0.920	0.969	0.929	0.913	0.918	0.931	0.919	0.952	0.920
3.20	0.992	0.958	0.996	0.968	1.00	0.978	0.966	0.947	0.974	0.952	0.986	0.958	0.950	0.951	0.960	0.951	0.974	0.952
3.60	1.00	0.972	1.00	0.980	1.00	0.987	0.985	0.966	0.988	0.971	0.995	0.975	0.973	0.971	0.978	0.971	0.986	0.971
4.00	1.00	0.979	1.00	0.986	1.00	0.991	0.996	0.977	0.996	0.981	1.00	0.984	0.986	0.982	0.988	0.983	0.994	0.982
4.40	1.00	0.983	1.00	0.989	1.00	0.992	1.00	0.984	1.00	0.987	1.00	0.989	0.994	0.989	0.994	0.990	0.998	0.989
4.80	1.00	0.985	1.00	0.991	1.00	0.993	1.00	0.987	1.00	0.991	1.00	0.992	0.998	0.992	0.997	0.994	1.00	0.992

$t_d^*=4.0$	C* = 0.2						C* = 0.6						C* = 1.0					
	R* = 0.5		R* = 1		R* = 2		R* = 0.5		R* = 1		R* = 2		R* = 0.5		R* = 1		R* = 2	
t*	$\varepsilon_{f,1}^*$	$\varepsilon_{f,2}^*$	$\varepsilon_{f,1}^*$	$\varepsilon_{f,2}^*$	$\varepsilon_{f,1}^*$	$\varepsilon_{f,2}^*$	$\varepsilon_{f,1}^*$	$\varepsilon_{f,2}^*$	$\varepsilon_{f,1}^*$	$\varepsilon_{f,2}^*$	$\varepsilon_{f,1}^*$	$\varepsilon_{f,2}^*$	$\varepsilon_{f,1}^*$	$\varepsilon_{f,2}^*$	$\varepsilon_{f,1}^*$	$\varepsilon_{f,2}^*$	$\varepsilon_{f,1}^*$	$\varepsilon_{f,2}^*$
0.30	0.058	0.134	0.077	0.138	0.095	0.152	0.049	0.127	0.067	0.125	0.083	0.126	0.042	0.102	0.058	0.097	0.073	0.094
0.60	0.199	0.341	0.266	0.354	0.322	0.384	0.175	0.318	0.234	0.317	0.286	0.324	0.158	0.265	0.210	0.258	0.256	0.255
0.90	0.385	0.530	0.484	0.555	0.567	0.595	0.346	0.498	0.434	0.504	0.511	0.519	0.316	0.434	0.394	0.430	0.464	0.429
1.20	0.562	0.679	0.665	0.708	0.751	0.751	0.514	0.645	0.608	0.657	0.690	0.677	0.475	0.582	0.559	0.582	0.634	0.584
1.50	0.706	0.786	0.795	0.815	0.866	0.854	0.656	0.756	0.740	0.770	0.812	0.791	0.614	0.702	0.689	0.704	0.757	0.708
1.80	0.812	0.860	0.879	0.884	0.932	0.915	0.767	0.835	0.832	0.848	0.888	0.868	0.725	0.792	0.785	0.794	0.840	0.800
2.10	0.887	0.908	0.933	0.928	0.968	0.951	0.848	0.890	0.895	0.902	0.936	0.918	0.811	0.858	0.855	0.860	0.897	0.866
2.40	0.936	0.939	0.965	0.955	0.987	0.971	0.904	0.926	0.936	0.936	0.965	0.948	0.872	0.904	0.904	0.906	0.934	0.911
2.70	0.968	0.959	0.985	0.971	0.998	0.982	0.943	0.951	0.963	0.958	0.982	0.967	0.916	0.936	0.937	0.938	0.959	0.941
3.00	0.988	0.970	0.996	0.980	1.00	0.987	0.968	0.966	0.979	0.972	0.992	0.979	0.946	0.957	0.960	0.959	0.975	0.961
3.30	1.00	0.977	1.00	0.985	1.00	0.990	0.984	0.976	0.990	0.981	0.998	0.985	0.967	0.971	0.975	0.973	0.986	0.974
3.60	1.00	0.981	1.00	0.988	1.00	0.992	0.994	0.982	0.996	0.986	1.00	0.989	0.980	0.981	0.984	0.982	0.992	0.983

Table 6.11: Transient Temperature Effectiveness Values for NTU = 1.0, Wall Capacitance Ratio = 10.0, Cross-Flow Heat Exchangers

NTU = 1.0 C_w^* = 10.0																		
$0.25 < t_d^* < 1.0$	C* = 0.2						C* = 0.6						C* = 1.0					
	R* = 0.5		R* = 1		R* = 2		R* = 0.5		R* = 1		R* = 2		R* = 0.5		R* = 1		R* = 2	
t*	$\varepsilon_{f,1}^*$	$\varepsilon_{f,2}^*$	$\varepsilon_{f,1}^*$	$\varepsilon_{f,2}^*$	$\varepsilon_{f,1}^*$	$\varepsilon_{f,2}^*$	$\varepsilon_{f,1}^*$	$\varepsilon_{f,2}^*$	$\varepsilon_{f,1}^*$	$\varepsilon_{f,2}^*$	$\varepsilon_{f,1}^*$	$\varepsilon_{f,2}^*$	$\varepsilon_{f,1}^*$	$\varepsilon_{f,2}^*$	$\varepsilon_{f,1}^*$	$\varepsilon_{f,2}^*$	$\varepsilon_{f,1}^*$	$\varepsilon_{f,2}^*$
2	0.282	0.184	0.463	0.203	0.624	0.237	0.242	0.172	0.399	0.181	0.541	0.196	0.214	0.163	0.355	0.166	0.482	0.169
4	0.482	0.423	0.661	0.458	0.807	0.517	0.425	0.390	0.584	0.406	0.717	0.430	0.386	0.364	0.529	0.367	0.651	0.370
6	0.637	0.609	0.780	0.649	0.889	0.711	0.576	0.568	0.706	0.584	0.812	0.610	0.532	0.534	0.651	0.534	0.750	0.537
8	0.754	0.739	0.860	0.775	0.937	0.829	0.696	0.699	0.796	0.712	0.876	0.737	0.653	0.666	0.746	0.663	0.823	0.665
10	0.839	0.827	0.914	0.856	0.967	0.899	0.787	0.792	0.861	0.803	0.921	0.825	0.748	0.763	0.817	0.759	0.877	0.762
12	0.899	0.885	0.949	0.907	0.984	0.940	0.855	0.857	0.907	0.865	0.951	0.884	0.821	0.834	0.870	0.829	0.915	0.832
14	0.940	0.923	0.972	0.940	0.994	0.963	0.904	0.902	0.939	0.908	0.970	0.924	0.875	0.885	0.909	0.880	0.943	0.883
16	0.967	0.947	0.986	0.960	1.00	0.977	0.938	0.933	0.961	0.938	0.983	0.949	0.914	0.921	0.937	0.916	0.962	0.919
18	0.985	0.962	0.996	0.973	1.00	0.984	0.962	0.953	0.976	0.957	0.992	0.966	0.942	0.945	0.957	0.942	0.976	0.944
20	0.997	0.972	1.00	0.980	1.00	0.989	0.978	0.967	0.986	0.970	0.997	0.977	0.962	0.962	0.971	0.960	0.985	0.961
22	1.00	0.978	1.00	0.985	1.00	0.991	0.989	0.975	0.993	0.978	1.00	0.983	0.975	0.974	0.980	0.972	0.991	0.973
24	1.00	0.982	1.00	0.988	1.00	0.993	0.996	0.981	0.998	0.984	1.00	0.988	0.985	0.982	0.987	0.981	0.995	0.981
$1.0 < t_d^* < 4.0$	C* = 0.2						C* = 0.6						C* = 1.0					
	R* = 0.5		R* = 1		R* = 2		R* = 0.5		R* = 1		R* = 2		R* = 0.5		R* = 1		R* = 2	
t*	$\varepsilon_{f,1}^*$	$\varepsilon_{f,2}^*$	$\varepsilon_{f,1}^*$	$\varepsilon_{f,2}^*$	$\varepsilon_{f,1}^*$	$\varepsilon_{f,2}^*$	$\varepsilon_{f,1}^*$	$\varepsilon_{f,2}^*$	$\varepsilon_{f,1}^*$	$\varepsilon_{f,2}^*$	$\varepsilon_{f,1}^*$	$\varepsilon_{f,2}^*$	$\varepsilon_{f,1}^*$	$\varepsilon_{f,2}^*$	$\varepsilon_{f,1}^*$	$\varepsilon_{f,2}^*$	$\varepsilon_{f,1}^*$	$\varepsilon_{f,2}^*$
2	0.283	0.256	0.464	0.281	0.626	0.323	0.245	0.231	0.403	0.240	0.545	0.252	0.218	0.213	0.360	0.211	0.488	0.208
4	0.485	0.497	0.664	0.537	0.812	0.600	0.432	0.455	0.592	0.470	0.727	0.493	0.395	0.422	0.539	0.421	0.663	0.420
6	0.641	0.665	0.784	0.705	0.894	0.767	0.584	0.620	0.716	0.636	0.823	0.663	0.545	0.584	0.665	0.584	0.765	0.586
8	0.758	0.778	0.865	0.812	0.942	0.864	0.705	0.738	0.806	0.752	0.887	0.779	0.666	0.707	0.759	0.704	0.838	0.709
10	0.843	0.853	0.917	0.880	0.970	0.920	0.796	0.821	0.869	0.832	0.929	0.856	0.761	0.796	0.830	0.792	0.890	0.798
12	0.902	0.903	0.952	0.923	0.986	0.952	0.863	0.878	0.914	0.887	0.957	0.906	0.832	0.859	0.881	0.855	0.926	0.861
14	0.942	0.934	0.974	0.950	0.996	0.970	0.910	0.917	0.945	0.923	0.975	0.939	0.884	0.903	0.918	0.900	0.951	0.905
16	0.969	0.954	0.988	0.966	1.00	0.980	0.943	0.943	0.965	0.948	0.987	0.960	0.922	0.934	0.944	0.931	0.969	0.935
18	0.986	0.967	0.997	0.977	1.00	0.986	0.966	0.960	0.979	0.964	0.994	0.973	0.948	0.955	0.962	0.953	0.980	0.956
20	1.00	0.975	1.00	0.983	1.00	0.989	0.981	0.971	0.989	0.975	0.999	0.981	0.966	0.969	0.975	0.968	0.988	0.970
22	1.00	0.980	1.00	0.987	1.00	0.991	0.991	0.978	0.995	0.982	1.00	0.986	0.978	0.978	0.984	0.978	0.993	0.979
24	1.00	0.983	1.00	0.989	1.00	0.992	0.998	0.983	0.999	0.986	1.00	0.989	0.987	0.985	0.990	0.985	0.997	0.985

Table 6.12: Transient Temperature Effectiveness Values for NTU =1.0 Wall Capacitance Ratio = 1000, Cross-Flow Heat Exchangers

NTU = 1.0																		
C_w^*=1000	$C^*=0.2$						$C^*=0.6$						$C^*=1.0$					
	$R^*=0.5$		$R^*=1$		$R^*=2$		$R^*=0.5$		$R^*=1$		$R^*=2$		$R^*=0.5$		$R^*=1$		$R^*=2$	
t^*	$\varepsilon_{f,1}^*$	$\varepsilon_{f,2}^*$	$\varepsilon_{f,1}^*$	$\varepsilon_{f,2}^*$	$\varepsilon_{f,1}^*$	$\varepsilon_{f,2}^*$	$\varepsilon_{f,1}^*$	$\varepsilon_{f,2}^*$	$\varepsilon_{f,1}^*$	$\varepsilon_{f,2}^*$	$\varepsilon_{f,1}^*$	$\varepsilon_{f,2}^*$	$\varepsilon_{f,1}^*$	$\varepsilon_{f,2}^*$	$\varepsilon_{f,1}^*$	$\varepsilon_{f,2}^*$	$\varepsilon_{f,1}^*$	$\varepsilon_{f,2}^*$
196	0.379	0.352	0.583	0.390	0.757	0.450	0.332	0.315	0.511	0.330	0.666	0.349	0.298	0.284	0.459	0.285	0.600	0.283
392	0.577	0.590	0.742	0.632	0.870	0.701	0.521	0.543	0.671	0.559	0.792	0.587	0.481	0.502	0.617	0.502	0.729	0.502
588	0.725	0.743	0.845	0.780	0.933	0.838	0.670	0.700	0.784	0.714	0.874	0.742	0.630	0.663	0.734	0.660	0.820	0.663
784	0.829	0.840	0.910	0.868	0.968	0.912	0.781	0.805	0.861	0.816	0.925	0.841	0.744	0.776	0.819	0.771	0.883	0.776
980	0.898	0.899	0.950	0.920	0.986	0.951	0.859	0.874	0.913	0.882	0.957	0.902	0.827	0.852	0.878	0.847	0.925	0.852
1176	0.943	0.935	0.975	0.951	0.997	0.972	0.912	0.918	0.947	0.924	0.977	0.939	0.886	0.903	0.920	0.899	0.953	0.903
1372	0.972	0.957	0.990	0.969	1.00	0.983	0.948	0.946	0.969	0.951	0.989	0.962	0.927	0.937	0.948	0.934	0.972	0.937
1568	0.990	0.970	0.999	0.979	1.00	0.988	0.971	0.964	0.983	0.967	0.996	0.976	0.954	0.959	0.966	0.957	0.983	0.959
1764	1.00	0.978	1.00	0.985	1.00	0.991	0.986	0.975	0.992	0.978	1.00	0.984	0.972	0.973	0.979	0.971	0.991	0.973
1960	1.00	0.982	1.00	0.988	1.00	0.993	0.995	0.981	0.997	0.984	1.00	0.988	0.983	0.982	0.987	0.981	0.995	0.982
2156	1.00	0.985	1.00	0.990	1.00	0.994	1.00	0.985	1.00	0.988	1.00	0.991	0.991	0.988	0.992	0.988	0.998	0.988
2352	1.00	0.986	1.00	0.991	1.00	0.994	1.00	0.988	1.00	0.991	1.00	0.992	0.996	0.991	0.996	0.992	1.00	0.991

7
Discussion of Results

The number of transfer units (NTU) noticeably affects the t^* range for $\overline{C}_w^* = 10$ and $\overline{C}_w^* = 1000$. The t^* range decreases as the NTU value increases for a given $\overline{C}_w^*$. It takes less time to achieve steady state for higher NTU values. NTU is the result of the basic parameters shown in equation 7.1.

$$\mathrm{NTU} = \frac{1}{\left(\dot{m}c_p\right)_{\min}\left[\frac{1}{(hA)_{\min}} + \frac{1}{(hA)_{\max}}\right]} \tag{7.1}$$

For NTU to increase, the mass flowrate, specific heat of the minimum capacity rate fluid, or both must decrease. This translates to slower fluid velocities or lower fluid specific heats. Conversely, the convection coefficients or surface areas must increase.

The ratio of the wall thermal capacitance to the fluid capacitance is defined by $\overline{C}_w^*$. The t^* range increases as $\overline{C}_w^*$ increases. It will take longer to reach steady-state with increased wall mass caused by either a higher density wall material, a thicker wall between the fluids, a higher specific heat material, or a combination of all three parameters. Equation 7.2 shows the practical parameters affecting $\overline{C}_w^*$.

$$\overline{C}_w^{\,*} = \frac{\overline{C}_w}{\overline{C}_{min}} = \frac{\left(Mc_p\right)_w}{\left(\rho c_p AL\right)_{min}} = \frac{\rho_{wall} L(wdth) thk_{wall} c_{pwall}}{\left(\rho c_p hgt(wdth)L\right)_{min}} \tag{7.2}$$

Conversely, an increased $\overline{C}_w^*$ could be caused by a less dense fluid, lower specific heat C_{min} fluid, or a narrower C_{min} fluid passage. $\overline{C}_w^*$ is one of the more important parameters in the transient performance of heat exchangers. The effects of t_d^*, R^*, C^*, and NTU are dependent on the value of $\overline{C}_w^*$.

As C^* increases, the time required to achieve the new steady state temperature effectiveness values increases for the C_{min} fluid, all other parameters held constant. An increasing C^* value appears to have no significant effect on the time for the C_{max} fluid. The C^* range for the tables generated are from 0.2 to 1.0 which indicates the lower capacity rate fluid heat capacity rate is increasing to approach the higher capacity rate fluid heat capacity. Equation 7.3 shows the parameters associated with C^*.

$$C^* = \frac{C_{min}}{C_{max}} = \frac{\left(\dot{m}c_p\right)_{min}}{\left(\dot{m}c_p\right)_{max}} = \frac{\left(\rho AVc_p\right)_{min}}{\left(\rho AVc_p\right)_{max}} = \frac{\left(\rho(hgt)wdthVc_p\right)_{min}}{\left(\rho(hgt)wdthVc_p\right)_{max}} \tag{7.3}$$

Increasing the mass flowrate of the C_{min} fluid will increase C^*, which increases the time to reach steady state temperature. Increasing the height of the fluid passage, or the velocity of the C_{min} fluid are two ways to achieve a larger C^*. An increased passage height increases the amount of fluid to be heated or cooled. An increased velocity, reduces the dwell time, which will increase the heat up or cool down time of the C_{min} fluid. The C_{max} fluid is not significantly changed over the range of C^* values due to it not being the stepped fluid, and having either a higher specific heat, fluid velocity, fluid passage height, or density relative to the stepped fluid. Those parameters translate into a higher mass flowrate or specific heat up until $C^* = 1$.

An increasing R^* leads to an increasing temperature effectiveness value for a given t^*, all other parameters held constant. This indicates the steady state condition is being achieved faster as R^* increases. Equation 7.4 shows the parameters for R^*.

$$R^* = \frac{(hA)_{max}}{(hA)_{min}} = \frac{(hLwdth)_{max}}{(hLwdth)_{min}} \tag{7.4}$$

An increase in h for the higher capacity rate fluid leads to an increase in R^*, which indicates the heat transfer or convective heat transfer coefficient of the C_{max} fluid is higher requiring less time to achieve the new steady state temperature effectiveness values for both fluids.

The parameter t_d^* affected the temperature effectiveness values for $\overline{C}_w^*$ equal to 1.0 and 10.0. It had negligible effect for $\overline{C}_w^*$ equal to 1000. For a thick wall, it reaches a point where the dwell time of the fluid has minimal effect on the temperature effectiveness values. Equation 7.5 shows the parameters associated with t_d^*.

$$t_d^* = \frac{t_{d,min}}{t_{d,max}} = \frac{\left(\frac{L}{V}\right)_{min}}{\left(\frac{L}{V}\right)_{max}} = \frac{\left(\frac{Lwdth(hgt)\rho}{\dot{m}}\right)_{min}}{\left(\frac{Lwdth(hgt)\rho}{\dot{m}}\right)_{max}} \tag{7.5}$$

The lower capacity rate fluid approaches the new steady state temperature effectiveness value faster than the higher capacity rate fluid with all other parameters held constant. The temperature effectiveness values exhibit an expected exponential relation with time.

The performance tables generated and published in the results section are very useful for determining transient outlet temperatures for each fluid over time for parallel and cross-flow heat exchangers. The dimensionless parameters cover the wide range of specific governing parameters for parallel-flow heat exchangers listed in Table 6.1. The sample tables generated for cross-flow are also very useful, yet limited in range.

This technique can be easily modified for other geometries, radiation, and wall thermal capacitance. Future considerations would be to calculate the temperature effectiveness values for a step input to the C_{max} fluid, determine a scheme and generate tables for modeling cross-flow heat exchangers with both or one fluid mixed, and complete the cross-flow effectiveness tables for a stepped C_{min} fluid validated in this thesis.

8
Conclusion

This thesis presents a new technique for solving the transient outlet temperature response for parallel-flow and cross-flow heat exchangers utilizing Thermonet - a thermal network solver. It also presents a new range of parameters investigated. Thermonet solutions are verified to within a maximum percent mean difference of 4 % of analytical solutions for parallel-flow, and 8 % of analytical solutions for cross-flow heat exchangers.

Parallel and cross-flow heat exchangers are modeled utilizing two fluids separated by a wall. The fluids and wall regions are represented by nodes. Resistors separate the fluid and wall nodes and represent convective and fluid flow resistances. Node linking and orientation determine the heat exchanger configuration to be either parallel or cross-flow. The cross-flow model is for a single-pass, both fluids unmixed cross-flow heat exchanger. Outlet temperatures calculated for cross-flow are mean outlet temperatures.

For accuracy and minimized computer run time, the parallel-flow heat exchanger was divided into 10 segments for NTU $\leq$ 2, and 20 segments for 2 $\leq$ NTU $\leq$ 10. The cross-flow heat exchanger was divided into 6 x 6 segments for NTU $\leq$ 1.0, and 10 x 10 segments for 1 $\leq$ NTU $\leq$ 2. A timestep of half the dwell time of the highest velocity fluid was sufficient for all cases.

Transient outlet temperature effectiveness (ε_1^* and ε_2^*) values were generated for a step change to the C_{min} fluid for a parallel-flow direct-transfer type heat exchanger. These values were generated for a new, wider range of dimensionless parameters which include NTU, C^*, R^*, $\overline{C}_w^*$, t_d^*, and t^*. Transient mean outlet temperature effectiveness (ε_1^* and ε_2^*) values were generated for a step change to the C_{min} fluid for a single pass, both fluids unmixed cross-flow direct-transfer type heat exchanger. New tables were generated for NTU = 1.0 and the following range of dimensionless parameters which include C^*, R^*, $\overline{C}_w^*$, t_d^*, and t^*.

The transient performance tables generated in this thesis are very useful for determining transient outlet temperatures for each fluid for parallel and cross-flow heat exchangers. Application of the new tables generated requires calculation of dimensionless parameters listed in the tables specific for one's application. The transient outlet temperature is calculated from the tables effectiveness values for the specific time or times of interest.

9
References

Bunce, D.J., 1995, "Transient Response of Heat Exchangers," Master's thesis, RIT Department of Mechanical Engineering, May, 1995.

Bunce, D.J., and Kandlikar, S.G., 1995, "Transient Response of Heat Exchangers ," Presented at the Second ASME-ISHMT conference in Mangalore, India, December 28-30, 1995.

Chen, H., Chen, K., 1992, "Transient Response of Crossflow Heat Exchangers with Finite Wall Capacitance," Transactions of ASME, *Journal of Heat Transfer*, Vol. 114, August, 1992, pp. 752 - 755.

Chen, H., Chen, K., 1991, "Simple Method for Transient Response of Gas-to-Gas Cross-Flow Heat Exchangers with Neither Gas Mixed," *International Journal of Heat and Mass Transfer*, Vol. 34, No. 11, November, 1991, pp. 2891 - 2898.

Cima, R.M., London, A.L., 1958, "The Transient Response of a Two-Fluid Counterflow Heat Exchanger- The Gas-Turbine Regenerator," Transactions of ASME, Vol. 80, No.5, pp.1169-1179.

Cole, B.D., Kandlikar, S.G., 1995, "Transient Performance of Parallel-Flow Heat Exchanger with a Step Temperature Change on Minimum Capacity Rate Fluid Stream," Presented at the 2nd European Thermal-Sciences and 14th UIT National Heat Transfer Conference, Rome, May 29 - 31, 1996.

Gvozdenac, D.D., 1987, "Analytical Solution of Transient Response of Gas-to-Gas Parallel and Counterflow Heat Exchangers," Transactions of ASME, *Journal of Heat Transfer*, Vol. 109, No. 4, pp. 848-855.

Gvozdenac, D.D., 1986, "Analytical Solution of Transient Response of Gas-to-Gas Crossflow Heat Exchanger with Both Fluids Unmixed," Transactions of ASME, *Journal of Heat Transfer*, Vol. 108, November, 1986, pp. 722 - 727.

Incropera, F.P., DeWitt, D.P., 1985, *Fundamentals of Heat and Mass Transfer*, 2nd Edition, John Wiley & Sons, New York.

Kandlikar, S.G., Bunce, D.J., and Cole, B.D., 1995, "Transient Performance of Counter-flow Heat Exchanger with a Step Temperature Change on Minimum Capacity Rate Fluid Stream," Presented at the Proceedings of the Symposium on Thermal Science and Engineering in honor of Chancellor Chang-Lin Tien at the University of California, Berkeley, November 14, 1995.

Kays, W.M., London, A.L., 1964, *Compact Heat Exchangers* , Second Edition, McGraw-Hill, New York.

Li, C.H., 1986, "Exact Transient Solutions of Parallel-Current Transfer Processes ," Transactions of ASME, *Journal of Heat Transfer*, Vol. 108, No. 2, pp. 365-369.

London, A.L., Sampsell, D.F., McGowan, J.G., 1964, "The Transient Response of Gas Turbine Plant Heat Exchangers--Additional Solutions for Regenerators of the Periodic-Flow and Direct-Transfer Types," Transactions of ASME, *Journal of Engineering for Power*, Vol. 86, pp. 127-135.

London, A.L., Biancardi, F.R., Mitchell, J.W., 1959, "The Transient Response of Gas-Turbine-Plant Heat Exchangers--Regenerators, Intercoolers, Precoolers, and Ducting ," Transactions of ASME, *Journal of Engineering for Power*, Vol 81, October, pp. 433-448.

Myers, G.E., Mitchell, J.W., Lindeman, C.F., 1970, "The Transient Response of Heat Exchangers Having an Infinite Capacitance Rate Fluid," Transactions of ASME, *Journal of Heat Transfer*, Vol. 92, Series C, No. 2, pp. 269-275.

Myers, G.E., Mitchell, J.W., Norman, R.F., 1967, "The Transient Response of Crossflow Heat Exchangers, Evaporators, and Condensers," Transactions of ASME, *Journal of Heat Transfer*, Vol. 89, No. 1, pp. 75-80.

Rizika, J.W., 1956, "Thermal Lags in Flowing Incompressible Fluid Systems Containing Heat Capacitors," Transactions of ASME, Vol. 78, October, pp.1407-1413.

Romie, F.E., 1985, "Transient Response of Parallel-Flow Heat Exchanger," *Journal of Heat Transfer*, Vol. 107, pp. 727-730.

Romie, F.E., 1983, "Transient Response of Gas-to-Gas Crossflow Heat Exchangers With Neither Gas Mixed," Transactions of ASME, *Journal of Heat Transfer*, Vol. 105, No. 3, pp. 563-570.

Shah, R.K., 1981, *Heat Exchangers - Thermal-Hydraulic Fundamentals and Design*, "Classification of Heat Exchangers," edited by Kakac, S., Bergles, A.E., and Mayinger, F., Hemisphere Corp., Washington.

Shah, R.K., 1981, *Heat Exchangers - Thermal-Hydraulic Fundamentals and Design*, "The Transient Response of Heat Exchangers," edited by Kakac, S., Bergles, A.E., and Mayinger, F., Hemisphere Corp., Washington.

Spiga, G., Spiga, M., 1988, "Transient Temperature Fields in Crossflow Heat Exchangers with Finite Wall Capacitance," Transactions of ASME, *Journal of Heat Transfer*, Vol. 110, February, 1988, pp. 49 - 53.

Spiga, G., Spiga, M., 1987, "Two-Dimensional Transient Solutions for Crossflow Heat Exchangers with Neither Gas Mixed," Transactions of ASME, *Journal of Heat Transfer*, Vol. 109, May, 1987, pp. 281 286.

THERMONET-TransHX, Thermal Network Solver, 1995, Commercial software developed by THERMONET Ltd., Rochester, NY.

Yamashita, H., Izumi, R., Yamaguchi, S., "Analysis of the Dynamic Characteristics of Cross-Flow Heat Exchangers with Both Fluids Unmixed," Bulletin of the JSME, Vol. 21, No. 153, March, 1978.

10
Appendices

Appendix A

Practical Application of Transient Temperature Effectiveness Tables:

Design Parameters Required for Applying tables to determine transient outlet temperature response to step input change of C_{min} fluid:

Heat Exchanger Dimensions:

L	Length
wdth	Width
hgt_{min}	Height of passage for C_{min} fluid
hgt_{max}	Height of passage for C_{max} fluid
thk_{wall}	Thickness of exchanger wall separating both fluids

Material Information:

Separating Wall:

ρ_{wall}	Density of material
$c_{p,wall}$	Specific heat at constant pressure
k_{wall}	Thermal conductivity

C_{min} Fluid:

$\dot{V}_{min}$	Volumetric flow rate
ρ_{min}	Density
$c_{p,min}$	Specific heat at constant pressure
h_{min}	Convective heat transfer coefficient

$T_{in,min}(0)$	Inlet temperature before step change
$T_{in,min}(\infty)$	Inlet temperature after step change

C_{max} Fluid:

$\dot{V}_{max}$	Volumetric flow rate
ρ_{max}	Density
$c_{p,max}$	Specific heat at constant pressure
h_{max}	Convective heat transfer coefficient
$T_{in,max}(0)$	Inlet temperature before step change
$T_{in,max}(\infty)$	Inlet temperature after step change

How to use Tables:

1. Determine dimensionless parameters NTU, C^*, R^*, $\overline{C}_w^*$, t_d^*, and t^* from design information listed above.
2. Find effectiveness values versus t^* from transient tables for dimensionless parameters calculated in step 1.
3. Calculate steady-state outlet temperatures for both fluids before and after the step input using the effectiveness-NTU method (Incropera et al. 1985), knowing NTU and C^*.
4. For a specific time, calculate t^* to find the appropriate effectiveness values for each fluid.

5. Calculate transient outlet temperature response by rearranging effectiveness equations (Fluid 1 => C_{min} fluid, Fluid 2 => C_{max} fluid):

$$\varepsilon_{f,1}^{*} = \frac{T_1(t) - T_1(0)}{T_1(\infty) - T_1(0)}$$
$$\Rightarrow T_{out,1}(t) = \varepsilon_1^{*}\left[T_{out,1}(\infty) - T_{out,1}(0)\right] + T_{out,1}(0)$$

$$\varepsilon_{f,2}^{*} = \frac{T_2(t) - T_2(0)}{T_2(\infty) - T_2(0)}$$
$$\Rightarrow T_{out,2}(t) = \varepsilon_2^{*}\left[T_{out,2}(\infty) - T_{out,2}(0)\right] + T_{out,2}(0)$$

ple Problem - Use of Tables:

GIVEN: Parallel-Flow Single Pass Heat Exchanger (Cooling Coil) with conditions shown in Figure 1

Figure 1: Direct Transfer Parallel-flow Heat Exchanger

Air - Stepped Fluid

T_{air} (0) = 70 C
T_{air} (0+) = 140 C
Flowrate = 48.9 m^3/min
h = 3135 W/m^2 °C

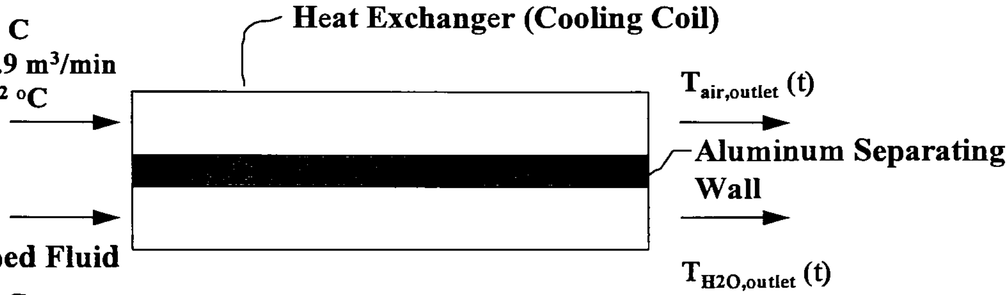

Water - Unstepped Fluid

T_{H2O} (0) = 20 C
T_{H2O} (0+) = 20 C
Flowrate = .072 m^3/min
h = 1568 W/m^2 °C

INITIAL CONDITIONS:	BOUNDARY CONDITIONS:
T_{air} (0) = 70 °C	T_{air} (0+) = 140 °C
T_{H2O} (0) = 20 °C	T_{H2O} (0+) = 20 °C

COIL DIMENSIONS:

Length = 1.6 meters
Width = 0.6 meters
Height of air passage = 2.000 meters
Height of water passage = 0.012 meters
Separating wall thickness = 0.01 meters

FIND: Outlet Temperature of Air and Water at time = 9.41 seconds, and time = 47.04 seconds after step input change.

EQUATIONS: Refer to Solutions.

ASSUMPTIONS:

1. Constant fluid properties
2. Negligible radiation effects
3. Negligible heat loss to surroundings
4. No thermal energy sources within coil
5. Wall thermal resistance is negligible

SOLUTION:

Design Parameters Required for Applying tables to determine transient outlet temperature response to step input change of
C_{min} fluid:

Heat Exchanger Dimensions:

L	Length = 1.6 meters
wdth	Width = 0.6 meters
hgt_{min}	Height of passage for C_{min} fluid = 2.000 m
hgt_{max}	Height of passage for C_{max} fluid = 0.012 m
thk_{wall}	Thickness of exchanger wall separating both fluids = 0.01 meters

Material Information:

Separating Wall - Aluminum:

ρ_{wall}	Density of material = 2702 kg/m^3
$c_{p,wall}$	Specific heat at constant pressure = 903 J/kg ^oC
k_{wall}	Thermal conductivity = 240 W/m ^oC

C_{min} Fluid - Air:

$\dot{V}_{min}$	Volumetric flowrate = 48.9 m^3/min
ρ_{min}	Density = 1.225 kg/m^3
$c_{p,min}$	Specific heat at constant pressure = 1003 J/kg ^oC
h_{min}	Convective heat transfer coefficient = 3135 W/m^2 ^oC
$T_{in,min}(0)$	Inlet temperature before step change = 70 ^oC
$T_{in,min}(\infty)$	Inlet temperature after step change = 140 ^oC

C_{max} Fluid - Water:

$\dot{V}_{max}$	Volumetric flowrate= 0.072 m^3/min
ρ_{max}	Density= 997.1 kg/m^3
$c_{p,max}$	Specific heat at constant pressure = 4180 J/kg ^oC
h_{max}	Convective heat transfer coefficient = 1568 W/m^2 ^{o} C

$T_{in,max}(0)$	Inlet temperature before step change = 20 °C
$T_{in,max}(\infty)$	Inlet temperature after step change = 20 °C

1. Determine dimensionless parameters NTU, C^*, R^*, $\overline{C}_w^*$, and t_d^* from design information listed above.

$$NTU = 1.000$$

$$\overline{C}_w^* = 10$$

$$C^* = 0.2$$

$$R^* = 0.5$$

$$t_d^* = 0.25$$

2. Find effectiveness values versus t^* from transient tables for dimensionless parameters calculated in step 1.

3. Calculate steady-state outlet temperatures for both fluids before and after the step input using the effectiveness-NTU method (Incropera et al. 1985), knowing NTU and C^*.

Parallel-Flow Formula:

$$\varepsilon = \frac{\left[1 - EXP\left(-NTU\left(1 + C^*\right)\right)\right]}{\left[1 + C^*\right]} = 0.5823$$

Steady-State Outlet Temperatures:

C_{min} : $$T_{out,min}(t) = T_{in,min}(t) - \varepsilon\left[T_{in,min}(t) - T_{in,max}(t)\right]$$

C_{max} : $$T_{out,max}(t) = T_{in,max}(t) + \varepsilon\, C^*\left[T_{in,min}(t) - T_{in,max}(t)\right]$$

Before Step Input:

C_{min}: T_{out} = 40.88 °C

C_{max}: T_{out} = 25.82 °C

After Step Input:

C_{min}: $T_{out} =$ 70.12 °C

C_{max}: $T_{out} =$ 33.97 °C

4. For a specific time, calculate t^* to find the appropriate effectiveness values for each fluid.

AT $t = 9.41$ seconds => $t^* = 4$ => $\varepsilon_{f,1}^* = 0.438$, $\varepsilon_{f,2}^* = 0.363$

AT $t = 47.04$ seconds => $t^* = 20$ => $\varepsilon_{f,1}^* = 0.987$, $\varepsilon_{f,2}^* = 0.984$

5. Calculate transient outlet temperature response by rearranging effectiveness equations:

C_{min}:

$$\varepsilon_{f,1}^* = \frac{T_1(t) - T_1(0)}{T_1(\infty) - T_1(0)} \Rightarrow T_{out,1}(t) = \varepsilon_1^*\left[T_{out,1}(\infty) - T_{out,1}(0)\right] + T_{out,1}(0)$$

C_{max} :

$$\varepsilon_{f,2}^* = \frac{T_2(t) - T_2(0)}{T_2(\infty) - T_2(0)} \Rightarrow T_{out,2}(t) = \varepsilon_2^*\left[T_{out,2}(\infty) - T_{out,2}(0)\right] + T_{out,2}(0)$$

AT $t = 9.41$ seconds:

Air: $T_{out}(9.41) = 53.68$ °C

Water: $T_{out}(9.41) = 28.78$ °C

AT $t = 47.04$ seconds:

Air: $T_{out}(47.04) = 69.74$ °C

Water: $T_{out}(47.04) = 33.84$ °C

Appendix B

Sample Spreadsheets for Parallel-flow and Cross-Flow Temperature Effectiveness Calculations:

Parallel-Flow:

1. **10 segment model**
2. **20 segment model**

Cross-Flow:

1. **3 x 3 segment model**
2. **6 x 6 segment model**
3. **10 x 10 segment model**

Data Generation
Parallel-Flow 10 Segment Model

Thermonet Input:											
NOTE: Values required as input are highlighted.											
NOTE: Change value of (h)min to obtain proper value of NTU											
Dimensions:			Cmin fluid a - Stepped			Cmax fluid b - Unstepped			Wall		
Total	Width	#	Mass			Mass			Thickness		
Length		Segments	Flowrate	h	Height	Flowrate	h	Height			
(Meters)	(Meters)		(Kg/s)	(W/m^2 Deg C)	(m)	(Kg/s)	(W/m^2 Deg C)	(m)	(Meters)		
6	0.6	10	1	5837.5	0.003175	5	2918.75	0.03175	0.021834034		
Materials:											
Cmin fluid - Engine Oil		Cmax fluid - Engine Oil		Wall - Aluminum							
Density	Cp	Density	Cp	Density	k	Cp					
(Kg/m^3)	(J/kg Deg. C)	(Kg/m^3)	(J/kg Deg. C)	(Kg/m^3)	(W/m Deg. C)	(J/kg Deg. C)					
890	1868	890	1868	2702	240	903					
										Effectiveness-NTU	
						Dwell time				Analytical Calculations:	
U	R*	Cw*	C*	NTU	td*	of Cmin fluid	Effectiveness	Tin, Fluid a	Tin, Fluid b	Tout, Fluid a	Tout, Fluid b
1846.833333	0.5	10	0.2	1	0.5	2.71272	0.582338157	70	20	40.883	25.823
								140	20	70.119	33.976
Resistor	Node A	Node B	Always Zero	& conduction	R - Value	Always Zero					
				3 = Fluid Flow							
101	101	102	0	3	0.000535332	0	0	0	0	0	
102	102	103	0	3	0.000535332	0	0	0	0	0	
103	103	104	0	3	0.000535332	0	0	0	0	0	
104	104	105	0	3	0.000535332	0	0	0	0	0	
105	105	106	0	3	0.000535332	0	0	0	0	0	
106	106	107	0	3	0.000535332	0	0	0	0	0	
107	107	108	0	3	0.000535332	0	0	0	0	0	
108	108	109	0	3	0.000535332	0	0	0	0	0	
109	109	110	0	3	0.000535332	0	0	0	0	0	
110	110	1	0	3	0.000535332	0	0	0	0	0	
201	201	202	0	3	0.000107066	0	0	0	0	0	
202	202	203	0	3	0.000107066	0	0	0	0	0	
203	203	204	0	3	0.000107066	0	0	0	0	0	
204	204	205	0	3	0.000107066	0	0	0	0	0	
205	205	206	0	3	0.000107066	0	0	0	0	0	
206	206	207	0	3	0.000107066	0	0	0	0	0	
207	207	209	0	3	0.000107066	0	0	0	0	0	
208	208	208	0	3	0.000107066	0	0	0	0	0	
209	209	210	0	3	0.000107066	0	0	0	0	0	
210	210	2	0	3	0.000107066	0	0	0	0	0	
301	101	301	0	0	0.00178444	0	0	0	0	0	
302	102	302	0	0	0.00178444	0	0	0	0	0	
303	103	303	0	0	0.00178444	0	0	0	0	0	
304	104	304	0	0	0.00178444	0	0	0	0	0	
305	105	305	0	0	0.00178444	0	0	0	0	0	
306	106	306	0	0	0.00178444	0	0	0	0	0	
307	107	307	0	0	0.00178444	0	0	0	0	0	
308	108	308	0	0	0.00178444	0	0	0	0	0	
309	109	309	0	0	0.00178444	0	0	0	0	0	

Data Generation
Parallel-Flow 10 Segment Model

310	110	310	0	0	0.00178444	0	0	0	0	0
401	201	301	0	0	0.003568878	0	0	0	0	0
402	202	302	0	0	0.003568878	0	0	0	0	0
403	203	303	0	0	0.003568878	0	0	0	0	0
404	204	304	0	0	0.003568878	0	0	0	0	0
405	205	305	0	0	0.003568878	0	0	0	0	0
406	206	306	0	0	0.003568878	0	0	0	0	0
407	207	307	0	0	0.003568878	0	0	0	0	0
408	208	308	0	0	0.003568878	0	0	0	0	0
408	208	308	0	0	0.003568879	0	0	0	0	0
410	210	310	0	0	0.003568878	0	0	0	0	0

Node #	Initial Temperature (Degrees C)	Always Zero	Always Zero	Node Volume (Meters^2)	Node Material	Time Classes
1	40.841025	0	0	0.0003	Oil	1
2	25.811777	0	0	0.0030	Oil	1
101	70	0	0	0.0003	Oil	2
102	85.305374	0	0	0.0003	Oil	1
103	81.138702	0	0	0.0003	Oil	1
104	57.443375	0	0	0.0003	Oil	1
105	54.183521	0	0	0.0003	Oil	1
106	51.253208	0	0	0.0003	Oil	1
107	48.670803	0	0	0.0003	Oil	1
108	46.37836	0	0	0.0003	Oil	1
109	44.348098	0	0	0.0003	Oil	1
110	42.54182	0	0	0.0003	Oil	1
201	20	0	0	0.0030	Oil	3
202	20.838925	0	0	0.0030	Oil	1
203	21.772057	0	0	0.0030	Oil	1
204	22.51132	0	0	0.0030	Oil	1
205	23.167288	0	0	0.0030	Oil	1
206	23.748348	0	0	0.0030	Oil	1
207	24.265827	0	0	0.0030	Oil	1
208	24.724113	0	0	0.0030	Oil	1
209	25.130766	0	0	0.0030	Oil	1
210	25.4816	0	0	0.0030	Oil	1
301	51.771637	0	0	0.0021	Aluminum	1
302	48.130817	0	0	0.0021	Aluminum	1
303	46.787544	0	0	0.0021	Aluminum	1
304	44.70828	0	0	0.0021	Aluminum	1
305	42.863304	0	0	0.0021	Aluminum	1
306	41.226196	0	0	0.0021	Aluminum	1
307	39.773544	0	0	0.0021	Aluminum	1
308	38.484562	0	0	0.0021	Aluminum	1
309	37.340813	0	0	0.0021	Aluminum	1
310	36.325932	0	0	0.0021	Aluminum	1

DATA GENERATION
PARALLEL-FLOW 10 SEGMENT MODEL

Interpolation Formulas:							
NOTE: Fluid a is Fluid 1 (Stepped Fluid), Fluid b is Fluid 2 (Unstepped Fluid)							
						Values for Table:	
					t*	**Eff (Fluid a)**	**Eff(Fluid b)**
					0	**0.000372447**	**-0.000620867**
		Interpolation formulas are highlighted =>			**4**	**0.341032728**	**0.260588492**
					8.023267476	**0.683674585**	**0.523317271**
Time							
(Seconds)	**Node #**	**Fluid a**	**Node #**	**Fluid b**		**Values for Table:**	
		Temperature		**Temperature**		**Eff (Fluid a)**	**Eff(Fluid b)**
		(Degrees F)		**(Degrees F)**	**t***		
0	1	40.941025	2	25.811777	0	0.001981536	-0.001423396
1	1	41.544785	2	25.82724	0.368633696	0.022632555	0.000473269
2	1	42.799114	2	25.886314	0.737267392	0.06553565	0.007719181
3	1	44.333191	2	26.014299	1.105901088	0.118007252	0.023417596
4	1	45.842503	2	26.2223	1.474534784	0.16963179	0.048930632
5	1	47.218601	2	26.505699	1.84316848	0.216699875	0.083691853
					2	0.234898959	0.10161169
6	1	48.469246	2	26.849098	2.211802176	0.259476962	0.125812569
7	1	49.632587	2	27.232771	2.580435872	0.299267902	0.172873223
8	1	50.739151	2	27.637672	2.949069569	0.337116839	0.222537665
9	1	51.805298	2	28.048134	3.317703265	0.373583353	0.27288421
10	1	52.837357	2	28.452673	3.686336961	0.408883921	0.322504251
					4	0.437962001	0.363312024
11	1	53.836483	2	28.843674	4.054970657	0.443058047	0.370463744
12	1	54.80183	2	29.216602	4.423604353	0.476076796	0.416206435
13	1	55.731915	2	29.56913	4.792238049	0.507889442	0.459446898
14	1	56.625305	2	29.900356	5.160871745	0.538446972	0.500074495
15	1	57.480942	2	30.210253	5.529505441	0.567713198	0.538085914
16	1	58.298328	2	30.49935	5.898139137	0.595671085	0.573546042
					6	0.603031666	0.582657408
17	1	59.077122	2	30.768473	6.266772833	0.622308971	0.606556195
18	1	59.817406	2	31.018593	6.635406529	0.64762966	0.637235473
19	1	60.519733	2	31.250782	7.004040225	0.671652067	0.665715367
20	1	61.184723	2	31.466148	7.372673921	0.694397399	-0.69213178
21	1	61.812988	2	31.665731	7.741307617	0.715886588	0.716612279
					8	0.73010835	0.732516575
22	1	62.405487	2	31.8505	8.109941314	0.736152436	0.739275719
23	1	62.963287	2	32.021366	8.47857501	0.755231439	0.760233841
24	1	63.487617	2	32.179218	8.847208706	0.773165633	0.779595689
25	1	63.979774	2	32.324924	9.215842402	0.789999361	0.79746773
26	1	64.441116	2	32.459343	9.584476098	0.805779132	0.813955328
27	1	64.872986	2	32.583294	9.953109794	0.820550823	0.829158939
					10	0.822307295	0.830941482
28	1	65.276703	2	32.697544	10.32174349	0.834359567	0.843172642
29	1	65.653679	2	32.802799	10.69037719	0.847253662	0.856083035
30	1	66.005424	2	32.899757	11.05901088	0.859284755	0.867975732
31	1	66.33316	2	32.989037	11.42764458	0.870494644	0.87892666
32	1	66.63813	2	33.071167	11.79627827	0.880925844	0.889000581
					12	0.886284139	0.894115362

DATA GENERATION
PARALLEL-FLOW 10 SEGMENT MODEL

33	1	66.9216	2	33.146622	12.16491197	0.890621658	0.898255758
34	1	67.185005	2	33.215919	12.53354567	0.899631168	0.906755606
35	1	67.429459	2	33.279552	12.90217936	0.907992478	0.914560717
36	1	67.656006	2	33.337944	13.27081306	0.915741296	0.921722977
37	1	67.665814	2	33.39146	13.63944675	0.922917573	0.928287155
					14	0.929412318	0.934165184
38	1	68.059952	2	33.440456	14.00808045	0.929557873	0.934296918
39	1	68.239479	2	33.485283	14.37671415	0.935698419	0.939795319
40	1	68.405502	2	33.526314	14.74534784	0.941377073	0.944828109
41	1	68.55896	2	33.563942	15.11398154	0.946625953	0.949443493
42	1	68.700645	2	33.598492	15.48261523	0.95147215	0.953681335
43	1	68.831177	2	33.630173	15.85124893	0.955936869	0.957567271
					16	0.957597775	0.959002776
44	1	68.951515	2	33.659176	16.21988263	0.960052913	0.961124728
45	1	69.062378	2	33.685699	16.58851632	0.963844873	0.964377992
46	1	69.164337	2	33.709908	16.95715002	0.967332281	0.967347425
47	1	69.258041	2	33.731937	17.32578372	0.970537334	0.970049464
48	1	69.344131	2	33.751945	17.69441741	0.973481958	0.97250361
					18	0.976723068	0.9743503
49	1	69.423172	2	33.770107	18.06305111	0.976185478	0.974731329
50	1	69.495903	2	33.786644	18.4316848	0.978673171	0.976759728
51	1	69.562737	2	33.801777	18.8003185	0.980959162	0.978615915
52	1	69.624008	2	33.815639	19.1689522	0.983054877	0.980316203
53	1	69.660038	2	33.828293	19.53758589	0.984971328	0.981868321
54	1	69.7313	2	33.839764	19.90621959	0.986724695	0.983275333
					20	0.987133178	0.983598859
55	1	69.778244	2	33.850132	20.27485328	0.988330368	0.984547054
56	1	69.821182	2	33.859497	20.64348698	0.989799021	0.985695748
57	1	69.860626	2	33.868023	21.01212068	0.991148164	0.986741532
58	1	69.896782	2	33.875847	21.38075437	0.992384845	0.98770121
59	1	69.929771	2	33.883045	21.74938807	0.993513201	0.988584104
					22	0.99421131	0.989131547
60	1	69.959793	2	33.88961	22.11802176	0.994540074	0.989389356
61	1	69.987221	2	33.89555	22.48665546	0.995478222	0.990117946
62	1	70.012344	2	33.900928	22.85528916	0.99633753	0.990777602
63	1	70.035347	2	33.90583	23.22392285	0.997124325	0.991378872
64	1	70.056381	2	33.910332	23.59255655	0.997843772	0.99193108
65	1	70.075516	2	33.914444	23.96119024	0.998498266	0.99243545
					24	0.998561013	0.992483527
66	1	70.092941	2	33.918167	24.32982394	0.999094271	0.992892107
67	1	70.108803	2	33.921524	24.69845764	0.999636815	0.993303871
68	1	70.123253	2	33.924549	25.06709133	1.000131063	0.993674912
69	1	70.13649	2	33.927311	25.43572503	1.000583822	0.994013694
70	1	70.148605	2	33.929863	25.80435872	1.000998204	0.994326718

Data Generation
Parallel-Flow 20 Segment Model

Thermonet input:											
NOTE: Values required as input are highlighted.											
NOTE: Change value of (h)min to obtain proper value of NTU											
Dimensions:			Cmin fluid - Stepped			Cmax fluid - Unstepped			Wall		
Total	Width	#	Mass			Mass			Thickness		
Length		Increments	Flowrate	h	Height	Flowrate	h	Height			
(Meters)	(Meters)		(Kg/s)	(W/m^2 Deg C)	(m)	(Kg/s)	(W/m^2 Deg C)	(m)	(Meters)		
16	0.6	20	1	17513	0.003175	5	6756.5	0.03175	0.021634034		
Materials:											
Cmin fluid - Engine Oil		Cmax fluid - Engine Oil		Wall - Aluminum							
Density	Cp	Density	Cp	Density	k	Cp					
(Kg/m^3)	(J/kg Deg. C)	(Kg/m^3)	(J/kg Deg. C)	(Kg/m^3)	(W/m Deg. C)	(J/kg Deg. C)					
890	1868	890	1868	2702	240	903					
										Effectiveness-NTU	
						Dwell time				Analytical Calculations:	
U	R*	Cw*	C*	NTU	Id*	of Cmin fluid	Effectivness	Tin, Fluid a	Tin, Fluid b	Tout, Fluid a	Tout, Fluid b
5637.666667	0.5	10	0.2	3.000065653	0.5	2.71272	0.610565905	70	20	29.47170476	26.10565905
								140	20	42.73209142	39.45356172
Resistor	Node A	Node B	Always Zero	& conduction	R - Value	Always Zero					
				3 = Fluid Flow							
101	101	102	0	3	0.000535332	0	0	0	0	0	
102	102	103	0	3	0.000535332	0	0	0	0	0	
103	103	104	0	3	0.000535332	0	0	0	0	0	
104	104	105	0	3	0.000535332	0	0	0	0	0	
105	105	106	0	3	0.000535332	0	0	0	0	0	
106	106	107	0	3	0.000535332	0	0	0	0	0	
107	107	108	0	3	0.000535332	0	0	0	0	0	
108	108	109	0	3	0.000535332	0	0	0	0	0	
109	109	110	0	3	0.000535332	0	0	0	0	0	
110	110	111	0	3	0.000535332	0	0	0	0	0	
111	111	112	0	3	0.000535332	0	0	0	0	0	
112	112	113	0	3	0.000535332	0	0	0	0	0	
113	113	114	0	3	0.000535332	0	0	0	0	0	
114	114	115	0	3	0.000535332	0	0	0	0	0	
115	115	116	0	3	0.000535332	0	0	0	0	0	
116	116	117	0	3	0.000535332	0	0	0	0	0	
117	117	118	0	3	0.000535332	0	0	0	0	0	
118	118	119	0	3	0.000535332	0	0	0	0	0	
119	119	120	0	3	0.000535332	0	0	0	0	0	
120	120	1	0	3	0.000535332	0	0	0	0	0	
201	201	202	0	3	0.000107066	0	0	0	0	0	
202	202	203	0	3	0.000107066	0	0	0	0	0	
203	203	204	0	3	0.000107066	0	0	0	0	0	
204	204	205	0	3	0.000107066	0	0	0	0	0	
205	205	206	0	3	0.000107066	0	0	0	0	0	
206	206	207	0	3	0.000107066	0	0	0	0	0	
207	207	208	0	3	0.000107066	0	0	0	0	0	
208	208	209	0	3	0.000107066	0	0	0	0	0	
209	209	210	0	3	0.000107066	0	0	0	0	0	

Data Generation
Parallel-Flow 20 Segment Model

210	210	211	0	3	0.000107066	0	0	0	0	0	
211	211	212	0	3	0.000107066	0	0	0	0	0	
212	212	213	0	3	0.000107066	0	0	0	0	0	
213	213	214	0	3	0.000107066	0	0	0	0	0	
214	214	215	0	3	0.000107066	0	0	0	0	0	
215	215	216	0	3	0.000107066	0	0	0	0	0	
216	216	217	0	3	0.000107066	0	0	0	0	0	
217	217	218	0	3	0.000107066	0	0	0	0	0	
218	218	219	0	3	0.000107066	0	0	0	0	0	
219	219	220	0	3	0.000107066	0	0	0	0	0	
220	220	2	0	3	0.000107066	0	0	0	0	0	
301	101	301	0	0	0.001189592	0	0	0	0	0	
302	102	302	0	0	0.001189592	0	0	0	0	0	
303	103	303	0	0	0.001189592	0	0	0	0	0	
304	104	304	0	0	0.001189592	0	0	0	0	0	
305	105	305	0	0	0.001189592	0	0	0	0	0	
306	106	306	0	0	0.001189592	0	0	0	0	0	
307	107	307	0	0	0.001189592	0	0	0	0	0	
308	108	308	0	0	0.001189592	0	0	0	0	0	
309	109	309	0	0	0.001189592	0	0	0	0	0	
310	110	310	0	0	0.001189592	0	0	0	0	0	
311	111	311	0	0	0.001189592	0	0	0	0	0	
312	112	312	0	0	0.001189592	0	0	0	0	0	
313	113	313	0	0	0.001189592	0	0	0	0	0	
314	114	314	0	0	0.001189592	0	0	0	0	0	
315	115	315	0	0	0.001189592	0	0	0	0	0	
316	116	316	0	0	0.001189592	0	0	0	0	0	
317	117	317	0	0	0.001189592	0	0	0	0	0	
318	118	318	0	0	0.001189592	0	0	0	0	0	
319	119	319	0	0	0.001189592	0	0	0	0	0	
320	120	320	0	0	0.001189592	0	0	0	0	0	
401	201	301	0	0	0.002379185	0	0	0	0	0	
402	202	302	0	0	0.002379185	0	0	0	0	0	
403	203	303	0	0	0.002379185	0	0	0	0	0	
404	204	304	0	0	0.002379185	0	0	0	0	0	
405	205	305	0	0	0.002379185	0	0	0	0	0	
406	206	306	0	0	0.002379185	0	0	0	0	0	
407	207	307	0	0	0.002379185	0	0	0	0	0	
408	208	308	0	0	0.002379185	0	0	0	0	0	
409	209	309	0	0	0.002379185	0	0	0	0	0	
410	210	310	0	0	0.002379185	0	0	0	0	0	
411	211	311	0	0	0.002379185	0	0	0	0	0	
412	212	312	0	0	0.002379185	0	0	0	0	0	
413	213	313	0	0	0.002379185	0	0	0	0	0	
414	214	314	0	0	0.002379185	0	0	0	0	0	
415	215	315	0	0	0.002379185	0	0	0	0	0	
416	216	316	0	0	0.002379185	0	0	0	0	0	
417	217	317	0	0	0.002379185	0	0	0	0	0	
418	218	318	0	0	0.002379185	0	0	0	0	0	
419	219	319	0	0	0.002379185	0	0	0	0	0	
420	220	320	0	0	0.002379185	0	0	0	0	0	

Data Generation
Parallel-Flow 20 Segment Model

	Initial			Node							
Node #	Temperature	Always Zero	Always Zero	Volume	Node	Time					
	(Degrees C)			(Meters^2)	Material	Classes					
1	29.506937	0	0	0.0002	Oil	1					
2	28.098578	0	0	0.0015	Oil	1					
101	70	0	0	0.0002	Oil	2					
102	83.189201	0	0	0.0002	Oil	1					
103	57.491888	0	0	0.0002	Oil	1					
104	52.725487	0	0	0.0002	Oil	1					
105	48.738361	0	0	0.0002	Oil	1					
106	45.402973	0	0	0.0002	Oil	1					
107	42.812778	0	0	0.0002	Oil	1					
108	40.278871	0	0	0.0002	Oil	1					
109	38.328092	0	0	0.0002	Oil	1					
110	36.89288	0	0	0.0002	Oil	1					
111	35.328283	0	0	0.0002	Oil	1					
112	34.183201	0	0	0.0002	Oil	1					
113	33.228982	0	0	0.0002	Oil	1					
114	32.427067	0	0	0.0002	Oil	1					
115	31.757904	0	0	0.0002	Oil	1					
116	31.198122	0	0	0.0002	Oil	1					
117	30.729841	0	0	0.0002	Oil	1					
118	30.338104	0	0	0.0002	Oil	1					
119	30.010403	0	0	0.0002	Oil	1					
120	29.738285	0	0	0.0002	Oil	1					
201	20	0	0	0.0015	Oil	3					
202	21.382148	0	0	0.0015	Oil	1					
203	22.501848	0	0	0.0015	Oil	1					
204	23.454864	0	0	0.0015	Oil	1					
205	24.252306	0	0	0.0015	Oil	1					
206	24.919382	0	0	0.0015	Oil	1					
207	25.477417	0	0	0.0015	Oil	1					
208	25.944239	0	0	0.0015	Oil	1					
209	26.334753	0	0	0.0015	Oil	1					
210	26.661434	0	0	0.0015	Oil	1					
211	26.934715	0	0	0.0015	Oil	1					
212	27.183328	0	0	0.0015	Oil	1					
213	27.35457	0	0	0.0015	Oil	1					
214	27.514553	0	0	0.0015	Oil	1					
215	27.648364	0	0	0.0015	Oil	1					
216	27.760342	0	0	0.0015	Oil	1					
217	27.853996	0	0	0.0015	Oil	1					
218	27.932344	0	0	0.0015	Oil	1					
219	27.997885	0	0	0.0015	Oil	1					
220	28.052711	0	0	0.0015	Oil	1					
301	50.960638	0	0	0.0010	Aluminum	1					
302	47.26199	0	0	0.0010	Aluminum	1					
303	44.187927	0	0	0.0010	Aluminum	1					
304	41.579613	0	0	0.0010	Aluminum	1					
305	39.414383	0	0	0.0010	Aluminum	1					
306	37.603081	0	0	0.0010	Aluminum	1					
307	36.087852	0	0	0.0010	Aluminum	1					
308	34.820301	0	0	0.0010	Aluminum	1					
309	33.769941	0	0	0.0010	Aluminum	1					

Data Generation
Parallel-Flow 20 Segment Model

310	32.87291	0	0	0.0010	Aluminum	1					
311	32.130887	0	0	0.0010	Aluminum	1					
312	31.510122	0	0	0.0010	Aluminum	1					
313	30.990843	0	0	0.0010	Aluminum	1					
314	30.556442	0	0	0.0010	Aluminum	1					
315	30.19305	0	0	0.0010	Aluminum	1					
316	29.889061	0	0	0.0010	Aluminum	1					
317	29.634754	0	0	0.0010	Aluminum	1					
318	29.422022	0	0	0.0010	Aluminum	1					
319	29.244061	0	0	0.0010	Aluminum	1					
320	29.095188	0	0	0.0010	Aluminum	1					

DATA GENERATION
PARALLEL-FLOW 20 SEGMENT MODEL

Interpolation Formulas:							
NOTE: Fluid a is Fluid 1 (Stepped Fluid), Fluid b is Fluid 2 (Unstepped Fluid)							
						Values for Table:	
					t*	Eff (Fluid a)	Eff(Fluid b)
					0	0.000372447	-0.000620867
		Interpolation formulas are highlighted =>			4	0.341032728	0.260588492
					8.023267476	0.683674585	0.523317271
Time							
(Seconds)	Node #	Fluid a	Node #	Fluid b		Values for Table:	
		Temperature		Temperature		Eff (Fluid a)	Eff(Fluid b)
		(Degrees F)		(Degrees F)	t*		
0	1	29.506937	2	28.098576	0	0.002656954	-0.000624171
1	1	29.514772	2	28.111872	0.368633696	0.003247812	0.000547497
2	1	29.549143	2	28.176859	0.737267392	0.005839818	0.006274272
3	1	29.63599	2	28.347429	1.105901088	0.012389174	0.021305217
					1.2	0.015584405	0.028514472
4	1	29.801975	2	28.667921	1.474534784	0.024906532	0.049547566
5	1	30.0681	2	29.153019	1.84316848	0.044975705	0.092295302
6	1	30.44117	2	29.788076	2.211802176	0.073109877	0.148257703
					2.4	0.091700717	0.181566643
7	1	30.924046	2	30.528461	2.580435872	0.109524804	0.213501803
8	1	31.503452	2	31.331205	2.949069569	0.153219306	0.284241094
9	1	32.16222	2	32.14896	3.317703265	0.202898702	0.356303182
					3.6	0.244272152	0.410290603
10	1	32.878639	2	32.948975	3.686336961	0.256925709	0.426801988
11	1	33.630074	2	33.709511	4.054970657	0.313593363	0.493821831
12	1	34.397282	2	34.413815	4.423604353	0.371450499	0.555886406
13	1	35.16116	2	35.058571	4.792238049	0.429056512	0.612703501
					4.8	0.430239631	0.6137858
14	1	35.90625	2	35.641865	5.160871745	0.485245673	0.664104451
15	1	36.622135	2	36.162083	5.529505441	0.539232409	0.709947026
16	1	37.299385	2	36.623974	5.898139137	0.59030558	0.750649718
					6	0.603505081	0.760541277
17	1	37.932819	2	37.030201	6.266772833	0.638074474	0.786447195
18	1	38.517735	2	37.386776	6.635406529	0.6821845	0.817869246
19	1	39.053841	2	37.696373	7.004040225	0.722613638	0.845151508
					7.2	0.742072733	0.857769968
20	1	39.539249	2	37.965744	7.372673921	0.759219509	0.86888898
21	1	39.975727	2	38.197784	7.741307617	0.792135442	0.889336775
22	1	40.36544	2	38.396946	8.109941314	0.821524705	0.9068873
					8.4	0.84203384	0.918695578
23	1	40.711071	2	38.567245	8.47857501	0.847589632	0.921894364
24	1	41.015709	2	38.712315	8.847208706	0.87056317	0.934678202
25	1	41.282646	2	38.835426	9.215842402	0.890693578	0.945526971
26	1	41.515289	2	38.939541	9.584476098	0.908237788	0.954701778
					9.6	0.908878399	0.955027458
27	1	41.717007	2	39.027302	9.953109794	0.923449863	0.96243544
28	1	41.89109	2	39.101063	10.32174349	0.936577912	0.968935397
29	1	42.040649	2	39.162872	10.69037719	0.947856542	0.97438212
					10.8	0.950725823	0.975735049

DATA GENERATION
PARALLEL-FLOW 20 SEGMENT MODEL

30	1	42.168594	2	39.2145	11.05901088	0.957505205	0.978931676
31	1	42.277607	2	39.257484	11.42764458	0.965726157	0.982719505
32	1	42.370136	2	39.293179	11.79627827	0.972704007	0.985865015
					12	0.97596503	0.987304723
33	1	42.448383	2	39.322742	12.16491197	0.978604816	0.988470161
34	1	42.514328	2	39.347168	12.53354567	0.983577898	0.990622626
35	1	42.569717	2	39.367287	12.90217936	0.987754926	0.992395549
					13.2	0.990580192	0.993570962
36	1	42.616089	2	39.383797	13.27081306	0.991251958	0.993850441
37	1	42.654789	2	39.397312	13.63944675	0.994170425	0.995041408
38	1	42.686996	2	39.408371	14.00808045	0.996599238	0.996015948
39	1	42.71373	2	39.417439	14.37671415	0.998615318	0.996815037
					14.4	0.998720805	0.996856418
40	1	42.735874	2	39.424873	14.74534784	1.000285254	0.997470135

Data Generation
Cross-Flow 3 x 3 Segment Model

Thermonet Input:	3 x 3 segment model										
NOTE: Values required as input are highlighted.											
NOTE: Change value of (h)min to obtain proper value of NTU											
Dimensions:			Cmin fluid - Stepped			Cmax fluid - Unstepped			Wall		
Total	Width	#	Mass			Mass			Thickness		
Length		Increments	Flowrate	h	Height	Flowrate	h	Height			
(Meters)	(Meters)		(Kg/s)	(W/m^2 Deg C)	(m)	(Kg/s)	(W/m^2 Deg C)	(m)	(Meters)		
1.6	1.0	3	1	2189.1	0.003175	5	1094.55	0.015875	0.021834034		
Materials:											
Cmin fluid - Engine Oil		Cmax fluid - Engine Oil		Wall - Aluminum							
Density	Cp	Density	Cp	Density	k	Cp					
(Kg/m^3)	(J/kg Deg. C)	(Kg/m^3)	(J/kg Deg. C)	(Kg/m^3)	(W/m Deg. C)	(J/kg Deg. C)					
890	1868	890	1868	2702	240	903					
						Dwell time	Both Fluids			Effectiveness-NTU	
						of Cmin fluid (Flow	Unmixed (Single pass)			Analytical Calculations:	
U	R*	Cw*	C*	NTU	td*	in Length direction)	Effectiveness	Tin, Fluid a	Tin, Fluid b	Tout, Fluid a	Tout, Fluid b
729.7	0.5	10	0.2	1.000017131	1	7.23392	0.596008156	100	20	52.31934749	29.5361305
								140	20	86.47902124	34.30419575
				0=Constant Resistance							
Resistor	Node A	Node B	Always Zero	Conduction/Conv.	R - Value	Always Zero					
				3 = Fluid Flow							
100	100	103	0	3	0.001805996	0	0	0	0	0	
101	101	104	0	3	0.001805996	0	0	0	0	0	
102	102	105	0	3	0.001805996	0	0	0	0	0	
103	103	106	0	3	0.001805996	0	0	0	0	0	
104	104	107	0	3	0.001805996	0	0	0	0	0	
105	105	108	0	3	0.001805996	0	0	0	0	0	
106	106	1	0	3	0.001805996	0	0	0	0	0	
107	107	1	0	3	0.001805996	0	0	0	0	0	
108	108	1	0	3	0.001805996	0	0	0	0	0	
200	200	201	0	3	0.000321199	0	0	0	0	0	
201	201	202	0	3	0.000321199	0	0	0	0	0	
202	202	2	0	3	0.000321199	0	0	0	0	0	
203	203	204	0	3	0.000321199	0	0	0	0	0	
204	204	205	0	3	0.000321199	0	0	0	0	0	
205	205	2	0	3	0.000321199	0	0	0	0	0	
206	206	207	0	3	0.000321199	0	0	0	0	0	
207	207	208	0	3	0.000321199	0	0	0	0	0	
208	208	2	0	3	0.000321199	0	0	0	0	0	
300	100	300	0	0	0.001805968	0	0	0	0	0	
301	101	301	0	0	0.001805968	0	0	0	0	0	
302	102	302	0	0	0.001805968	0	0	0	0	0	
303	103	303	0	0	0.001805968	0	0	0	0	0	
304	104	304	0	0	0.001805968	0	0	0	0	0	
305	105	305	0	0	0.001805969	0	0	0	0	0	
306	106	306	0	0	0.001805968	0	0	0	0	0	
307	107	307	0	0	0.001805968	0	0	0	0	0	
308	108	308	0	0	0.001805968	0	0	0	0	0	
400	200	300	0	0	0.003211936	0	0	0	0	0	
401	201	301	0	0	0.003211936	0	0	0	0	0	

Data Generation
Cross-Flow 3 x 3 Segment Model

402	202	302	0	0	0.003211936	0	0	0	0	0	
403	203	303	0	0	0.003211936	0	0	0	0	0	
404	204	304	0	0	0.003211936	0	0	0	0	0	
405	205	305	0	0	0.003211936	0	0	0	0	0	
406	206	306	0	0	0.003211936	0	0	0	0	0	
407	207	307	0	0	0.003211936	0	0	0	0	0	
408	208	308	0	0	0.003211936	0	0	0	0	0	
	Initial			Node							
Node #	Temperature	Always Zero	Always Zero	Volume	Node	Time					
	(Degrees C)			(Meters^2)	Material	Classes					
1	53.481577	0	0	0.0009	Oil	1					
2	29.301678	0	0	0.0045	Oil	1					
100	100	0	0	0.0009	Oil	2					
101	100	0	0	0.0009	Oil	2					
102	100	0	0	0.0009	Oil	2					
103	76.669769	0	0	0.0009	Oil	1					
104	79.625104	0	0	0.0009	Oil	1					
105	80.488118	0	0	0.0009	Oil	1					
106	63.056156	0	0	0.0009	Oil	1					
107	64.721939	0	0	0.0009	Oil	1					
108	66.058228	0	0	0.0009	Oil	1					
200	20	0	0	0.0045	Oil	3					
201	24.262037	0	0	0.0045	Oil	1					
202	28.297014	0	0	0.0045	Oil	1					
203	20	0	0	0.0045	Oil	3					
204	23.126719	0	0	0.0045	Oil	1					
205	26.14735	0	0	0.0045	Oil	1					
206	20	0	0	0.0045	Oil	3					
207	22.369797	0	0	0.0045	Oil	1					
208	24.647453	0	0	0.0045	Oil	1					
300	64.821646	0	0	0.0062	Aluminum	1					
301	66.895793	0	0	0.0062	Aluminum	1					
302	87.806755	0	0	0.0062	Aluminum	1					
303	52.862137	0	0	0.0062	Aluminum	1					
304	54.893124	0	0	0.0062	Aluminum	1					
305	56.66111	0	0	0.0062	Aluminum	1					
306	45.132287	0	0	0.0062	Aluminum	1					
307	46.132397	0	0	0.0062	Aluminum	1					
308	47.400021	0	0	0.0062	Aluminum	1					

Data Generation
Cross-Flow 6 x 6 Segment Model

Thermonet Input:	6 x 6 segment model										
NOTE: Values required as input are highlighted.											
NOTE: Change value of (h)min to obtain proper value of NTU											
Dimensions:			Cmin fluid - Stepped			Cmax fluid - Unstepped			Wall		
Total	Width	#	Mass			Mass			Thickness		
Length		Increments	Flowrate	h	Height	Flowrate	h	Height			
(Meters)	(Meters)		(Kg/s)	(W/m^2 Deg C)	(m)	(Kg/s)	(W/m^2 Deg C)	(m)	(Meters)		
1.6	1.6	6	1	1469.4	0.003175	5	1459.4	0.03175	0.021634034		
Materials:											
Cmin fluid - Engine Oil		Cmax fluid - Engine Oil		Wall - Aluminum							
Density	Cp	Density	Cp	Density	k	Cp					
(Kg/m^3)	(J/kg Deg. C)	(Kg/m^3)	(J/kg Deg. C)	(Kg/m^3)	(W/m Deg. C)	(J/kg Deg. C)					
890	1868	890	1868	2702	240	903					
						Dwell time	Both Fluids			Effectiveness-NTU	
						of Cmin fluid (Flow	Unmixed (Single Pass)			Analytical Calculations:	
U	R*	Cw*	C*	NTU	td*	In Length direction)	Effectiveness	Tin, Fluid a	Tin, Fluid b	Tout, Fluid a	Tout, Fluid b
729.7	[illegible]	10	0.2	1.000017131	0.5	7.23392	0.596006156	70	20	40.19959218	25.96008156
								140	20	68.47902124	34.30419575
				0=Constant Resistance							
Resistor	Node A	Node B	Always Zero	Conduction/Conv.	R - Value	Always Zero					
				3 = Fluid Flow							
100	100	106	0	3	0.003211991	0	0	0	0	0	
101	101	107	0	3	0.003211991	0	0	0	0	0	
102	102	108	0	3	0.003211991	0	0	0	0	0	
103	103	109	0	3	0.003211991	0	0	0	0	0	
104	104	110	0	3	0.003211991	0	0	0	0	0	
105	105	111	0	3	0.003211991	0	0	0	0	0	
106	106	112	0	3	0.003211991	0	0	0	0	0	
107	107	113	0	3	0.003211991	0	0	0	0	0	
108	108	114	0	3	0.003211991	0	0	0	0	0	
109	109	115	0	3	0.003211991	0	0	0	0	0	
110	110	116	0	3	0.003211991	0	0	0	0	0	
111	111	117	0	3	0.003211991	0	0	0	0	0	
112	112	118	0	3	0.003211991	0	0	0	0	0	
113	113	119	0	3	0.003211991	0	0	0	0	0	
114	114	120	0	3	0.003211991	0	0	0	0	0	
115	115	121	0	3	0.003211991	0	0	0	0	0	
116	116	122	0	3	0.003211991	0	0	0	0	0	
117	117	123	0	3	0.003211991	0	0	0	0	0	
118	118	124	0	3	0.003211991	0	0	0	0	0	
119	119	125	0	3	0.003211991	0	0	0	0	0	
120	120	126	0	3	0.003211991	0	0	0	0	0	
121	121	127	0	3	0.003211991	0	0	0	0	0	
122	122	128	0	3	0.003211991	0	0	0	0	0	
123	123	129	0	3	0.003211991	0	0	0	0	0	
124	124	130	0	3	0.003211991	0	0	0	0	0	
125	125	131	0	3	0.003211991	0	0	0	0	0	
126	126	132	0	3	0.003211991	0	0	0	0	0	
127	127	133	0	3	0.003211991	0	0	0	0	0	
128	128	134	0	3	0.003211991	0	0	0	0	0	
129	129	135	0	3	0.003211991	0	0	0	0	0	
130	130	1	0	3	0.003211991	0	0	0	0	0	
131	131	1	0	3	0.003211991	0	0	0	0	0	
132	132	1	0	3	0.003211991	0	0	0	0	0	
133	133	1	0	3	0.003211991	0	0	0	0	0	

Data Generation
Cross-Flow 6 x 6 Segment Model

134	134	1	0	3	0.003211991	0	0	0	0	0	
135	135	1	0	3	0.003211991	0	0	0	0	0	
200	200	201	0	3	0.000642398	0	0	0	0	0	
201	201	202	0	3	0.000642398	0	0	0	0	0	
202	202	203	0	3	0.000642398	0	0	0	0	0	
203	203	204	0	3	0.000642398	0	0	0	0	0	
204	204	205	0	3	0.000642398	0	0	0	0	0	
205	205	2	0	3	0.000642398	0	0	0	0	0	
209	206	207	0	3	0.000642398	0	0	0	0	0	
207	207	206	0	3	0.000642398	0	0	0	0	0	
208	208	209	0	3	0.000642398	0	0	0	0	0	
209	209	210	0	3	0.000642398	0	0	0	0	0	
210	210	211	0	3	0.000642398	0	0	0	0	0	
211	211	2	0	3	0.000642398	0	0	0	0	0	
212	212	213	0	3	0.000642398	0	0	0	0	0	
213	213	214	0	3	0.000642398	0	0	0	0	0	
214	214	215	0	3	0.000642398	0	0	0	0	0	
215	215	216	0	3	0.000642398	0	0	0	0	0	
216	216	217	0	3	0.000642398	0	0	0	0	0	
217	217	2	0	3	0.000642398	0	0	0	0	0	
218	218	219	0	3	0.000642398	0	0	0	0	0	
219	219	220	0	3	0.000642398	0	0	0	0	0	
220	220	221	0	3	0.000642398	0	0	0	0	0	
221	221	222	0	3	0.000642398	0	0	0	0	0	
222	222	223	0	3	0.000642398	0	0	0	0	0	
223	223	2	0	3	0.000642398	0	0	0	0	0	
224	224	225	0	3	0.000642398	0	0	0	0	0	
225	225	226	0	3	0.000642398	0	0	0	0	0	
226	226	227	0	3	0.000642398	0	0	0	0	0	
227	227	228	0	3	0.000642398	0	0	0	0	0	
228	228	229	0	3	0.000642398	0	0	0	0	0	
229	229	2	0	3	0.000642398	0	0	0	0	0	
230	230	231	0	3	0.000642398	0	0	0	0	0	
231	231	232	0	3	0.000642398	0	0	0	0	0	
232	232	233	0	3	0.000642398	0	0	0	0	0	
233	233	234	0	3	0.000642398	0	0	0	0	0	
234	234	235	0	3	0.000642398	0	0	0	0	0	
235	235	2	0	3	0.000642398	0	0	0	0	0	
300	100	300	0	0	0.009635809	0	0	0	0	0	
301	101	301	0	0	0.009635809	0	0	0	0	0	
302	102	302	0	0	0.009635809	0	0	0	0	0	
303	103	303	0	0	0.009635809	0	0	0	0	0	
304	104	304	0	0	0.009635809	0	0	0	0	0	
305	105	305	0	0	0.009635809	0	0	0	0	0	
306	106	306	0	0	0.009635809	0	0	0	0	0	
307	107	307	0	0	0.009635809	0	0	0	0	0	
308	108	308	0	0	0.009635809	0	0	0	0	0	
309	109	309	0	0	0.009635809	0	0	0	0	0	
310	110	310	0	0	0.009635809	0	0	0	0	0	
311	111	311	0	0	0.009635809	0	0	0	0	0	
312	112	312	0	0	0.009635809	0	0	0	0	0	
313	113	313	0	0	0.009635809	0	0	0	0	0	
314	114	314	0	0	0.009635809	0	0	0	0	0	
315	115	315	0	0	0.009635809	0	0	0	0	0	
316	116	316	0	0	0.009635809	0	0	0	0	0	
317	117	317	0	0	0.009635809	0	0	0	0	0	
318	118	318	0	0	0.009635809	0	0	0	0	0	
319	119	319	0	0	0.009635809	0	0	0	0	0	
320	120	320	0	0	0.009635809	0	0	0	0	0	

Data Generation
Cross-Flow 6 x 6 Segment Model

321	121	321	0	0	0.009635809	0	0	0	0	0	
322	122	322	0	0	0.009635809	0	0	0	0	0	
323	123	323	0	0	0.009635809	0	0	0	0	0	
324	124	324	0	0	0.009635809	0	0	0	0	0	
325	125	325	0	0	0.009635809	0	0	0	0	0	
326	126	326	0	0	0.009635809	0	0	0	0	0	
327	127	327	0	0	0.009635809	0	0	0	0	0	
328	128	328	0	0	0.009635809	0	0	0	0	0	
329	129	329	0	0	0.009635809	0	0	0	0	0	
330	130	330	0	0	0.009635809	0	0	0	0	0	
331	131	331	0	0	0.009635809	0	0	0	0	0	
332	132	332	0	0	0.009635809	0	0	0	0	0	
333	133	333	0	0	0.009635809	0	0	0	0	0	
334	134	334	0	0	0.009635809	0	0	0	0	0	
335	135	335	0	0	0.009635809	0	0	0	0	0	
400	200	300	0	0	0.009635809	0	0	0	0	0	
401	201	301	0	0	0.009635809	0	0	0	0	0	
402	202	302	0	0	0.009635809	0	0	0	0	0	
403	203	303	0	0	0.009635809	0	0	0	0	0	
404	204	304	0	0	0.009635809	0	0	0	0	0	
405	205	305	0	0	0.009635809	0	0	0	0	0	
406	206	306	0	0	0.009635809	0	0	0	0	0	
407	207	307	0	0	0.009635809	0	0	0	0	0	
408	208	308	0	0	0.009635809	0	0	0	0	0	
409	209	309	0	0	0.009635809	0	0	0	0	0	
410	210	310	0	0	0.009635809	0	0	0	0	0	
411	211	311	0	0	0.009635809	0	0	0	0	0	
412	212	312	0	0	0.009635809	0	0	0	0	0	
413	213	313	0	0	0.009635809	0	0	0	0	0	
414	214	314	0	0	0.009635809	0	0	0	0	0	
415	215	315	0	0	0.009635809	0	0	0	0	0	
416	216	316	0	0	0.009635809	0	0	0	0	0	
417	217	317	0	0	0.009635809	0	0	0	0	0	
418	218	318	0	0	0.009635809	0	0	0	0	0	
419	219	319	0	0	0.009635809	0	0	0	0	0	
420	220	320	0	0	0.009635809	0	0	0	0	0	
421	221	321	0	0	0.009635809	0	0	0	0	0	
422	222	322	0	0	0.009635809	0	0	0	0	0	
423	223	323	0	0	0.009635809	0	0	0	0	0	
424	224	324	0	0	0.009635809	0	0	0	0	0	
425	225	325	0	0	0.009635809	0	0	0	0	0	
426	226	326	0	0	0.009635809	0	0	0	0	0	
427	227	327	0	0	0.009635809	0	0	0	0	0	
428	228	328	0	0	0.009635809	0	0	0	0	0	
429	229	329	0	0	0.009635809	0	0	0	0	0	
430	230	330	0	0	0.009635809	0	0	0	0	0	
431	231	331	0	0	0.009635809	0	0	0	0	0	
432	232	332	0	0	0.009635809	0	0	0	0	0	
433	233	333	0	0	0.009635809	0	0	0	0	0	
434	234	334	0	0	0.009635809	0	0	0	0	0	
435	235	335	0	0	0.009635809	0	0	0	0	0	
	Initial			Node							
Node #	Temperature	Always Zero	Always Zero	Volume	Node	Time					
	(Degrees C)			(Meters^2)	Material	Classes					
1	40.328789	0	0	0.0002	Oil	1					
2	25.934237	0	0	0.0023	Oil	1					

Data Generation
Cross-Flow 6 x 6 Segment Model

100	70	0	0	0.0002	Oil	2					
101	70	0	0	0.0002	Oil	2					
102	70	0	0	0.0002	Oil	2					
103	70	0	0	0.0002	Oil	2					
104	70	0	0	0.0002	Oil	2					
105	70	0	0	0.0002	Oil	2					
100	62.469075	0	0	0.0002	Oil	1					
107	62.714733	0	0	0.0002	Oil	1					
108	62.933609	0	0	0.0002	Oil	1					
109	63.145912	0	0	0.0002	Oil	1					
110	63.35183	0	0	0.0002	Oil	1					
111	63.365795	0	0	0.0002	Oil	1					
112	56.106434	0	0	0.0002	Oil	1					
113	56.469952	0	0	0.0002	Oil	1					
114	66.662965	0	0	0.0002	Oil	1					
115	57.225761	0	0	0.0002	Oil	1					
116	57.576609	0	0	0.0002	Oil	1					
117	57.665909	0	0	0.0002	Oil	1					
118	50.682583	0	0	0.0002	Oil	1					
119	51.17144	0	0	0.0002	Oil	1					
120	51.648209	0	0	0.0002	Oil	1					
121	52.113174	0	0	0.0002	Oil	1					
122	52.56662	0	0	0.0002	Oil	1					
123	52.771019	0	0	0.0002	Oil	1					
124	46.073494	0	0	0.0002	Oil	1					
125	46.627366	0	0	0.0002	Oil	1					
126	47.169056	0	0	0.0002	Oil	1					
127	47.69675	0	0	0.0002	Oil	1					
128	46.216702	0	0	0.0002	Oil	1					
129	46.570053	0	0	0.0002	Oil	1					
130	42.156773	0	0	0.0002	Oil	1					
131	42.745136	0	0	0.0002	Oil	1					
132	43.322075	0	0	0.0002	Oil	1					
133	43.667775	0	0	0.0002	Oil	1					
134	44.442417	0	0	0.0002	Oil	1					
135	44.967646	0	0	0.0002	Oil	1					
200	20	0	0	0.0023	Oil	3					
201	21.502182	0	0	0.0023	Oil	1					
202	22.959234	0	0	0.0023	Oil	1					
203	24.372511	0	0	0.0023	Oil	1					
204	25.743326	0	0	0.0023	Oil	1					
205	27.072962	0	0	0.0023	Oil	1					
200	20	0	0	0.0023	Oil	3					
207	21.276524	0	0	0.0023	Oil	1					
208	22.521461	0	0	0.0023	Oil	1					
209	23.735609	0	0	0.0023	Oil	1					
210	24.91964	0	0	0.0023	Oil	1					
211	26.074264	0	0	0.0023	Oil	1					
212	20	0	0	0.0023	Oil	3					
213	21.084766	0	0	0.0023	Oil	1					
214	22.148466	0	0	0.0023	Oil	1					
215	23.19142	0	0	0.0023	Oil	1					
216	24.213936	0	0	0.0023	Oil	1					
217	25.216333	0	0	0.0023	Oil	1					
218	20	0	0	0.0023	Oil	3					
219	20.921612	0	0	0.0023	Oil	1					
220	21.830622	0	0	0.0023	Oil	1					
221	22.726462	0	0	0.0023	Oil	1					
222	23.609337	0	0	0.0023	Oil	1					

Data Generation

Cross-Flow 6 x 6 Segment Model

223	24.479319	0	0	0.0023	Oil	1						
224	20	0	0	0.0023	Oil	3						
225	20.78334	0	0	0.0023	Oil	1						
226	21.559792	0	0	0.0023	Oil	1						
227	22.329187	0	0	0.0023	Oil	1						
228	23.091363	0	0	0.0023	Oil	1						
229	23.646239	0	0	0.0023	Oil	1						
230	20	0	0	0.0023	Oil	3						
231	20.694492	0	0	0.0023	Oil	1						
232	21.374508	0	0	0.0023	Oil	1						
233	22.039944	0	0	0.0023	Oil	1						
234	22.690712	0	0	0.0023	Oil	1						
235	23.326733	0	0	0.0023	Oil	1						
300	43.300152	0	0	0.0015	Aluminum	1						
301	44.102314	0	0	0.0015	Aluminum	1						
302	44.880375	0	0	0.0015	Aluminum	1						
303	45.635063	0	0	0.0015	Aluminum	1						
304	46.367073	0	0	0.0015	Aluminum	1						
305	46.416714	0	0	0.0015	Aluminum	1						
306	39.800037	0	0	0.0015	Aluminum	1						
307	40.586857	0	0	0.0015	Aluminum	1						
308	41.353657	0	0	0.0015	Aluminum	1						
309	42.100933	0	0	0.0015	Aluminum	1						
310	42.829159	0	0	0.0015	Aluminum	1						
311	43.103817	0	0	0.0015	Aluminum	1						
312	36.825706	0	0	0.0015	Aluminum	1						
313	37.583691	0	0	0.0015	Aluminum	1						
314	38.325527	0	0	0.0015	Aluminum	1						
315	39.051525	0	0	0.0015	Aluminum	1						
316	39.761974	0	0	0.0015	Aluminum	1						
317	40.265545	0	0	0.0015	Aluminum	1						
318	34.268172	0	0	0.0015	Aluminum	1						
319	35.01823	0	0	0.0015	Aluminum	1						
320	35.725708	0	0	0.0015	Aluminum	1						
321	36.42075	0	0	0.0015	Aluminum	1						
322	37.103519	0	0	0.0015	Aluminum	1						
323	37.83741	0	0	0.0015	Aluminum	1						
324	32.150326	0	0	0.0015	Aluminum	1						
325	32.826748	0	0	0.0015	Aluminum	1						
326	33.493786	0	0	0.0015	Aluminum	1						
327	34.151482	0	0	0.0015	Aluminum	1						
328	34.799858	0	0	0.0015	Aluminum	1						
329	35.764214	0	0	0.0015	Aluminum	1						
330	30.772232	0	0	0.0015	Aluminum	1						
331	31.242113	0	0	0.0015	Aluminum	1						
332	31.895988	0	0	0.0015	Aluminum	1						
333	32.133911	0	0	0.0015	Aluminum	1						
334	32.555954	0	0	0.0015	Aluminum	1						
335	33.504757	0	0	0.0015	Aluminum	1						

Data Generation
Cross-Flow 6 x 6 Segment Model

Interpolation Formulas:							
NOTE: Fluid a is Fluid 1 (Stepped Fluid), Fluid b is Fluid 2 (Unstepped Fluid)							
						Values for Table:	
					t*	Eff (Fluid a)	Eff(Fluid b)
					0	0.000372447	-0.000620867
		Interpolation formulas are highlighted =>			4	0.341032728	0.260588492
					8.023267476	0.683674585	0.523317271
Time		Fluid a		Fluid b			
(Seconds)	Node #	Mean Outlet	Node #	Mean Outlet		Values for Table:	
		Temperature		Temperature		Eff (Fluid a)	Eff(Fluid b)
		(Degrees F)		(Degrees F)	t*		
0	1	40.328789	2	25.934237	0	0.004568579	-0.003097341
5	1	45.43993	2	26.333601	0.69118818	0.185305644	0.044764421
10	1	50.305859	2	26.978453	1.38237636	0.357371671	0.12204668
					2	0.462622425	0.203105918
15	1	53.63681	2	27.735382	2.07356454	0.475158738	0.212760803
20	1	55.944912	2	28.51177	2.764752721	0.556776439	0.305806989
25	1	57.722397	2	29.252237	3.455940901	0.619630785	0.394548224
					4	0.66086449	0.458340271
30	1	59.2038	2	29.928471	4.147129081	0.672015258	0.475591458
35	1	60.48193	2	30.53063	4.838317261	0.717211715	0.547757178
40	1	61.596489	2	31.058849	5.529505441	0.756624074	0.61106156

Data Generation

Cross-Flow 6 x 6 Segment Model

					6	0.780065003	0.648507681
45	1	62.570328	2	31.517866	6.220693621	0.791060377	0.666072433
50	1	63.420303	2	31.914614	6.911881801	0.821116677	0.713620679
55	1	64.16082	2	32.256233	7.603069981	0.84730239	0.754561994
					8	0.860376358	0.774713889
60	1	64.804634	2	32.549038	8.294258162	0.870068549	0.789653196
65	1	65.36338	2	32.800041	8.985446342	0.889826586	0.81973464
70	1	65.847527	2	33.015335	9.676634522	0.906946698	0.84553654
					10	0.913874973	0.855863697
75	1	66.266319	2	33.199524	10.3678227	0.921755767	0.867610662
80	1	66.627945	2	33.356712	11.05901088	0.934543366	0.886448851
85	1	66.939774	2	33.4907	11.75019906	0.945570074	0.902506637
					12	0.949001091	0.907439763
90	1	67.208244	2	33.604595	12.44138724	0.955063547	0.916156378
95	1	67.439102	2	33.701794	13.13257542	0.963227007	0.927805188
100	1	67.637383	2	33.784595	13.8237636	0.9702385	0.937728471
					14	0.971771939	0.939879175
105	1	67.807457	2	33.854977	14.51495178	0.976252553	0.946163398
110	1	67.953186	2	33.914921	15.20613996	0.981405733	0.953347384
115	1	68.077927	2	33.965954	15.89732814	0.985816749	0.959463432
					16	0.986377157	0.960225457
120	1	68.184616	2	34.008759	16.58851632	0.989589421	0.964593395
125	1	68.275681	2	34.044907	17.2797045	0.992809606	0.968925551
130	1	68.353371	2	34.075615	17.97089268	0.995556832	0.97260575
					18	0.995655335	0.972737186
135	1	68.419518	2	34.101658	18.66208086	0.997895883	0.975726872
140	1	68.475853	2	34.12328	19.35326904	0.999887967	0.97831816
					20	1.001473758	0.980402666
145	1	68.523781	2	34.141869	20.04445722	1.001582767	0.980545958
150	1	68.564537	2	34.157761	20.7356454	1.003023956	0.982450534

Data Generation

Cross-Flow 6 x 6 Segment Model

155	1	68.599174	2	34.171253	21.42683358	1.004248769	0.984067482
					22	1.005111228	0.985192676
160	1	68.628586	2	34.182575	22.11802176	1.005288818	0.985424366
165	1	68.653557	2	34.192135	22.80920994	1.006171828	0.986570084
170	1	68.674683	2	34.200172	23.50039812	1.006918872	0.987533278
					24	1.007376162	0.988139399
175	1	68.692574	2	34.207169	24.1915863	1.007551523	0.988371833
180	1	68.707611	2	34.212635	24.88277448	1.008083252	0.989026906

Data Generation
Cross-Flow 10 x 10 Segment Model

Thermonet Input:	10 x 10 segment model										
NOTE: Values required as input are highlighted.											
NOTE: Change value of (h)min to obtain proper value of NTU											
Dimensions:			Cmin fluid - Stepped			Cmax fluid - Unstepped			Wall		
Total	Width	#	Mass			Mass			Thickness		
Length		Increments	Flowrate	h	Height	Flowrate	h	Height			
(Meters)	(Meters)		(Kg/s)	(W/m^2 Deg C)	(m)	(Kg/s)	(W/m^2 Deg C)	(m)	(Meters)		
1.6	1.6	10	1	1094.6	0.003175	5	2189.2	0.015875	0.021834034		
Materials:											
Cmin fluid - Engine Oil		Cmax fluid - Engine Oil		Wall - Aluminum							
Density	Cp	Density	Cp	Density	k	Cp					
(Kg/m^3)	(J/kg Deg. C)	(Kg/m^3)	(J/kg Deg. C)	(Kg/m^3)	(W/m Deg. C)	(J/kg Deg. C)					
890	1868	890	1868	2702	240	903					
						Dwell time	Both Fluids			Effectiveness-NTU	
						of Cmin fluid (Flow	Unmixed (Single Pass)			Analytical Calculations:	
U	R*	Cw*	C*	NTU	td*	in Length direction)	Effectiveness	Tin, Fluid a	Tin, Fluid b	Tout, Fluid a	Tout, Fluid b
729.7333333	2	10	0.2	1.000062812	1	7.23392	0.596023621	100	20	52.31811029	29.53637794
								140	20	68.47716544	34.30456691
				0=Constant Resistance							
Resistor	Node A	Node B	Always Zero	Conduction/Conv.	R - Value	Always Zero					
				3 = Fluid Flow							
100	100	110	0	3	0.005353319	0	0	0	0	0	
101	101	111	0	3	0.005353319	0	0	0	0	0	
102	102	112	0	3	0.005353319	0	0	0	0	0	
103	103	113	0	3	0.005353319	0	0	0	0	0	
104	104	114	0	3	0.005353319	0	0	0	0	0	
105	105	115	0	3	0.005353319	0	0	0	0	0	
106	106	116	0	3	0.005353319	0	0	0	0	0	
107	107	117	0	3	0.005353319	0	0	0	0	0	
108	108	118	0	3	0.005353319	0	0	0	0	0	
109	109	119	0	3	0.005353319	0	0	0	0	0	
110	110	120	0	3	0.005353319	0	0	0	0	0	
111	111	121	0	3	0.005353319	0	0	0	0	0	
112	112	122	0	3	0.005353319	0	0	0	0	0	
113	113	123	0	3	0.005353319	0	0	0	0	0	
114	114	124	0	3	0.005353319	0	0	0	0	0	
115	115	125	0	3	0.005353319	0	0	0	0	0	
116	118	128	0	3	0.005353319	0	0	0	0	0	
117	117	127	0	3	0.005353319	0	0	0	0	0	
118	118	128	0	3	0.005353319	0	0	0	0	0	
119	119	129	0	3	0.005353319	0	0	0	0	0	
120	120	130	0	3	0.005353319	0	0	0	0	0	
121	121	131	0	3	0.005353319	0	0	0	0	0	
122	122	132	0	3	0.005353319	0	0	0	0	0	
123	123	133	0	3	0.005353319	0	0	0	0	0	
124	124	134	0	3	0.005353319	0	0	0	0	0	
125	125	135	0	3	0.005353319	0	0	0	0	0	
128	128	138	0	3	0.005353319	0	0	0	0	0	
127	127	137	0	3	0.005353319	0	0	0	0	0	
128	128	138	0	3	0.005353319	0	0	0	0	0	

Data Generation
Cross-Flow 10 x 10 Segment Model

129	129	139	0	3	0.005353319	0	0	0	0	0	
130	130	140	0	3	0.005353319	0	0	0	0	0	
131	131	141	0	3	0.005353319	0	0	0	0	0	
132	132	142	0	3	0.005353319	0	0	0	0	0	
133	133	143	0	3	0.005353319	0	0	0	0	0	
134	134	144	0	3	0.005353319	0	0	0	0	0	
135	135	145	0	3	0.005353319	0	0	0	0	0	
136	136	146	0	3	0.005353319	0	0	0	0	0	
137	137	147	0	3	0.005353319	0	0	0	0	0	
138	138	148	0	3	0.005353319	0	0	0	0	0	
139	139	149	0	3	0.005353319	0	0	0	0	0	
140	140	150	0	3	0.005353319	0	0	0	0	0	
141	141	151	0	3	0.005353319	0	0	0	0	0	
142	142	152	0	3	0.005353319	0	0	0	0	0	
143	143	153	0	3	0.005353319	0	0	0	0	0	
144	144	154	0	3	0.005353319	0	0	0	0	0	
145	145	155	0	3	0.005353319	0	0	0	0	0	
146	146	156	0	3	0.005353319	0	0	0	0	0	
147	147	157	0	3	0.005353319	0	0	0	0	0	
148	148	158	0	3	0.005353319	0	0	0	0	0	
149	149	159	0	3	0.005353319	0	0	0	0	0	
150	150	160	0	3	0.005353319	0	0	0	0	0	
151	151	161	0	3	0.005353319	0	0	0	0	0	
152	152	162	0	3	0.005353319	0	0	0	0	0	
153	153	183	0	3	0.005353319	0	0	0	0	0	
154	154	164	0	3	0.005353319	0	0	0	0	0	
155	155	165	0	3	0.005353319	0	0	0	0	0	
156	156	166	0	3	0.005353319	0	0	0	0	0	
157	157	167	0	3	0.005353319	0	0	0	0	0	
158	158	168	0	3	0.005353319	0	0	0	0	0	
159	159	169	0	3	0.005353319	0	0	0	0	0	
160	160	170	0	3	0.005353319	0	0	0	0	0	
161	161	171	0	3	0.005353319	0	0	0	0	0	
162	162	172	0	3	0.005353319	0	0	0	0	0	
163	163	173	0	3	0.005353319	0	0	0	0	0	
184	184	174	0	3	0.005353319	0	0	0	0	0	
165	165	175	0	3	0.005353319	0	0	0	0	0	
166	166	176	0	3	0.005353319	0	0	0	0	0	
167	167	177	0	3	0.005353319	0	0	0	0	0	
168	168	178	0	3	0.005353319	0	0	0	0	0	
169	169	179	0	3	0.005353319	0	0	0	0	0	
170	170	180	0	3	0.005353319	0	0	0	0	0	
171	171	181	0	3	0.005353319	0	0	0	0	0	
172	172	182	0	3	0.005353319	0	0	0	0	0	
173	173	183	0	3	0.005353319	0	0	0	0	0	
174	174	184	0	3	0.005353319	0	0	0	0	0	
175	175	185	0	3	0.005353319	0	0	0	0	0	
176	176	186	0	3	0.005353319	0	0	0	0	0	
177	177	187	0	3	0.005353319	0	0	0	0	0	
178	178	188	0	3	0.005353319	0	0	0	0	0	
179	179	189	0	3	0.005353319	0	0	0	0	0	
180	180	190	0	3	0.005353319	0	0	0	0	0	
181	181	191	0	3	0.005353319	0	0	0	0	0	
182	182	192	0	3	0.005353319	0	0	0	0	0	

Data Generation

Cross-Flow 10 x 10 Segment Model

183	183	193	0	3	0.005353319	0	0	0	0	0
184	184	194	0	3	0.005353319	0	0	0	0	0
185	185	195	0	3	0.005353319	0	0	0	0	0
186	186	196	0	3	0.005353319	0	0	0	0	0
187	187	197	0	3	0.005353319	0	0	0	0	0
188	188	198	0	3	0.005353319	0	0	0	0	0
189	189	199	0	3	0.005353319	0	0	0	0	0
190	190	1	0	3	0.005353319	0	0	0	0	0
191	191	1	0	3	0.005353319	0	0	0	0	0
192	192	1	0	3	0.005353319	0	0	0	0	0
193	193	1	0	3	0.005353319	0	0	0	0	0
194	194	1	0	3	0.005353319	0	0	0	0	0
195	195	1	0	3	0.005353319	0	0	0	0	0
196	196	1	0	3	0.005353319	0	0	0	0	0
197	197	1	0	3	0.005353319	0	0	0	0	0
198	198	1	0	3	0.005353319	0	0	0	0	0
199	199	1	0	3	0.005353319	0	0	0	0	0
200	200	201	0	3	0.001070664	0	0	0	0	0
201	201	202	0	3	0.001070664	0	0	0	0	0
202	202	203	0	3	0.001070664	0	0	0	0	0
203	203	204	0	3	0.001070664	0	0	0	0	0
204	204	205	0	3	0.001070664	0	0	0	0	0
205	205	206	0	3	0.001070664	0	0	0	0	0
206	206	207	0	3	0.001070664	0	0	0	0	0
207	207	208	0	3	0.001070664	0	0	0	0	0
208	208	209	0	3	0.001070664	0	0	0	0	0
209	209	2	0	3	0.001070664	0	0	0	0	0
210	210	211	0	3	0.001070664	0	0	0	0	0
211	211	212	0	3	0.001070664	0	0	0	0	0
212	212	213	0	3	0.001070664	0	0	0	0	0
213	213	214	0	3	0.001070664	0	0	0	0	0
214	214	215	0	3	0.001070664	0	0	0	0	0
215	215	216	0	3	0.001070664	0	0	0	0	0
216	216	217	0	3	0.001070664	0	0	0	0	0
217	217	218	0	3	0.001070664	0	0	0	0	0
218	218	219	0	3	0.001070664	0	0	0	0	0
219	219	2	0	3	0.001070664	0	0	0	0	0
220	220	221	0	3	0.001070664	0	0	0	0	0
221	221	222	0	3	0.001070664	0	0	0	0	0
222	222	223	0	3	0.001070664	0	0	0	0	0
223	223	224	0	3	0.001070664	0	0	0	0	0
224	224	225	0	3	0.001070664	0	0	0	0	0
225	225	226	0	3	0.001070664	0	0	0	0	0
226	226	227	0	3	0.001070664	0	0	0	0	0
227	227	228	0	3	0.001070664	0	0	0	0	0
228	228	229	0	3	0.001070664	0	0	0	0	0
229	229	2	0	3	0.001070664	0	0	0	0	0
230	230	231	0	3	0.001070664	0	0	0	0	0
231	231	232	0	3	0.001070664	0	0	0	0	0
232	232	233	0	3	0.001070664	0	0	0	0	0
233	233	234	0	3	0.001070664	0	0	0	0	0
234	234	235	0	3	0.001070664	0	0	0	0	0
235	235	236	0	3	0.001070664	0	0	0	0	0
236	236	237	0	3	0.001070664	0	0	0	0	0

Data Generation
Cross-Flow 10 x 10 Segment Model

237	237	238	0	3	0.001070664	0	0	0	0	0	
238	238	239	0	3	0.001070664	0	0	0	0	0	
239	239	2	0	3	0.001070664	0	0	0	0	0	
240	240	241	0	3	0.001070664	0	0	0	0	0	
241	241	242	0	3	0.001070664	0	0	0	0	0	
242	242	243	0	3	0.001070664	0	0	0	0	0	
243	243	244	0	3	0.001070664	0	0	0	0	0	
244	244	245	0	3	0.001070664	0	0	0	0	0	
245	245	246	0	3	0.001070664	0	0	0	0	0	
246	246	247	0	3	0.001070664	0	0	0	0	0	
247	247	248	0	3	0.001070664	0	0	0	0	0	
248	248	249	0	3	0.001070664	0	0	0	0	0	
249	249	2	0	3	0.001070664	0	0	0	0	0	
250	250	251	0	3	0.001070664	0	0	0	0	0	
251	251	252	0	3	0.001070664	0	0	0	0	0	
252	252	253	0	3	0.001070664	0	0	0	0	0	
253	253	254	0	3	0.001070664	0	0	0	0	0	
254	254	255	0	3	0.001070664	0	0	0	0	0	
255	255	256	0	3	0.001070664	0	0	0	0	0	
256	256	257	0	3	0.001070664	0	0	0	0	0	
257	257	258	0	3	0.001070664	0	0	0	0	0	
258	258	259	0	3	0.001070664	0	0	0	0	0	
259	259	2	0	3	0.001070664	0	0	0	0	0	
260	260	261	0	3	0.001070664	0	0	0	0	0	
261	261	262	0	3	0.001070664	0	0	0	0	0	
262	262	263	0	3	0.001070664	0	0	0	0	0	
263	263	264	0	3	0.001070664	0	0	0	0	0	
264	264	265	0	3	0.001070664	0	0	0	0	0	
265	265	266	0	3	0.001070664	0	0	0	0	0	
266	266	267	0	3	0.001070664	0	0	0	0	0	
267	267	268	0	3	0.001070664	0	0	0	0	0	
268	268	269	0	3	0.001070664	0	0	0	0	0	
269	269	2	0	3	0.001070664	0	0	0	0	0	
270	270	271	0	3	0.001070664	0	0	0	0	0	
271	271	272	0	3	0.001070664	0	0	0	0	0	
272	272	273	0	3	0.001070664	0	0	0	0	0	
273	273	274	0	3	0.001070664	0	0	0	0	0	
274	274	275	0	3	0.001070664	0	0	0	0	0	
275	275	276	0	3	0.001070664	0	0	0	0	0	
276	276	277	0	3	0.001070664	0	0	0	0	0	
277	277	278	0	3	0.001070664	0	0	0	0	0	
278	278	279	0	3	0.001070664	0	0	0	0	0	
279	279	2	0	3	0.001070664	0	0	0	0	0	
280	280	281	0	3	0.001070664	0	0	0	0	0	
281	281	282	0	3	0.001070664	0	0	0	0	0	
282	282	283	0	3	0.001070664	0	0	0	0	0	
283	283	284	0	3	0.001070664	0	0	0	0	0	
284	284	285	0	3	0.001070664	0	0	0	0	0	
285	285	286	0	3	0.001070664	0	0	0	0	0	
286	286	287	0	3	0.001070664	0	0	0	0	0	
287	287	288	0	3	0.001070664	0	0	0	0	0	
288	288	289	0	3	0.001070664	0	0	0	0	0	
289	289	2	0	3	0.001070664	0	0	0	0	0	
290	290	291	0	3	0.001070664	0	0	0	0	0	

Data Generation
Cross-Flow 10 x 10 Segment Model

291	291	292	0	3	0.001070664	0	0	0	0	0
292	292	293	0	3	0.001070664	0	0	0	0	0
293	293	294	0	3	0.001070664	0	0	0	0	0
294	294	295	0	3	0.001070664	0	0	0	0	0
295	295	296	0	3	0.001070664	0	0	0	0	0
296	296	297	0	3	0.001070664	0	0	0	0	0
297	297	298	0	3	0.001070664	0	0	0	0	0
298	298	299	0	3	0.001070664	0	0	0	0	0
299	299	2	0	3	0.001070664	0	0	0	0	0
300	100	300	0	0	0.035688552	0	0	0	0	0
301	101	301	0	0	0.035688552	0	0	0	0	0
302	102	302	0	0	0.035688552	0	0	0	0	0
303	103	303	0	0	0.035688552	0	0	0	0	0
304	104	304	0	0	0.035688552	0	0	0	0	0
305	105	305	0	0	0.035688552	0	0	0	0	0
306	106	306	0	0	0.035688552	0	0	0	0	0
307	107	307	0	0	0.035688552	0	0	0	0	0
308	108	308	0	0	0.035688552	0	0	0	0	0
309	109	309	0	0	0.035688552	0	0	0	0	0
310	110	310	0	0	0.035688552	0	0	0	0	0
311	111	311	0	0	0.035688552	0	0	0	0	0
312	112	312	0	0	0.035688552	0	0	0	0	0
313	113	313	0	0	0.035688552	0	0	0	0	0
314	114	314	0	0	0.035688552	0	0	0	0	0
315	115	315	0	0	0.035688552	0	0	0	0	0
316	116	316	0	0	0.035688552	0	0	0	0	0
317	117	317	0	0	0.035688552	0	0	0	0	0
318	118	318	0	0	0.035688552	0	0	0	0	0
319	119	319	0	0	0.035688552	0	0	0	0	0
320	120	320	0	0	0.035688552	0	0	0	0	0
321	121	321	0	0	0.035688552	0	0	0	0	0
322	122	322	0	0	0.035688552	0	0	0	0	0
323	123	323	0	0	0.035688552	0	0	0	0	0
324	124	324	0	0	0.035688552	0	0	0	0	0
325	125	325	0	0	0.035688552	0	0	0	0	0
326	126	326	0	0	0.035688552	0	0	0	0	0
327	127	327	0	0	0.035688552	0	0	0	0	0
328	128	328	0	0	0.035688552	0	0	0	0	0
329	129	329	0	0	0.035688552	0	0	0	0	0
330	130	330	0	0	0.035688552	0	0	0	0	0
331	131	331	0	0	0.035688552	0	0	0	0	0
332	132	332	0	0	0.035688552	0	0	0	0	0
333	133	333	0	0	0.035688552	0	0	0	0	0
334	134	334	0	0	0.035688552	0	0	0	0	0
335	135	335	0	0	0.035688552	0	0	0	0	0
336	136	336	0	0	0.035688552	0	0	0	0	0
337	137	337	0	0	0.035688552	0	0	0	0	0
338	138	338	0	0	0.035688552	0	0	0	0	0
339	139	339	0	0	0.035688552	0	0	0	0	0
340	140	340	0	0	0.035688552	0	0	0	0	0
341	141	341	0	0	0.035688552	0	0	0	0	0
342	142	342	0	0	0.035688552	0	0	0	0	0
343	143	343	0	0	0.035688552	0	0	0	0	0
344	144	344	0	0	0.035688552	0	0	0	0	0

Data Generation

Cross-Flow 10 x 10 Segment Model

345	145	345	0	0	0.035888552	0	0	0	0	0	
346	146	346	0	0	0.035688552	0	0	0	0	0	
347	147	347	0	0	0.035688552	0	0	0	0	0	
348	148	348	0	0	0.035888552	0	0	0	0	0	
349	149	349	0	0	0.035888552	0	0	0	0	0	
350	150	350	0	0	0.035688552	0	0	0	0	0	
351	151	351	0	0	0.035888552	0	0	0	0	0	
352	152	352	0	0	0.035688552	0	0	0	0	0	
353	153	353	0	0	0.035688552	0	0	0	0	0	
354	154	354	0	0	0.035656552	0	0	0	0	0	
355	155	355	0	0	0.035688552	0	0	0	0	0	
356	156	356	0	0	0.035688552	0	0	0	0	0	
357	157	357	0	0	0.035688552	0	0	0	0	0	
358	158	358	0	0	0.035656552	0	0	0	0	0	
359	159	359	0	0	0.035686552	0	0	0	0	0	
360	160	360	0	0	0.035688552	0	0	0	0	0	
361	181	361	0	0	0.035688552	0	0	0	0	0	
362	162	382	0	0	0.035688552	0	0	0	0	0	
363	163	363	0	0	0.035686552	0	0	0	0	0	
364	184	364	0	0	0.035688552	0	0	0	0	0	
365	165	365	0	0	0.035688552	0	0	0	0	0	
366	156	356	0	0	0.035686552	0	0	0	0	0	
367	167	367	0	0	0.035686552	0	0	0	0	0	
368	168	368	0	0	0.035686552	0	0	0	0	0	
369	169	369	0	0	0.035688552	0	0	0	0	0	
370	170	370	0	0	0.035686552	0	0	0	0	0	
371	171	371	0	0	0.035688552	0	0	0	0	0	
372	172	372	0	0	0.035688552	0	0	0	0	0	
373	173	373	0	0	0.035688552	0	0	0	0	0	
374	174	374	0	0	0.035688552	0	0	0	0	0	
375	175	375	0	0	0.035688552	0	0	0	0	0	
376	176	376	0	0	0.035686552	0	0	0	0	0	
377	177	377	0	0	0.035688552	0	0	0	0	0	
378	178	378	0	0	0.035686552	0	0	0	0	0	
379	179	379	0	0	0.035688552	0	0	0	0	0	
380	180	380	0	0	0.035688552	0	0	0	0	0	
381	181	381	0	0	0.035888552	0	0	0	0	0	
382	182	382	0	0	0.035688552	0	0	0	0	0	
383	183	383	0	0	0.035686552	0	0	0	0	0	
384	184	384	0	0	0.035686552	0	0	0	0	0	
385	185	385	0	0	0.035686552	0	0	0	0	0	
386	188	388	0	0	0.035688552	0	0	0	0	0	
387	187	387	0	0	0.035688552	0	0	0	0	0	
388	188	398	0	0	0.035688552	0	0	0	0	0	
389	189	389	0	0	0.035688552	0	0	0	0	0	
390	190	390	0	0	0.035656552	0	0	0	0	0	
391	191	391	0	0	0.035888552	0	0	0	0	0	
392	192	392	0	0	0.035888552	0	0	0	0	0	
393	193	393	0	0	0.035888552	0	0	0	0	0	
394	194	394	0	0	0.035888552	0	0	0	0	0	
395	195	395	0	0	0.035686552	0	0	0	0	0	
396	196	396	0	0	0.035686552	0	0	0	0	0	
397	197	397	0	0	0.035688552	0	0	0	0	0	
398	198	398	0	0	0.035888552	0	0	0	0	0	

Data Generation
Cross-Flow 10 x 10 Segment Model

399	199	399	0	0	0.035686552	0	0	0	0	0
400	200	300	0	0	0.017843276	0	0	0	0	0
401	201	301	0	0	0.017843276	0	0	0	0	0
402	202	302	0	0	0.017843276	0	0	0	0	0
403	203	303	0	0	0.017843276	0	0	0	0	0
404	204	304	0	0	0.017843276	0	0	0	0	0
405	205	305	0	0	0.017843276	0	0	0	0	0
406	206	306	0	0	0.017843276	0	0	0	0	0
407	207	307	0	0	0.017843276	0	0	0	0	0
408	208	308	0	0	0.017843276	0	0	0	0	0
409	209	309	0	0	0.017843276	0	0	0	0	0
410	210	310	0	0	0.017843276	0	0	0	0	0
411	211	311	0	0	0.017843276	0	0	0	0	0
412	212	312	0	0	0.017843276	0	0	0	0	0
413	213	313	0	0	0.017843276	0	0	0	0	0
414	214	314	0	0	0.017843276	0	0	0	0	0
415	215	315	0	0	0.017843276	0	0	0	0	0
416	216	316	0	0	0.017843276	0	0	0	0	0
417	217	317	0	0	0.017843276	0	0	0	0	0
418	218	318	0	0	0.017843276	0	0	0	0	0
419	219	319	0	0	0.017843276	0	0	0	0	0
420	220	320	0	0	0.017843276	0	0	0	0	0
421	221	321	0	0	0.017843276	0	0	0	0	0
422	222	322	0	0	0.017843276	0	0	0	0	0
423	223	323	0	0	0.017843276	0	0	0	0	0
424	224	324	0	0	0.017843276	0	0	0	0	0
425	225	325	0	0	0.017843276	0	0	0	0	0
426	226	326	0	0	0.017843276	0	0	0	0	0
427	227	327	0	0	0.017843276	0	0	0	0	0
428	228	328	0	0	0.017843276	0	0	0	0	0
429	229	329	0	0	0.017843276	0	0	0	0	0
430	230	330	0	0	0.017843276	0	0	0	0	0
431	231	331	0	0	0.017843276	0	0	0	0	0
432	232	332	0	0	0.017843276	0	0	0	0	0
433	233	333	0	0	0.017843276	0	0	0	0	0
434	234	334	0	0	0.017843276	0	0	0	0	0
435	235	335	0	0	0.017843276	0	0	0	0	0
436	236	336	0	0	0.017843276	0	0	0	0	0
437	237	337	0	0	0.017843276	0	0	0	0	0
438	238	338	0	0	0.017843276	0	0	0	0	0
439	239	339	0	0	0.017843276	0	0	0	0	0
440	240	340	0	0	0.017843276	0	0	0	0	0
441	241	341	0	0	0.017843276	0	0	0	0	0
442	242	342	0	0	0.017843276	0	0	0	0	0
443	243	343	0	0	0.017843276	0	0	0	0	0
444	244	344	0	0	0.017843276	0	0	0	0	0
445	245	345	0	0	0.017843276	0	0	0	0	0
446	246	346	0	0	0.017843276	0	0	0	0	0
447	247	347	0	0	0.017843276	0	0	0	0	0
448	248	348	0	0	0.017843276	0	0	0	0	0
449	249	349	0	0	0.017843276	0	0	0	0	0
450	250	350	0	0	0.017843276	0	0	0	0	0
451	251	351	0	0	0.017843276	0	0	0	0	0
452	252	352	0	0	0.017843276	0	0	0	0	0

Data Generation
Cross-Flow 10 x 10 Segment Model

453	253	353	0	0	0.017843276	0	0	0	0	0	
454	254	354	0	0	0.017843276	0	0	0	0	0	
455	255	355	0	0	0.017843276	0	0	0	0	0	
456	256	356	0	0	0.017843276	0	0	0	0	0	
457	257	357	0	0	0.017843276	0	0	0	0	0	
458	258	358	0	0	0.017843276	0	0	0	0	0	
459	259	359	0	0	0.017843276	0	0	0	0	0	
460	260	360	0	0	0.017843276	0	0	0	0	0	
461	261	361	0	0	0.017843276	0	0	0	0	0	
462	262	362	0	0	0.017843276	0	0	0	0	0	
463	263	363	0	0	0.017843276	0	0	0	0	0	
464	264	364	0	0	0.017843276	0	0	0	0	0	
465	265	365	0	0	0.017843276	0	0	0	0	0	
466	266	366	0	0	0.017843276	0	0	0	0	0	
467	267	367	0	0	0.017843276	0	0	0	0	0	
468	268	368	0	0	0.017843276	0	0	0	0	0	
469	269	369	0	0	0.017843276	0	0	0	0	0	
470	270	370	0	0	0.017843276	0	0	0	0	0	
471	271	371	0	0	0.017843276	0	0	0	0	0	
472	272	372	0	0	0.017843276	0	0	0	0	0	
473	273	373	0	0	0.017843276	0	0	0	0	0	
474	274	374	0	0	0.017843276	0	0	0	0	0	
475	275	375	0	0	0.017843276	0	0	0	0	0	
476	276	376	0	0	0.017843276	0	0	0	0	0	
477	277	377	0	0	0.017843276	0	0	0	0	0	
478	278	378	0	0	0.017843276	0	0	0	0	0	
479	279	379	0	0	0.017843276	0	0	0	0	0	
480	280	380	0	0	0.017843276	0	0	0	0	0	
481	281	381	0	0	0.017843276	0	0	0	0	0	
482	282	382	0	0	0.017843276	0	0	0	0	0	
483	283	383	0	0	0.017843276	0	0	0	0	0	
484	284	384	0	0	0.017843276	0	0	0	0	0	
485	285	385	0	0	0.017843276	0	0	0	0	0	
486	286	386	0	0	0.017843276	0	0	0	0	0	
487	287	387	0	0	0.017843276	0	0	0	0	0	
488	288	388	0	0	0.017843276	0	0	0	0	0	
489	289	389	0	0	0.017843276	0	0	0	0	0	
490	290	390	0	0	0.017843276	0	0	0	0	0	
491	291	391	0	0	0.017843276	0	0	0	0	0	
492	292	392	0	0	0.017843276	0	0	0	0	0	
493	293	393	0	0	0.017843276	0	0	0	0	0	
494	294	394	0	0	0.017843276	0	0	0	0	0	
495	295	395	0	0	0.017843276	0	0	0	0	0	
496	296	396	0	0	0.017843276	0	0	0	0	0	
497	297	397	0	0	0.017843276	0	0	0	0	0	
498	298	398	0	0	0.017843276	0	0	0	0	0	
499	299	399	0	0	0.017843276	0	0	0	0	0	
	Initial			Node							
Node #	Temperature	Always Zero	Always Zero	Volume	Node	Time					
	(Degrees C)			(Meters^2)	Material	Classes					
1	52.380241	0	0	0.0001	Oil	1					

Data Generation
Cross-Flow 10 x 10 Segment Model

2	29.527943	0	0	0.0004	Oil	1					
100	100	0	0	0.0001	Oil	2					
101	100	0	0	0.0001	Oil	2					
102	100	0	0	0.0001	Oil	2					
103	100	0	0	0.0001	Oil	2					
104	100	0	0	0.0001	Oil	2					
105	100	0	0	0.0001	Oil	2					
106	100	0	0	0.0001	Oil	2					
107	100	0	0	0.0001	Oil	2					
108	100	0	0	0.0001	Oil	2					
109	100	0	0	0.0001	Oil	2					
110	92.471504	0	0	0.0001	Oil	1					
111	92.813197	0	0	0.0001	Oil	1					
112	92.752235	0	0	0.0001	Oil	1					
113	92.888641	0	0	0.0001	Oil	1					
114	93.022484	0	0	0.0001	Oil	1					
115	93.153809	0	0	0.0001	Oil	1					
116	93.282877	0	0	0.0001	Oil	1					
117	93.409096	0	0	0.0001	Oil	1					
118	93.533142	0	0	0.0001	Oil	1					
119	93.455338	0	0	0.0001	Oil	1					
120	85.851489	0	0	0.0001	Oil	1					
121	85.908218	0	0	0.0001	Oil	1					
122	88.160382	0	0	0.0001	Oil	1					
123	86.407997	0	0	0.0001	Oil	1					
124	86.651222	0	0	0.0001	Oil	1					
125	86.890106	0	0	0.0001	Oil	1					
126	87.124733	0	0	0.0001	Oil	1					
127	87.355156	0	0	0.0001	Oil	1					
128	87.581474	0	0	0.0001	Oil	1					
129	87.478799	0	0	0.0001	Oil	1					
130	79.473289	0	0	0.0001	Oil	1					
131	79.822136	0	0	0.0001	Oil	1					
132	80.1851	0	0	0.0001	Oil	1					
133	80.502274	0	0	0.0001	Oil	1					
134	80.833755	0	0	0.0001	Oil	1					
135	81.159653	0	0	0.0001	Oil	1					
136	81.480057	0	0	0.0001	Oil	1					
137	81.795029	0	0	0.0001	Oil	1					
138	82.104898	0	0	0.0001	Oil	1					
139	82.018579	0	0	0.0001	Oil	1					
140	73.876488	0	0	0.0001	Oil	1					
141	74.297844	0	0	0.0001	Oil	1					
142	74.712509	0	0	0.0001	Oil	1					
143	75.120575	0	0	0.0001	Oil	1					
144	75.522158	0	0	0.0001	Oil	1					
145	75.917351	0	0	0.0001	Oil	1					
146	78.306274	0	0	0.0001	Oil	1					
147	76.88898	0	0	0.0001	Oil	1					
148	77.065813	0	0	0.0001	Oil	1					
149	77.030998	0	0	0.0001	Oil	1					
150	88.806381	0	0	0.0001	Oil	1					
151	89.283518	0	0	0.0001	Oil	1					
152	89.753532	0	0	0.0001	Oil	1					

Data Generation
Cross-Flow 10 x 10 Segment Model

153	70.21653	0	0	0.0001	Oil	1					
154	70.672623	0	0	0.0001	Oil	1					
155	71.121902	0	0	0.0001	Oil	1					
156	71.564476	0	0	0.0001	Oil	1					
157	72.00042	0	0	0.0001	Oil	1					
158	72.429646	0	0	0.0001	Oil	1					
159	72.460179	0	0	0.0001	Oil	1					
160	64.213409	0	0	0.0001	Oil	1					
161	64.732079	0	0	0.0001	Oil	1					
162	65.24353	0	0	0.0001	Oil	1					
163	65.747641	0	0	0.0001	Oil	1					
164	66.245117	0	0	0.0001	Oil	1					
165	66.735451	0	0	0.0001	Oil	1					
166	67.216933	0	0	0.0001	Oil	1					
167	67.695641	0	0	0.0001	Oil	1					
168	66.16566	0	0	0.0001	Oil	1					
169	66.327713	0	0	0.0001	Oil	1					
170	60.052654	0	0	0.0001	Oil	1					
171	60.60063	0	0	0.0001	Oil	1					
172	61.141903	0	0	0.0001	Oil	1					
173	61.675953	0	0	0.0001	Oil	1					
174	62.203072	0	0	0.0001	Oil	1					
175	62.723335	0	0	0.0001	Oil	1					
176	63.236635	0	0	0.0001	Oil	1					
177	63.743626	0	0	0.0001	Oil	1					
178	64.243613	0	0	0.0001	Oil	1					
179	64.540344	0	0	0.0001	Oil	1					
180	56.263455	0	0	0.0001	Oil	1					
181	56.650986	0	0	0.0001	Oil	1					
182	57.411716	0	0	0.0001	Oil	1					
183	57.965717	0	0	0.0001	Oil	1					
184	56.513062	0	0	0.0001	Oil	1					
185	59.053614	0	0	0.0001	Oil	1					
186	59.566055	0	0	0.0001	Oil	1					
187	60.115629	0	0	0.0001	Oil	1					
188	60.637226	0	0	0.0001	Oil	1					
189	61.067736	0	0	0.0001	Oil	1					
190	52.866965	0	0	0.0001	Oil	1					
191	53.44735	0	0	0.0001	Oil	1					
192	54.019375	0	0	0.0001	Oil	1					
193	54.565067	0	0	0.0001	Oil	1					
194	55.14455	0	0	0.0001	Oil	1					
195	55.697615	0	0	0.0001	Oil	1					
196	56.244942	0	0	0.0001	Oil	1					
197	56.765973	0	0	0.0001	Oil	1					
198	57.320976	0	0	0.0001	Oil	1					
199	57.942204	0	0	0.0001	Oil	1					
200	20	0	0	0.0004	Oil	3					
201	21.505666	0	0	0.0004	Oil	1					
202	22.963044	0	0	0.0004	Oil	1					
203	24.432596	0	0	0.0004	Oil	1					
204	25.654666	0	0	0.0004	Oil	1					
205	27.250366	0	0	0.0004	Oil	1					
206	26.619606	0	0	0.0004	Oil	1					

Data Generation
Cross-Flow 10 x 10 Segment Model

207	29.963072	0	0	0.0004	Oil	1					
208	31.281252	0	0	0.0004	Oil	1					
209	32.574823	0	0	0.0004	Oil	1					
210	20	0	0	0.0004	Oil	3					
211	21.383989	0	0	0.0004	Oil	1					
212	22.704987	0	0	0.0004	Oil	1					
213	24.023381	0	0	0.0004	Oil	1					
214	25.319489	0	0	0.0004	Oil	1					
215	26.593742	0	0	0.0004	Oil	1					
216	27.846483	0	0	0.0004	Oil	1					
217	29.078072	0	0	0.0004	Oil	1					
218	30.28868	0	0	0.0004	Oil	1					
219	31.479195	0	0	0.0004	Oil	1					
220	20	0	0	0.0004	Oil	3					
221	21.23563	0	0	0.0004	Oil	1					
222	22.452847	0	0	0.0004	Oil	1					
223	23.651899	0	0	0.0004	Oil	1					
224	24.833048	0	0	0.0004	Oil	1					
225	25.996538	0	0	0.0004	Oil	1					
226	27.14283	0	0	0.0004	Oil	1					
227	28.271566	0	0	0.0004	Oil	1					
228	29.383591	0	0	0.0004	Oil	1					
229	30.478947	0	0	0.0004	Oil	1					
230	20	0	0	0.0004	Oil	3					
231	21.119349	0	0	0.0004	Oil	1					
232	22.224207	0	0	0.0004	Oil	1					
233	23.314728	0	0	0.0004	Oil	1					
234	24.391064	0	0	0.0004	Oil	1					
235	25.453384	0	0	0.0004	Oil	1					
236	26.501844	0	0	0.0004	Oil	1					
237	27.5366	0	0	0.0004	Oil	1					
238	28.55781	0	0	0.0004	Oil	1					
239	29.565628	0	0	0.0004	Oil	1					
240	20	0	0	0.0004	Oil	3					
241	21.014011	0	0	0.0004	Oil	1					
242	22.018878	0	0	0.0004	Oil	1					
243	23.005675	0	0	0.0004	Oil	1					
244	23.989483	0	0	0.0004	Oil	1					
245	24.959391	0	0	0.0004	Oil	1					
246	25.918482	0	0	0.0004	Oil	1					
247	26.866842	0	0	0.0004	Oil	1					
248	27.804554	0	0	0.0004	Oil	1					
249	28.731709	0	0	0.0004	Oil	1					
250	20	0	0	0.0004	Oil	3					
251	20.918585	0	0	0.0004	Oil	1					
252	21.828873	0	0	0.0004	Oil	1					
253	22.730873	0	0	0.0004	Oil	1					
254	23.624811	0	0	0.0004	Oil	1					
255	24.510111	0	0	0.0004	Oil	1					
256	25.387402	0	0	0.0004	Oil	1					
257	26.25851	0	0	0.0004	Oil	1					
258	27.117488	0	0	0.0004	Oil	1					
259	27.970301	0	0	0.0004	Oil	1					
260	20	0	0	0.0004	Oil	3					

Data Generation
Cross-Flow 10 x 10 Segment Model

261	20.832136	0	0	0.0004	Oil	1					
282	21.858388	0	0	0.0004	Oil	1					
283	22.478712	0	0	0.0004	Oil	1					
284	23.293089	0	0	0.0004	Oil	1					
285	24.101498	0	0	0.0004	Oil	1					
286	24.903921	0	0	0.0004	Oil	1					
287	25.70034	0	0	0.0004	Oil	1					
288	28.490744	0	0	0.0004	Oil	1					
289	27.275118	0	0	0.0004	Oil	1					
270	20	0	0	0.0004	Oil	3					
271	20.753834	0	0	0.0004	Oil	1					
272	21.503803	0	0	0.0004	Oil	1					
273	22.24984	0	0	0.0004	Oil	1					
274	22.991888	0	0	0.0004	Oil	1					
275	23.729889	0	0	0.0004	Oil	1					
278	24.483793	0	0	0.0004	Oil	1					
277	25.19355	0	0	0.0004	Oil	1					
278	25.919109	0	0	0.0004	Oil	1					
279	28.840427	0	0	0.0004	Oil	1					
280	20	0	0	0.0004	Oil	3					
281	20.882901	0	0	0.0004	Oil	1					
282	21.363828	0	0	0.0004	Oil	1					
283	22.042097	0	0	0.0004	Oil	1					
284	22.718224	0	0	0.0004	Oil	1					
285	23.391928	0	0	0.0004	Oil	1					
288	24.063128	0	0	0.0004	Oil	1					
287	24.731749	0	0	0.0004	Oil	1					
288	25.39772	0	0	0.0004	Oil	1					
289	28.06097	0	0	0.0004	Oil	1					
290	20	0	0	0.0004	Oil	3					
291	20.845697	0	0	0.0004	Oil	1					
292	21.284203	0	0	0.0004	Oil	1					
293	21.91548	0	0	0.0004	Oil	1					
294	22.539505	0	0	0.0004	Oil	1					
295	23.156256	0	0	0.0004	Oil	1					
296	23.765711	0	0	0.0004	Oil	1					
297	24.367849	0	0	0.0004	Oil	1					
298	24.96285	0	0	0.0004	Oil	1					
299	25.550097	0	0	0.0004	Oil	1					
300	45.881283	0	0	0.0006	Aluminum	1					
301	48.880222	0	0	0.0006	Aluminum	1					
302	47.880001	0	0	0.0006	Aluminum	1					
303	48.860962	0	0	0.0006	Aluminum	1					
304	49.82346	0	0	0.0006	Aluminum	1					
305	50.787845	0	0	0.0006	Aluminum	1					
306	51.894458	0	0	0.0006	Aluminum	1					
307	52.803822	0	0	0.0006	Aluminum	1					
308	53.495682	0	0	0.0006	Aluminum	1					
309	52.936184	0	0	0.0006	Aluminum	1					
310	43.427559	0	0	0.0006	Aluminum	1					
311	44.396431	0	0	0.0006	Aluminum	1					
312	45.348877	0	0	0.0006	Aluminum	1					
313	48.28518	0	0	0.0006	Aluminum	1					
314	47.205583	0	0	0.0006	Aluminum	1					

Data Generation
Cross-Flow 10 x 10 Segment Model

315	48.110344	0	0	0.0006	Aluminum	1					
316	48.999775	0	0	0.0006	Aluminum	1					
317	49.8741	0	0	0.0006	Aluminum	1					
318	50.733582	0	0	0.0006	Aluminum	1					
319	50.462582	0	0	0.0006	Aluminum	1					
320	41.222885	0	0	0.0006	Aluminum	1					
321	42.142075	0	0	0.0006	Aluminum	1					
322	43.047318	0	0	0.0006	Aluminum	1					
323	43.938808	0	0	0.0006	Aluminum	1					
324	44.816757	0	0	0.0006	Aluminum	1					
325	45.681355	0	0	0.0006	Aluminum	1					
326	46.532803	0	0	0.0006	Aluminum	1					
327	47.371277	0	0	0.0006	Aluminum	1					
328	48.196983	0	0	0.0008	Aluminum	1					
329	48.211327	0	0	0.0006	Aluminum	1					
330	39.225681	0	0	0.0006	Aluminum	1					
331	40.095959	0	0	0.0006	Aluminum	1					
332	40.954525	0	0	0.0006	Aluminum	1					
333	41.80151	0	0	0.0006	Aluminum	1					
334	42.637066	0	0	0.0006	Aluminum	1					
335	43.481323	0	0	0.0006	Aluminum	1					
336	44.274426	0	0	0.0006	Aluminum	1					
337	45.076504	0	0	0.0006	Aluminum	1					
338	45.887895	0	0	0.0006	Aluminum	1					
339	46.164356	0	0	0.0006	Aluminum	1					
340	37.416428	0	0	0.0006	Aluminum	1					
341	38.236861	0	0	0.0006	Aluminum	1					
342	39.051582	0	0	0.0006	Aluminum	1					
343	39.854875	0	0	0.0006	Aluminum	1					
344	40.648243	0	0	0.0006	Aluminum	1					
345	41.432365	0	0	0.0006	Aluminum	1					
346	42.207138	0	0	0.0006	Aluminum	1					
347	42.972645	0	0	0.0006	Aluminum	1					
348	43.728977	0	0	0.0006	Aluminum	1					
349	44.305229	0	0	0.0006	Aluminum	1					
350	35.777435	0	0	0.0006	Aluminum	1					
351	36.553318	0	0	0.0006	Aluminum	1					
352	37.321281	0	0	0.0006	Aluminum	1					
353	38.081367	0	0	0.0006	Aluminum	1					
354	38.83383	0	0	0.0006	Aluminum	1					
355	39.578114	0	0	0.0006	Aluminum	1					
356	40.314877	0	0	0.0006	Aluminum	1					
357	41.043957	0	0	0.0006	Aluminum	1					
358	41.765415	0	0	0.0006	Aluminum	1					
359	42.618996	0	0	0.0006	Aluminum	1					
360	34.292879	0	0	0.0006	Aluminum	1					
361	35.023491	0	0	0.0006	Aluminum	1					
362	35.747978	0	0	0.0006	Aluminum	1					
363	36.488148	0	0	0.0006	Aluminum	1					
364	37.178017	0	0	0.0006	Aluminum	1					
365	37.883802	0	0	0.0006	Aluminum	1					
366	38.582924	0	0	0.0006	Aluminum	1					
367	39.27599	0	0	0.0006	Aluminum	1					
368	39.96283	0	0	0.0006	Aluminum	1					

Data Generation
Cross-Flow 10 x 10 Segment Model

369	41.092052	0	0	0 0008	Aluminum	1					
370	32.947855	0	0	0 0008	Aluminum	1					
371	33.63501	0	0	0.0006	Aluminum	1					
372	34.317451	0	0	0.0006	Aluminum	1					
373	34.994961	0	0	0 0008	Aluminum	1					
374	35.667528	0	0	0.0006	Aluminum	1					
375	36.335144	0	0	0 0006	Aluminum	1					
376	36.997795	0	0	0 0006	Aluminum	1					
377	37.655476	0	0	0 0006	Aluminum	1					
378	38.308182	0	0	0 0008	Aluminum	1					
379	39.712025	0	0	0 0006	Aluminum	1					
380	31.729206	0	0	0.0008	Aluminum	1					
381	32.374609	0	0	0 0008	Aluminum	1					
382	33.016747	0	0	0.0006	Aluminum	1					
383	33.65496	0	0	0 0008	Aluminum	1					
384	34.289474	0	0	0 0006	Aluminum	1					
385	34.9202	0	0	0 0006	Aluminum	1					
386	35.547134	0	0	0 0006	Aluminum	1					
387	36.170216	0	0	0 0008	Aluminum	1					
388	36.789452	0	0	0 0008	Aluminum	1					
389	36.467813	0	0	0 0006	Aluminum	1					
390	31.090399	0	0	0 0008	Aluminum	1					
391	31.612404	0	0	0.0006	Aluminum	1					
392	32.126774	0	0	0.0006	Aluminum	1					
393	32.633503	0	0	0.0006	Aluminum	1					
394	33.132591	0	0	0 0006	Aluminum	1					
395	33.624023	0	0	0 0008	Aluminum	1					
396	34 107796	0	0	0 0006	Aluminum	1					
397	34.563927	0	0	0 0008	Aluminum	1					
398	35.052391	0	0	0 0006	Aluminum	1					
399	36.636928	0	0	0 0008	Aluminum	1					

Appendix C

Excel Spreadsheet Formulas:

$\dot{m}_{\max}$:

$$C^{*}=\frac{\left(\dot{m}c_{p}\right)_{\min}}{\left(\dot{m}c_{p}\right)_{\max}}$$

$$\Rightarrow \dot{m}_{\max}=\frac{\left(\dot{m}c_{p}\right)_{\min}}{C^{*}c_{p_{\max}}}$$

h_{max}:

$$R^{*}=\frac{(hA)_{\max}}{(hA)_{\min}}$$

$$\Rightarrow h_{\max}=R^{*}h_{\min}\frac{A_{\min}}{A_{\max}}=R^{*}h_{\min}$$

hgt_{max}:

$$t_{d}^{*}=\frac{\left(\frac{Lw(hgt)\rho}{\dot{m}}\right)_{\min}}{\left(\frac{Lw(hgt)\rho}{\dot{m}}\right)_{\max}}$$

$$\Rightarrow hgt_{\max}=\frac{hgt_{\min}\rho_{\min}\dot{m}_{\max}}{\rho_{\max}\dot{m}_{\min}t_{d}^{*}}$$

thk_{wall}:

$$\overline{C}_w^* = \frac{\rho_{wall} L(wdth) c_{p_{wall}} thk_{wall}}{\left(\rho c_p L(wdth) hgt\right)_{\min}}$$

$$\Rightarrow thk_{wall} = \overline{C}_w^* \frac{\left(\rho c_p L(wdth) hgt\right)_{\min}}{\rho_{wall} L(wdth) c_{p_{wall}}} = \overline{C}_w^* \frac{\left(\rho c_p hgt\right)_{\min}}{\rho_{wall} c_{p_{wall}}}$$

U:

$$NTU = \frac{UA}{\left(\dot{m} c_p\right)_{\min}} = \frac{1}{\left(\dot{m} c_p\right)_{\min} \left[\frac{1}{(hA)_{\min}} + \frac{1}{(hA)_{\max}}\right]}$$

$$\Rightarrow U = \frac{1}{\left[\left(\frac{1}{h}\right)_{\min} + \left(\frac{1}{h}\right)_{\max}\right]}$$

NTU:

$$NTU = \frac{UA}{C_{\min}} = \frac{1}{\left(\dot{m} c_p\right)_{\min} \left[\frac{1}{(hA)_{\min}} + \frac{1}{(hA)_{\max}}\right]} = \frac{UA}{\left(\dot{m} c_p\right)_{\min}}$$

$$\Rightarrow NTU = \frac{UA}{\left(\dot{m} c_p\right)_{\min}}$$

$t_{d,\min}$:

$$t_{d,\min} = \left[\frac{\rho L(wdth) hgt}{\dot{m}}\right]_{\min}$$

Steady-State Outlet Temperature Calculations (Effectiveness-NTU Method Incropera et al. (1985)):

ε:

Parallel-Flow Formula:

$$\varepsilon = \frac{\left[1 - EXP\left(-NTU\left(1 + C^{*}\right)\right)\right]}{\left[1 + C^{*}\right]}$$

Cross-Flow Formula (Single pass/Both fluids unmixed):

$$\varepsilon = 1 - EXP\left[\left(\frac{1}{C^{*}}\right) NTU^{0.22}\left[EXP\left(-C^{*} NTU^{0.78}\right) - 1\right]\right]$$

$T_{out:}$

Parallel-Flow Formulas and
Cross-Flow Formulas (Single pass/Both fluids unmixed):

$$T_{out,\min}(t) = T_{in,\min}(t) - \varepsilon\left[T_{in,\min}(t) - T_{in,\max}(t)\right]$$

$$T_{out,\max}(t) = T_{in,\max}(t) - \varepsilon C^{*}\left[T_{in,\min}(t) - T_{in,\max}(t)\right]$$

Appendix D

Dimensionless Parameter Equations Expanded to Practical Terms:

NTU:
$$NTU = \frac{UA}{C_{\min}} = \frac{UA}{\left(\dot{m}c_p\right)_{\min}} = \frac{1}{\left(\dot{m}c_p\right)_{\min}\left[\frac{1}{\left(\eta_0 hA\right)_{\min}} + \frac{thk_w}{\left(kA\right)} + \frac{1}{\left(\eta_0 hA\right)_{\max}}\right]}$$

$\overline{C}_w{}^*$:
$$\overline{C}_w{}^* = \frac{\overline{C}_w}{\overline{C}_{\min}} = \frac{\left(Mc_p\right)_w}{\left(\rho c_p AL\right)_{\min}} = \frac{\rho_{wall} L\left(wdth\right)thk_{wall}c_{p_{wall}}}{\left(\rho c_p hgt\left(wdth\right)L\right)_{\min}}$$

C^*:
$$C^* = \frac{C_{\min}}{C_{\max}} = \frac{\left(\dot{m}c_p\right)_{\min}}{\left(\dot{m}c_p\right)_{\max}} = \frac{\left(\rho AVc_p\right)_{\min}}{\left(\rho AVc_p\right)_{\max}} = \frac{\left(\rho\left(hgt\right)wdthVc_p\right)_{\min}}{\left(\rho\left(hgt\right)wdthVc_p\right)_{\max}}$$

R^*:
$$R^* = \frac{\left(\eta_0 hA\right)_{\max}}{\left(\eta_0 hA\right)_{\min}} = \frac{\left(\eta_0 hLwdth\right)_{\max}}{\left(\eta_0 hLwdth\right)_{\min}}$$

t_d^*:
$$t_d^* = \frac{t_{d,\min}}{t_{d,\max}} = \frac{\left(\frac{L}{V}\right)_{\min}}{\left(\frac{L}{V}\right)_{\max}} = \frac{\left(\frac{Lwdth\left(hgt\right)\rho}{\dot{m}}\right)_{\min}}{\left(\frac{Lwdth\left(hgt\right)\rho}{\dot{m}}\right)_{\max}}$$

t^*:

$$t^* = \frac{t}{t_{d,\min}} = \frac{t}{\left(\frac{L}{V}\right)_{\min}} = \frac{t}{\left(\frac{Lwdth(hgt)\rho}{\dot{m}}\right)_{\min}}$$

$\varepsilon_{f,1}^*$:

$$\varepsilon_{f,1}^* = \frac{T_1(t) - T_1(0)}{T_1(\infty) - T_1(0)}$$

$\varepsilon_{f,2}^*$:

$$\varepsilon_{f,2}^* = \frac{T_2(t) - T_2(0)}{T_2(\infty) - T_2(0)}$$

**NOTE: min refers to C_{min} fluid, and max refers to C_{max} fluid

Appendix E

I. PROCEDURE FOR PARALLEL AND CROSS-FLOW DATA GENERATION

** NOTE: Record different macros for 10 and 20 segment models

A. Open Excel spreadsheet

B. Change spreadsheet input values to match desired table values (NTU, C^*, R^*, Cw^*)

C. <u>Macro</u> (Shortcut Key CTRL. a)
   [Transfers resistor values from spreadsheet to Thermonet model]
   1. Highlight, copy, point to 1 cell, paste special, values, OK
   2. Delete the rest of the spreadsheet leaving only the resistor portion
   3. File, save as, text(tab delimited), steadyst.rdt file, OK, yes, OK
   4. Close spreadsheet, yes, OK, yes, OK [Close all open Excel files]

D. File manager, copy steadyst.rdt to trans.rdt [Same files]

E. Open Thermonet file steadyst.prj and run
   1. Model, get model, steadyst.prj, OK,OK
   2. Data, steady state, input node, node # (existing), recall, enter, exit (Make sure node # 101 is at 70° F, and #201 is at 20°F)
   3. Model, save model input, OK
   4. Solver, steady state, OK

F. Open Excel spreadsheet

G. Open steadyst.nop file from Excel
   1. File, open, steadyst.nop, OK, delimited, next, space, finish

H. Highlight and copy steady state temperature profile (Column 2)

I. Switch to spreadsheet model

J. Paste special, values, into initial steady state temperature column

K. Save spreadsheet

L. <u>Macro</u> (Shortcut Key CTRL. b)
   [Transfers node values from spreadsheet to Thermonet model]
   3. Highlight, copy, point to cell, paste special, values the spreadsheet node table values
   4. Delete rest of spreadsheet
   5. File, save as, text (Tab delimited), trans.ndt file, OK, yes, OK
   6. Close spreadsheet, yes, OK, yes, OK [Close all open excel files]

M. Open Thermonet file trans.prj and run
   [Make sure materials agree with spreadsheet materials. Make sure time class for 1=> no temperature or heat input, 2=> 140°F, 3= 20°F and all have same total time]
   1. Model, get model, trans.prj, OK,OK

2. Solver, transient, yes, time step #, yes, OK

N. Open Excel spreadsheet (Sheet 2)

O. Open trans.his file from Excel

1. File, open, trans.his, OK, delimited, next, space, finish

P. Highlight and copy transient temperature profile and nodes (Five columns)

Q. Switch to spreadsheet model

R. Paste special, values, into transient temperature columns (Sheet 2)

S. Macro (Shortcut Key CTRL. c)

[E calculation]

2. Copy, and paste 1st row, last 3 columns all the way down to match transient data
3. Determine delta t^* to evenly fill in 12 blanks in chart and get E range of 0 => .999
4. Write all 12 t^* values below the t^* column
5. Highlight table
6. Data, sort, ascending, column F, no header row, OK, copy, paste interpolation equations to
   fill blanks for E values
7. Save file

T. Copy all files (Transient and Excel spreadsheet) to floppy disk, and print spreadsheets and Thermonet .HIS files